Evaluation of CT and MR angiography for the diagnosis of renal artery stenosis

Evaluation of CT and MR Angiography for the Diagnosis of Renal Artery Stenosis

Evaluation of CT and MR Angiography for the Diagnosis of Renal Artery Stenosis

proefschrift ter verkrijging van de graad van doctor
aan de Universiteit Maastricht,
op gezag van de Rector Magnificus
Prof. Dr. A.C. Nieuwenhuijzen Kruseman,
volgens het besluit van het College van Decanen,
in het openbaar te verdedigen
op donderdag 30 oktober 2003 om 16.00 uur

door

Godfried Boudewijn Christoffel Vasbinder
geboren 9 januari 1969 te Nijmegen

Promotores

Prof. Dr. J.M.A. van Engelshoven

Prof. Dr. P.W. de Leeuw

Co-promotores

Dr. P.J. Nelemans

Dr. A.A. Kroon

Beoordelingscommissie

Prof. Dr. K.M.L. Leunissen (voorzitter)

Prof. Dr. P.J.E.H.M. Kitslaar

Dr. C.T. Postma (Katholieke Universiteit Nijmegen)

Prof. Dr. M.H. Prins

Priv.-Doz. Dr. med. S.O. Schönberg (Ludwig-Maximilians-Universität München)

ISBN 90-9017412-5

design and lay out: Geertjan van Zonneveld, Maastricht, The Netherlands
print: Drukkerij Schrijen/Huntjens, Voerendaal, The Netherlands

Financial support by The Dutch Kidney Foundation for the publication of this thesis is gratefully acknowledged

Additional financial support was generously provided by: Amersham Health, Bard Benelux N.V., Medis medical imaging systems B.V., Merit Medical B.V., Schering Nederland B.V. and Toshiba Medical Systems Europe B.V.

Fere libenter homines id qoud volunt credunt

–Julius Caesar–

Men willingly believe what they wish
De mensen geloven gaarne wat ze willen dat zo is

To Suuske,
Charlotte, Madeleine & Diederik
and my parents

Contents

introduction

Renovascular hypertension is the most common form of secondary hypertension with a reported prevalence ranging from 1% to 5% in a general hypertensive population (1, 2). The pathophysiology of renovascular hypertension was first described in the early 20th century. Although earlier studies by the group of Franz Volhard contributed to elucidate the role of renal perfusion in hypertension, the experimental work by Harry Goldblatt in the early 1930s is indisputable considered to be the first evidence of the relationship between constriction of the renal artery, hypertension, and decreased renal function (3, 4). The experiments of Goldblatt provided an important basis for the further elucidation of the role of the renin-angiotensin system and our current knowledge of renovascular hypertension.

Renovascular hypertension is caused by renal artery stenosis (RAS). Two distinct causes of RAS can be identified. The most common cause is atherosclerosis which is mainly seen in older patients and commonly affects the proximal part of the renal artery. Fibromuscular dysplasia (FMD) is a less common cause of RAS (16% to 40% of all patients with RAS) and is typically seen in the more distal part of the renal artery (5, 6). FMD predominantly affects females and is relatively more often seen in younger patients. Renal artery stenosis is potentially treatable by percutaneous transluminal angioplasty with or without stent placement or surgery, which may result in improvement or cure of hypertension and halt the associated deterioration of renal function (7-9). The possibility to treat RAS created a need for a valid diagnostic test to identify subjects who may benefit from intervention.

Diagnostic tests for renal artery stenosis

The relatively low prevalence of renal artery stenosis demands a careful selection of patients who are more likely to have the condition and are, therefore, eligible for referral to a diagnostic test. Generally accepted specific clinical clues that raise the likelihood for the presence of a renal artery stenosis to 20% to 40% have been identified by the Working Group on Renovascular Hypertension and others, and are widely used in current clinical practice (10-12).

Traditionally, intra-arterial digital subtraction angiography (DSA) of the renal arteries is considered to be the best test for the detection of renal artery stenosis. However, this test is invasive and harbors small risks for serious complications

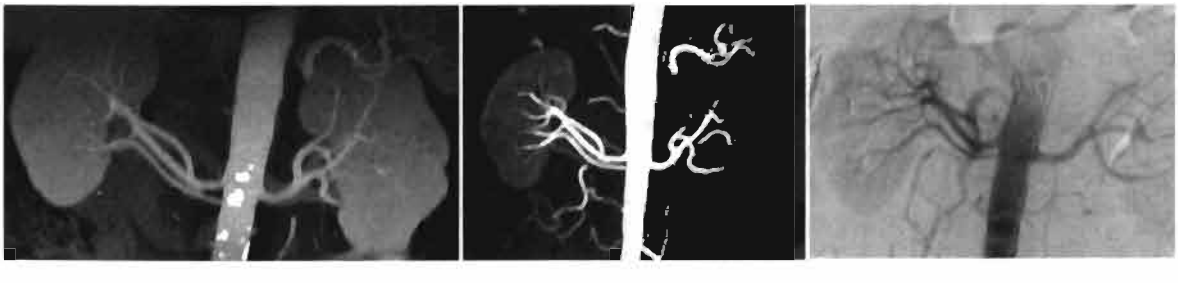

Images of a CTA, MRA, and DSA exam, respectively, show enhancement of the aorta, the renal arteries, and the renal parenchyma.

such as arterial dissection (13, 14). Moreover, patients who undergo DSA are subjected to radiation and iodinated contrast agents that are known for their adverse reactions, such as renal failure (15, 16). Over the past decades, several non invasive or minimally invasive diagnostic tests for RAS have been advocated. These tests include spiral computed tomographic angiography (CTA), 3D contrast-enhanced magnetic resonance angiography (MRA), non contrast-enhanced magnetic resonance angiographic techniques (2D and 3D time-of-flight, and 3D phase-contrast magnetic resonance angiography), ultrasonography, captopril renal scintigraphy, and the captopril test. The tests can be divided into those that rely upon assessment of the functional (or physiological) effects of RAS and those that rely upon direct imaging of the anatomy of the renal artery. Based on favorable reports in the literature, the anatomical tests CTA and MRA are currently considered to be the best minimally invasive diagnostic alternatives to DSA for the assessment of the renal arteries (17).

CTA and MRA for the diagnosis of renal artery stenosis

While DSA requires a short hospitalization because of the intra-arterial catheterization, both CTA and MRA can be performed as an outpatient routine. This fact, in addition to the minimally invasive nature of both CTA and MRA, has resulted in widespread enthusiasm in patients, health care insurances, and physicians and contributed to the rapid implementation of these techniques for the diagnosis of RAS since the introduction of CTA and MRA in the 1990s.

CTA and MRA offer the possibility to acquire volumetric data of the arterial system, which allow for 3D visualization and 3D quantification of abnormalities. This is not attainable with DSA, which acquires 2D images that may miss stenoses due to superposition of contrast agent filled vascular structures located anterior or posterior of the lesion.

However, CTA and MRA do have some disadvantages. As with DSA, CTA requires the administration of a large amount of a potential nephrotoxic contrast agent and exposes the patient to radiation (18). MRA overcomes these drawbacks by using non-nephrotoxic gadolinium-chelates as contrast agent and a magnetic field instead of X-rays. This magnetic field is, however, contra-indicated in some patients with metallic implants and pacemakers (19). Moreover, in a sizable number of patients MRA cannot be performed due to claustrophobia. Nevertheless, over 90% of all patients are capable to undergo a complete MRA exam. Despite the aforementioned limitations of CTA and MRA, both techniques seem to be preferred above DSA for the diagnosis of RAS. Before CTA or MRA can become the new standard of reference for this purpose, the results and conclusions of the studies included in this thesis should be considered.

The current thesis

This thesis addresses the validity of several non invasive or minimally invasive diagnostic tests for the detection of renal artery stenosis and, in particular, assesses the diagnostic accuracy of CTA and MRA using DSA as the reference test. Moreover, current limitations and pitfalls of MRA are discussed.

The objectives of this thesis are

- To summarize and compare the validity as found in the literature of CTA, MRA, non contrast-enhanced magnetic resonance angiographic techniques, ultrasonography, captopril renal scintigraphy, and the captopril test for the diagnosis of renal artery stenosis in patients suspected of having renovascular hypertension, using DSA as reference standard.
- To determine the validity of CTA and MRA as compared to the reference standard DSA for the detection of clinically relevant renal artery stenosis in a prospective multicenter study that included a large group of patients suspected of having renovascular hypertension.
- To quantify motion of the proximal renal artery during the cardiac cycle and discuss its potential effects on MRA image quality.
- To investigate whether respiratory-like motion is present despite sustained breath-hold and the effects of this motion on the MRA image quality of the distal renal artery.
- To identify causes that can explain discrepancies between MRA and DSA with respect to the observed severity of atherosclerotic renal artery stenosis.

Outline of this thesis

- In chapter 2, a meta-analysis is performed using the construction of summary receiver-operating characteristics (ROC) curves and the calculation of areas under the ROC curves, in order to summarize and compare the validity of five noninvasive or minimally invasive diagnostic tests for the detection of renal artery stenosis.
- In chapter 3, the diagnostic accuracy of CTA and MRA versus DSA for the detection of clinically relevant renal artery stenosis is determined in a large group of hypertensive patients with clinical clues for the presence of renovascular hypertension.
- In chapter 4, motion of the proximal renal artery during the cardiac cycle is quantified and objective arguments are provided for the improvement of renal MRA.
- In chapter 5, the presence of respiratory-like motion of the distal renal artery during sustained breath-hold is studied and the effects of this motion on renal MRA image quality is explored by using a computer model and the evaluation of patient MRA image data.
- In chapter 6, discrepancies between MRA and DSA with respect to the measured severity of atherosclerotic renal artery stenosis in a large group of patients that underwent both tests are retrospectively evaluated and the observed causes of the discrepancies are quantified and discussed.
- In chapter 7, the several noninvasive and minimally invasive diagnostic tests for the detection of clinically relevant renal artery stenosis are placed in perspective and the use of CTA and MRA as alternatives to DSA in current practice is discussed. Moreover, the limitations of MRA are addressed. Finally, recent developments that may improve the accuracy of CTA and MRA for the detection of renal artery stenosis are discussed and recommendations for future developments will be given.

The research for this thesis was funded by grant OG 97-003 of the Dutch Health Care Insurance Board.

References

1. Eardley KS, Lipkin GW. Atherosclerotic renal artery stenosis: is it worth diagnosing? J Hum Hypertens 1999; 13(4):217-20.
2. Derkx FH, Schalekamp MA. Renal artery stenosis and hypertension. Lancet 1994; 344(8917):237-239.
3. Wolf G. Franz Volhard and his students' tortuous road to renovascular hypertension. Kidney Int 2000; 57(5):2156-66.
4. Laragh J. Harry Goldblatt 1891-1977. Trans Assoc Am Physicians 1978; 91:24-7.:24-27.
5. Pohl MA, Novick AC. Natural history of atherosclerotic and fibrous renal artery disease: clinical implications. Am J Kidney Dis 1985; 5(4):A120-A130.
6. Textor SC. Epidemiology and clinical presentation. Semin Nephrol 2000; 20(5):426-31.
7. Plouin PF, Chatellier G, Darne B, Raynaud A. Blood pressure outcome of angioplasty in atherosclerotic renal artery stenosis: a randomized trial. Essai Multicentrique Medicaments vs Angioplastie (EMMA) Study Group. Hypertension 1998; 31(3):823-29.
8. van Jaarsveld BC, Krijnen P, Pieterman H, Derkx FH, Deinum J, Postma CT et al. The effect of balloon angioplasty on hypertension in atherosclerotic renal artery stenosis. Dutch Renal Artery Stenosis Intervention Cooperative Study Group. N Engl J Med 2000; 342(14): 1007-14.
9. Webster J, Marshall F, Abdalla M, Dominiczak A, Edwards R, Isles CG et al. Randomised comparison of percutaneous angioplasty vs continued medical therapy for hypertensive patients with atheromatous renal artery stenosis. Scottish and Newcastle Renal Artery Stenosis Collaborative Group. J Hum Hypertens 1998; 12(5):329-35.
10. Detection, evaluation, and treatment of renovascular hypertension. Final report. Working Group on Renovascular Hypertension. Arch Intern Med 1987; 147(5):820-29.
11. Anderson GH, Jr., Blakeman N, Streeten DH. Prediction of renovascular hypertension. Comparison of clinical diagnostic indices. Am J Hypertens 1988; 1(3 Pt 1):301-304.
12. Krijnen P, van Jaarsveld BC, Steyerberg EW, Man in 't Veld AJ, Schalekamp MA, Habbema JD. A clinical prediction rule for renal artery stenosis. Ann Intern Med 1998; 129(9):705-11.
13. Waugh JR, Sacharias N. Arteriographic complications in the DSA era. Radiology 1992; 182(1):243-46.
14. Young N, Chi KK, Ajaka J, McKay L, O'Neill D, Wong KP. Complications with outpatient angiography and interventional procedures. Cardiovasc Intervent Radiol 2002; 25(2):123-26.
15. Rudnick MR, Berns JS, Cohen RM, Goldfarb S. Nephrotoxic risks of renal angiography: contrast media-associated nephrotoxicity and atheroembolism--a critical review. Am J Kidney Dis 1994; 24(4):713-27.
16. Cochran ST, Bomyea K, Sayre JW. Trends in adverse events after IV administration of contrast media. AJR Am J Roentgenol 2001; 176(6):1385-88.
17. Vasbinder GB, Nelemans PJ, Kessels AG, Kroon AA, de Leeuw PW, van Engelshoven JM. Diagnostic tests for renal artery stenosis in patients suspected of having renovascular hypertension: a meta-analysis. Ann Intern Med. 2001;135:401-11.
18. Kemerink GJ, de Haan MW, Vasbinder GB, Frantzen MJ, Schultz FW, Zoetelief J, Jansen JT et al. The effect of equipment set up on patient radiation dose in conventional and computed tomographic angiography of the renal arteries. BJR; in press.
19. Kanal E, Shellock FG. Policies, guidelines, and recommendations for MR imaging safety and patient management. SMRI Safety Committee. J Magn Reson Imaging 1991; 1(1):97-101.

Diagnostic tests for renal artery stenosis in patients suspected of having renovascular hypertension: a meta-analysis

Annals of Internal Medicine 2001;135:401-411.

G.B.C. Vasbinder, P.J. Nelemans, A.G.H. Kessels, A.A. Kroon, P.W. de Leeuw, J.M.A. van Engelshoven.

Abstract

Purpose
To summarize and compare the validity of computed tomographic angiography, magnetic resonance angiography, ultrasonography, captopril renal scintigraphy, and the captopril test for diagnosis of renal artery stenosis in patients suspected of having renovascular hypertension.

Data sources
For each diagnostic modality, published studies were identified by MEDLINE literature searches.

Original studies were selected if they met the following criteria: 1) suspicion of renovascular hypertension was the indication for the test; 2) intra-arterial x-ray angiography was used as the gold standard; 3) a cutoff point for a positive test result was explicitly defined; and 4) absolute numbers of true-positive, false-negative, true-negative, and false-positive results were available or could be derived from the presented data.

Data extraction
A standard form was used to extract relevant data.

Data synthesis
Data on the accuracy of the different diagnostic methods were analyzed and compared by constructing summary receiver-operating characteristic (ROC) curves and by computation areas under the summary ROC curves.

Results
Although accuracy varied greatly for all diagnostic modalities, summary ROC curves found that computed tomographic angiography and gadolinium-enhanced, three-dimensional magnetic resonance angiography performed significantly better than the other diagnostic tests.

Conclusions
Computed tomographic angiography and gadolinium-enhanced, three-dimensional magnetic resonance angiography seem to be preferred in patients referred for evaluation of renovascular hypertension. However, because few studies of these tests have been published, further research is recommended.

Introduction

In a general hypertensive population, the prevalence of renovascular disease varies between 1% and 5% (1,2). In patients who exhibit specific clinical clues that indicate renovascular hypertension, the probability of having the disease increases to 20% to 40% (3). Renovascular hypertension is currently treated with drugs; surgery; or less invasive techniques, such as percutaneous transluminal renal angioplasty with or without stent placement. A recent study found no significant difference between treatment with percutaneous transluminal renal angioplasty and antihypertensive drug therapy. However, in that study, 44% of patients who received drug therapy still underwent percutaneous transluminal renal angioplasty (4). Because a large proportion of patients are still preferably treated with angioplasty, a valid diagnostic test is needed in the presence of one or more clinical clues (5). Intra-arterial x-ray angiography is considered the gold standard; however, it is invasive and carries small risks for serious complications, such as arterial dissection or adverse contrast reactions.

During the past few decades, many researchers have reported results of other, less invasive diagnostic tests. It is, however, difficult to compare the tests' diagnostic performance. Reviews have reported rather broad ranges of sensitivity and specificity for a certain test that overlap the ranges reported for other tests. Furthermore, studies differ in case mix, specific test characteristics, and cut-off points for a positive test result, all of which may affect estimates of sensitivity and specificity.

The objective of our meta-analysis was to compare five non-invasive or minimally invasive modalities currently used in clinical practice to detect renal artery stenosis. The tests were computed tomographic angiography (CTA), magnetic resonance angiography (MRA), ultrasonography, captopril renal scintigraphy, and the captopril test. Intravenous renal angiography, and conventional renography were not considered because earlier studies showed that their accuracy was limited (6, 7).

Methods

Data sources

We searched MEDLINE using the following terms: magnetic resonance imaging and angiography and (renal artery or hypertension, renovascular); tomography, x-ray computed and angiography and (renal artery or hypertension, renovascular); ultrasonography and angiography and (renal artery or hypertension, renovascular); captopril and angiography and (renal artery or hypertension, renovascular).

No beginning date limit was used. The search was updated until 1 August 2000. Only English-, German-, or French-language studies were considered because the investigators were familiar with these languages. The bibliographies of selected articles were screened for potentially suitable references, which were then retrieved. We also searched the EMBASE and Cochrane databases using the same strategy.

Study selection

Studies were included in the meta-analysis if they met the following criteria:

1) intra-arterial x-ray angiography was used as the gold standard; 2) clinical suspicion of renovascular hypertension was the reason for referral; 3) the criteria and cutoff values for a positive result for each test (for example, hemodynamically significant stenosis) were explicitly defined; and 4) the absolute numbers of true-positive, false-negative, false-positive, and true-negative results had to be available or could be derived from the data presented.

Two investigators screened the full text of potentially relevant articles using the inclusion criteria. In all cases of disagreement, the investigators reached consensus. Studies that included patients who had received renal transplants were excluded. Another reason for exclusion was the possibility of verification bias, which appears when patients with a positive outcome of the index test (that is, test under investigation) are referred to the gold standard test more often than patients with a negative results on the index test. The presence of verification bias was assumed if only some of the patients who had the index test were referred for intra-arterial x-ray angiography. If an author or research group published more than one study about the same diagnostic test, the most recent study was included. All articles by the same author or research group were included for analysis only when it was obvious that a different patient sample had been used. In cases where an author or research group discussed more than one diagnostic technique within one journal article (for example, MRA vs. ultrasonography, or two-dimensional time-of-flight MRA vs. three-dimensional time-of-flight MRA), each modality was considered separately.

Data extraction

We used a standard form to extract relevant data from the included articles. Several studies reported more than one pair of sensitivity and specificity estimates because they used several approaches to analyze data on accuracy. These approaches included inclusion compared with exclusion of the accessory renal arteries in the analysis; estimation of sensitivity and specificity using renal arteries, kidneys, or patients as unit of analysis; exclusion compared with inclusion of missing observations (such as technical failures, poor examination quality, or arteries not identified at the index test); and presentation of sensitivity and specificity estimates based on evaluation by more than one reviewer. We prefered sensitivity and specificity estimates based on inclusion of accessory renal arteries, on patients as unit of analysis, or on inclusion of missing observations in the analysis. If a study presented results based on more than one reviewer, the accuracy data representing the highest estimates were extracted.

For each ultrasonography study, we noted whether measurements were performed at the level of the intrarenal arteries or at the level of the extrarenal arteries. For captopril renal scintigraphy studies, we noted whether the analysis was based on changes between baseline (precaptopril) and postcaptopril measurements or only postcaptopril measurements. When captopril renal scintigraphy studies presented estimates based on evaluation of postcaptopril renograms and captopril-induced changes, the highest estimates were extracted.

Data synthesis

We based our meta-analysis method on the construction of summary receiver-operating characteristic (ROC) curves. This method accounts for the mutual dependence between sensitivity and specificity; evaluates the extent to which the

variation in sensitivity and specificity can be explained by variation in positivity thresholds between studies; makes it possible to assess the effects of other between-study differences, such as differences in test design and analysis characteristics, on the estimates of diagnostic accuracy; and is very useful to compare different diagnostic tests (8, 9). Areas under the summary ROC curves were used as measure of the diagnostic performance of the tests. We calculated a diagnostic odds ratio on the basis of the sensitivity and specificity reported in each study and then derived areas under the ROC curve for each study.

We used linear regression analyses to compare the diagnostic tests. In the analysis, indicator variables represented the tests and the presence or absence of specific study characteristics. The coefficients resulting from the model were translated into areas under the summary ROC curves, differences between areas under the summary ROC curves, and the 95%-CIs of these differences. Details of the statistical analysis are discussed in the Appendix. All statistical calculations were performed using SPSS (SPSS, Inc. Chicago, Illinois).

Results

Included studies

We identified 343, 306, 314, 172, and 172 studies for CTA, MRA, ultrasonography, captopril renal scintigraphy, and the captopril test, respectively. We retrieved the full text of 22, 39, 58, 25, and 13 studies. Five of 22 involving CTA (10-14), 16 of 39 studies involving MRA (15-30), 24 of 58 studies involving ultrasonography (7, 10, 18, 29, 31-50), 14 of 25 studies involving captopril renal scintigraphy (7, 16, 35, 37, 51-60), and 4 of 13 involving the captopril test (59, 61-63) met the inclusion criteria. Subsequent searches on the EMBASE and Cochrane databases did not reveal any additional references. A list of all studies that we excluded after reading the full text, as well as the reasons for exclusion is available from the authors or at http://www.unimaas.nl/~radiolog/radish.html.

Ten journal articles studied more than one diagnostic modality (7, 10, 15, 16, 18, 21, 29, 35, 37, 59). In the MRA articles a distinction was made between techniques. Studies evaluating gadolinium-enhanced MRA (n = 6) were combined and compared with studies evaluating non-gadolinium-enhanced MRA, representing the two-dimensional and three-dimensional time-of-flight and the phase-contrast techniques (n = 12). In the ultrasonography studies, a distinction was made between studies performed at the level of the extrarenal arteries (n = 13), and studies performed at the level of the intrarenal arteries (n = 7); 4 studies performed measurements at both levels.

Data extraction and synthesis

We extracted the evaluated technique, the year of publication, test characteristics, patient characteristics, design characateristics, and results from the 55 included studies (evaluating 65 modalities); this information is partly summarized the Table.

The summary ROC curves for the compared diagnostic modalities are shown in Figure 1. The summary ROC curve representing the CTA studies and the summary ROC curve representing the gadolinium-enhanced MRA studies pass through the upper left area of the ROC-area, which indicates that high sensitivity could

be reached at low false positive rates. Figure 1 also shows that the captopril test has the lowest diagnostic performance. The areas under the ROC curves for the diagnostic modalities were 0.99 for CTA, 0.99 for gadolinium-enhanced MRA, 0.97 for non-gadolinium-enhanced MRA, 0.93 for ultrasonography, 0.92 for captopril renal scintigraphy, and 0.72 for the captopril test.

We used a multivariate regression model to compare studies of CTA, gadolinium-enhanced MRA, non gadolinium-enhanced MRA, captopril renal scintigraphy, and the captopril test with ultrasonography as a reference test. We chose ultrasonography as the reference test because it had the largest number of available studies. The differences between the area under the summary ROC curve of a particular test and the area under the summary ROC curve of the reference test (ultrasonography), as well as the 95% confidence intervals of these differences are displayed in Figure 2. This analysis showed that CTA and MRA have significantly better diagnostic accuracy than ultrasonography, while the captopril test performs significantly worse than ultrasonography.

In addition, we performed many between-test comparisons. These analyses showed that both CTA and gadolinium-enhanced MRA were significantly better than all other studied tests ($P < 0.05$), while CTA and gadolinium-enhanced MRA had similar diagnostic performance ($P > 0.2$). Non-gadolinium-enhanced MRA was significantly better than captopril renal scintigraphy and the captopril test

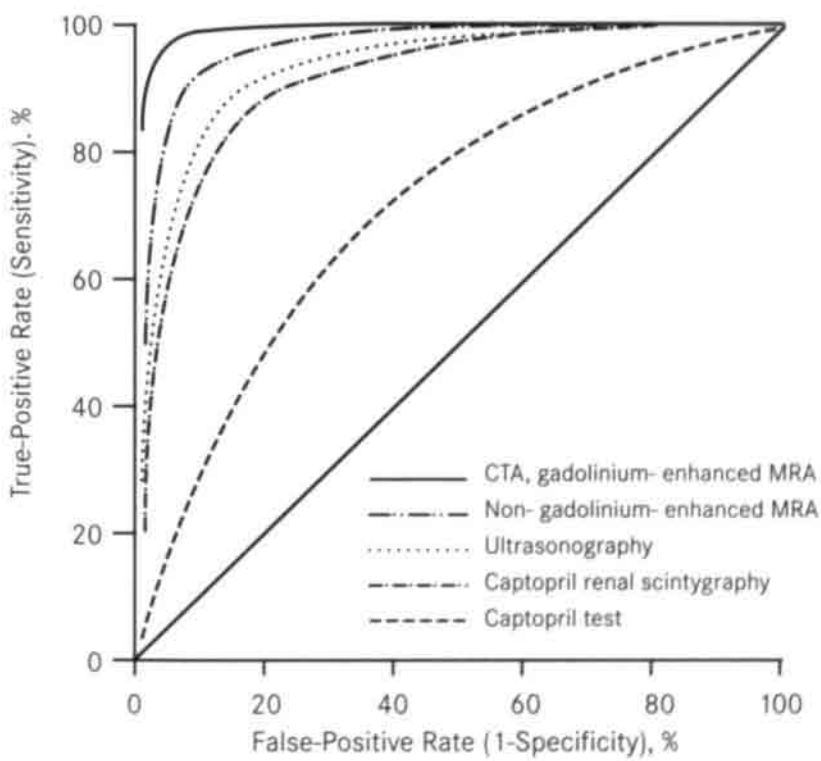

Figure 1. Summary receiver-operating characteristic (ROC) curves. For each diagnostic technique, the concurrent ROC curve is shown. The boldface, diagonal line indicates the point at which sensitivity equals 1 - specificity. Because data for computed tomographic angiography (CTA) and gadolinium-enhanced magnetic resonance (MRA) were nearly identical, both tests are represented by the same line pattern.

Table. Extracted data from studies that met the inclusion criteria

Study (reference)	Year	Test*	Patient	Definition of Hemodynamically Significant Stenosis†	Blinded review	Accessory Arteries Included*
			n	%		
Bongers et al. (16)	2000	Gadolinium-enhanced MRA	43	50	Yes	No
De Cobelli et al. (18)	2000	Gadolinium-enhanced MRA	45	50	Yes	Yes
Korst et al. (22)	2000	Gadolinium-enhanced MRA	88	50	Yes	Yes
Leung et al. (24)	1998	Gadolinium-enhanced MRA	20	60	Not mentioned	No
Rieumont et al. (27)	1997	Gadolinium-enhanced MRA	30	50	Yes	Yes
Thornton et al. (30)	1999	Gadolinium-enhanced MRA	62	50	Yes	Yes
Arlart et al. (15)	1992	2-D time-of-flight MRA[1]	41	50	Yes	No
Fellner et al. (21)	1995	2-D time-of-flight MRA[1]	46	60	Yes	No
Laissy et al. (23)	1996	2-D time-of-flight MRA[1]	36	50	Yes	Yes
Arlart et al. (15)	1992	3-D time-of-flight MRA[1]	41	50	Yes	Yes
Borrello et al. (17)	1995	3-D time-of-flight MRA[1]	15	50	Yes	No
Fellner et al. (21)	1995	3-D time-of-flight MRA[1]	46	60	Yes	No
Postma et al. (26)	1997	3-D time-of-flight MRA[1]	37	50	Yes	No
Smith and Bakke (28)	1993	3-D time-of-flight MRA[1]	12	75	Yes	Yes
Strotzer et al. (29)	1995	3-D time-of-flight MRA[1]	55	60	Not mentioned	No
De Cobelli et al. (19)	1996	Phase-contrast MRA[1]	50	50	Yes	Yes
De Haan et al. (20)	1996	Phase-contrast MRA[1]	33	50	Yes	Yes
Loubeyre et al. (25)	1996	Phase-contrast MRA[1]	46	50	Yes	No
Equine et al. (10)	1999	CTA	50	50	Not mentioned	No
Galanski et al. (11)	1994	CTA	52	50	Yes	Yes
Kaatee et al. (12)	1997	CTA	71	50	Yes	Yes
Olbricht et al. (13)	1995	CTA	62	50	Yes	Yes
Wittenberg et al. (14)	1999	CTA	82	50	No	Yes
Bardelli et al. (31)	1992	Ultrasonography[2]	49	50	Yes	NA
Baxter et al. (32)	1996	Ultrasonography[2]	73	70	Yes	NA
Breitenseher et al. (33)	1992	Ultrasonography[3]	17	50	Not mentioned	No
Claudon et al. (34)	2000	Ultrasonography[3]	116	50	Yes	No
De Cobelli et al. (18)	2000	Ultrasonography[4]	45	50	Yes	Yes
Dondi et al. (35)	1992	Ultrasonography[3]	63	50	Not mentioned	No
Equine et al. (10)	1999	Ultrasonography[4]	53	50	Not mentioned	No
Handa et al. (36)	1988	Ultrasonography[3]	20	50	Not mentioned	No
Kaplan-Pavlovcic (37)	1998	Ultrasonography[3]	28	60	Not mentioned	No
Karasch et al. (38)	1993	Ultrasonography[3]	53	50	Not mentioned	No
Kliewer et al. (39)	1993	Ultrasonography[3]	46	50	Yes	No
Lucas et al. (40)	1996	Ultrasonography[2]	53	60	Yes	NA
Miralles et al. (41)	1993	Ultrasonography[3]	46	60	Not mentioned	No
Miralles et al. (42)	1996	Ultrasonography[3]	78	60	Not mentioned	No
Olin et al. (43)	1995	Ultrasonography[3]	102	60	Yes	No

Missing Observations	Unit of Analysis	TP	FN	TN	FP	Sum	Sensitivity	Specificity	Area under the ROC Curve*
None	Patient	29	0	14	0	43	100	100	1.00
Excluded	Artery	32	0	65	5	102	100	93	1.00
Excluded	Artery	26	0	57	5	88	100	92	1.00
None	Artery	8	0	31	1	40	100	97	1.00
Excluded	Artery	46	0	15	5	66	100	75	1.00
Excluded	Artery	23	3	101	2	129	88	98	0.99
Excluded	Artery	23	3	28	5	59	88	85	0.93
Included	Artery	7	0	71	14	92	100	84	1.00
None	Artery	15	1	60	1	77	94	98	0.99
None	Artery	18	2	24	9	53	90	73	0.90
None	Artery	7	6	20	1	34	54	95	0.89
Included	Artery	7	0	76	9	92	100	89	1.00
None	Patient	12	0	24	1	37	100	96	1.00
None	Artery	7	0	18	1	26	100	95	1.00
Included	Artery	10	0	90	10	110	100	90	1.00
Excluded	Artery	18	2	80	1	101	90	99	0.99
Excluded	Patient	6	0	26	1	33	100	96	1.00
None	Artery	11	0	55	29	95	100	65	1.00
Excluded	Artery	45	3	41	2	91	94	95	0.98
None	Artery	53	0	65	6	124	100	92	1.00
None	Artery	91	5	68	2	166	95	97	0.99
Excluded	Artery	60	1	89	6	156	98	94	0.99
None	Artery	23	1	172	1	197	96	99	0.99
None	Patient	26	7	15	1	49	79	94	0.95
None	Patient	32	4	36	1	73	89	97	0.98
Excluded	Artery	1	5	16	2	24	17	89	0.58
Excluded	Patient	36	7	59	14	116	84	81	0.89
Excluded	Artery	22	6	57	4	89	79	93	0.94
Included	Artery	34	6	66	19	125	85	78	0.89
Excluded	Artery	40	13	38	6	97	75	86	0.88
None	Artery	10	0	28	2	40	100	93	1.00
Excluded	Artery	15	3	22	5	45	83	81	0.89
Excluded	Artery	47	4	34	3	88	92	92	0.97
None	Artery	16	12	43	21	92	57	67	0.66
Included	Kidney	15	7	75	7	104	68	91	0.89
None	Artery	34	4	49	5	92	89	91	0.96
Excluded	Artery	48	7	86	8	149	87	91	0.95
Excluded	Artery	122	2	62	1	187	98	98	1.00

table continues on the next pages

Table. Extracted data from studies that met the inclusion criteria* Continued

Study (reference)	Year	Test*	Patient	Definition of Hemodynamically Significant Stenosis†	Blinded review	Accessory Arteries Included*
			n	%		
Oliva et al. (44)	1998	Ultrasonography[2]	71	50	Yes	NA
Pedersen et al. (7)	1996	Ultrasonography[2]	131	50	Not mentioned	NA
Postma et al. (45)	1992	Ultrasonography[4]	61	50	Yes	No
Postma et al. (46)	1996	Ultrasonography[2]	57	50	Yes	NA
Spies et al. (47)	1995	Ultrasonography[4]	135	50	Yes	No
Strotzer et al. (29)	1995	Ultrasonography[3]	55	60	Not mentioned	No
Strunk et al. (48)	1995	Ultrasonography[2]	50	50	Not mentioned	NA
Vigna et al. (49)	1998	Ultrasonography[3]	104	50	Yes	No
Zoller et al. (50)	1990	Ultrasonography[3]	86	50	Yes	No
Bongers et al. (16)	2000	Captopril renal scintigraphy[5]	43	50	Yes	NA
Dondi et al. (51)	1990	Captopril renal scintigraphy[6]	132	50	Not mentioned	NA
Dondi et al. (35)	1992	Captopril renal scintigraphy[5]	63	50	Not mentioned	NA
Fommei et al. (52)	1993	Captopril renal scintigraphy[5]	272	70	Yes	NA
Gezici et al. (53)	1999	Captopril renal scintigraphy[6]	45	50	Not mentioned	NA
Kahn et al. (54)	1994	Captopril renal scintigraphy[6]	28	50	Yes	NA
Kaplan-Pavlovcic (37)	1998	Captopril renal scintigraphy[6]	28	60	Not mentioned	NA
Mann et al. (55)	1991	Captopril renal scintigraphy[6]	55	70	Not mentioned	NA
Mittal et al. (56)	1996	Captopril renal scintigraphy[6]	86	0	Not mentioned	NA
Nitzsche et al. (57)	1991	Captopril renal scintigraphy[5]	68	60	Not mentioned	NA
Pedersen et al. (7)	1996	Captopril renal scintigraphy[5]	131	50	Not mentioned	NA
Setaro et al. (58)	1991	Captopril renal scintigraphy[7]	113	75	Yes	NA
Svetkey et al. (59)	1991	Captopril renal scintigraphy[5]	140	50	Not mentioned	NA
Tremel et al. (60)	1996	Captopril renal scintigraphy[5]	45	70	Not mentioned	NA
Postma et al. (61)	1990	Captopril test	149	50	Not mentioned	NA
Schreij et al. (62)	1995	Captopril test	46	50	Not mentioned	NA
Stephan et al. (63)	1993	Captopril test	88	75	Not mentioned	NA
Svetkey et al. (59)	1991	Captopril test	130	50	Not mentioned	NA

* 2-D = two-dimensional; 3-D = three-dimensional; CTA = computed tomography angiography; MRA = magnetic resonance angiography; NA = not applicable; ROC = receiver-operating characteristic.
† Cutoff value for a positive result on the gold standard test.
‡ The index test and conventional angiography were judged without knowledge of the outcome of the opposite test.
§ Missing observations or technical failures were included in analysis.
‖ Total of true-positive results, false-positive results, false-negative results, and true-negative results.
¶ Areas for individual studies are computed by assuming logistically distributed data for healthy and diseased persons with equal variances (9).

Missing Observations	Unit of Analysis	TP	FN	TN	FP	Sum	Sensitivity	Specificity	Area under the ROC Curve*
None	Kidney	39	9	85	2	135	81	98	0.98
None	Patient	21	7	78	25	131	75	76	0.82
Excluded	Patient	15	9	19	3	46	63	86	0.83
Excluded	Patient	9	10	32	1	52	47	97	0.91
Excluded	Artery	45	3	135	12	195	94	92	0.98
Included	Artery	9	1	85	15	110	90	85	0.94
Excluded	Patient	9	4	32	3	48	69	91	0.90
Excluded	Kidney	40	5	143	4	192	89	97	0.98
None	Artery	21	4	131	2	158	84	98	0.98
None	Patient	26	3	11	3	43	90	79	0.92
None	Patient	48	4	78	2	132	92	98	0.99
None	Kidney	36	4	80	5	125	90	94	0.97
None	Patient	89	15	137	31	272	86	82	0.91
None	Kidney	21	8	32	12	73	72	73	0.79
None	Patient	13	1	10	4	28	93	71	0.92
Excluded	Kidney	14	4	22	5	45	78	81	0.87
None	Patient	33	2	19	1	55	94	95	0.98
None	Patient	37	8	37	4	86	82	90	0.93
None	Patient	17	1	44	6	68	94	88	0.97
None	Patient	18	10	85	18	131	64	83	0.81
None	Patient	53	5	48	7	113	91	87	0.95
None	Patient	24	7	48	61	140	77	44	0.66
None	Patient	8	6	30	1	45	57	97	0.93
None	Patient	15	29	98	7	149	34	93	0.79
Excluded	Patient	3	17	20	6	46	15	77	0.41
None	Patient	13	6	61	8	88	68	88	0.87
None	Patient	13	9	82	26	130	59	76	0.74

TP = true-positive results; FN = false-negative results; TN = true-negative results; FP = false-positive results.

[1] Included in the "non-gadolinium-enhanced MRA" subgroup.

[2] Intrarenal ultrasonography measurements.

[3] Extrarenal ultrasonography measurements.

[4] Both intrarenal and extrarenal ultrasonography measurements.

[5] Analysis based on postcaptopril measurements.

[6] Analysis based on changes between baseline (precaptopril) and postcaptopril measurements.

[7] Analysis based on postcaptopril measurements and on changes between baseline (precaptopril) and postcaptopril measurements.

(P = 0.022 and P < 0.001, respectively), and both ultrasonography and captopril renal scintigraphy were better than the captopril test (P = 0.010 and P = 0.017, respectively). Ultrasonography and captopril renal scintigraphy did not differ significantly in diagnostic performance (P > 0.2).

An additional analysis comparing the diagnostic performance of two-dimensional time-of-flight MRA with three-dimensional time-of-flight MRA, two-dimensional time-of-flight MRA with phase-contrast MRA, three-dimensional time-of-flight MRA with phase-contrast MRA, and intrarenal ultrasonography with extrarenal ultrasonography, showed no significant differences in diagnostic performance.

For captopril renal scintigraphy, performance was similar in studies that based the analysis on changes between baseline (precaptopril) and postcaptopril measurements and those that based the analysis only on postcaptopril measurements. Eight studies of captopril renal scintigraphy using technetium-99m-mercapto-acetyl-triglycine reported diagnostic accuracy similar to that of six studies using technetium-99m-diethylenetriaminepentaacetic acid.

The effect of study characteristics on diagnostic performance is shown in Figure 3. Studies that included more than 50 patients showed a statistical better diagnostic performance than studies that included 50 or fewer patients (difference in area under the ROC curve, 0.052 [95% CI: 0.004 to 0.099]. The other evaluated study characteristics, such as a stringent definition of hemodynamically significant stenosis (≥ 60%, ≥ 70%, or ≥ 75%) compared with a less stringent definition (≥ 50%), inclusion or exclusion of missing observations in the analysis, inclusion or exclusion of accessory renal arteries in the analysis, and publication year, were poor predictors of diagnostic performance. The differences between the areas under the ROC curves with and without these study characteristics were small and not statistically significant. The

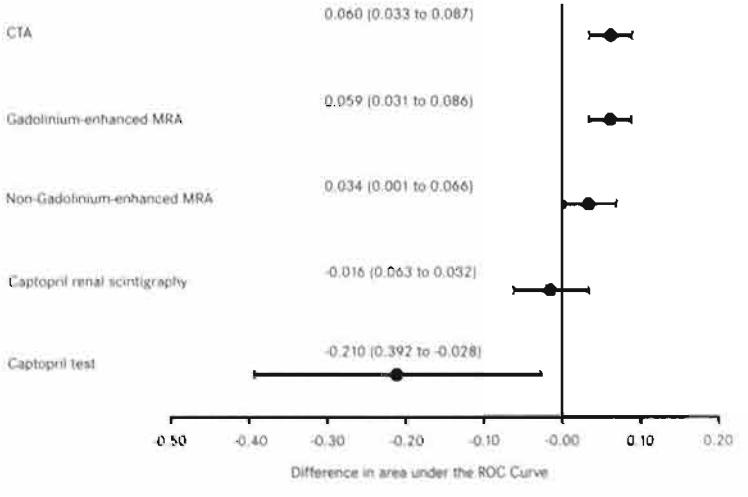

Figure 2. Differences between the areas under the summary receiver-operating characteristic (ROC) curve for a particular test and the area under under the area under the summary ROC curve for the reference test (ultrasonography). Values in parenthesis are 95% CIs. CTA = computed tomographic angiography; MRA = magnetic resonance angiography.

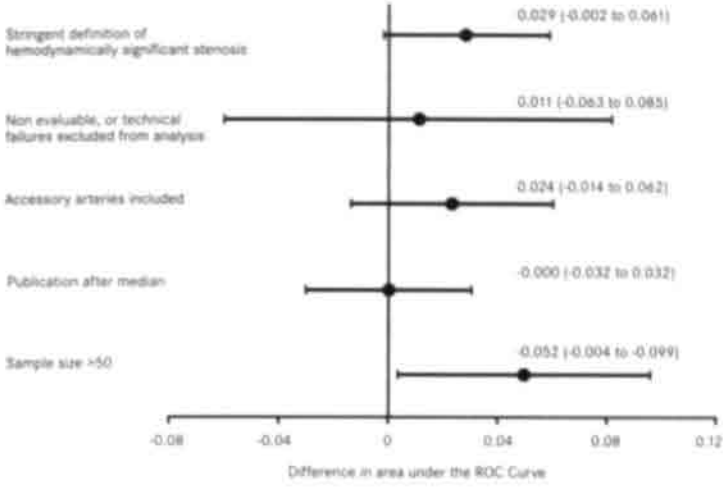

Figure 3. Differences between the areas under the summary receiver-operating characteristics (ROC) curve for studies with and without the evaluated study characteristics. Values in parenthesis are 95% CIs.

analysis comparing inclusion or exclusion of accessory arteries pertains only to CTA, MRA, and extrarenal ultrasonography studies. Intrarenal ultrasonography, captopril renal scintigraphy, and the captopril test were excluded from this analysis because these tests do not intend to visualize accessory renal arteries.

Discussion

Our study is an up-to-date meta-analysis of CTA, MRA, ultrasonography, captopril renal scintigraphy, and the captopril test as diagnostic tests for renal artery stenosis. We demonstrate that CTA and gadolinium-enhanced MRA had the highest diagnostic performance for the detection of renal artery stenosis compared with the other studied tests.

It must be emphasized that only 55 articles met the predefined inclusion criteria. This is partly because many studies poorly defined their study population or did not primarily aim at determining the diagnostic performance of a test for the detection of renal artery stenosis. Studies were frequently excluded because 1) the indication for referral was not primarily suspicion of renal artery stenosis, but the presence of other types of atherosclerotic disease, such as peripheral arterial occlusive disease or aneurysms, and 2) verification bias, which is known to inflate sensitivity and to deflate specificity, was possible.The included studies varied greatly in their analyses of data on accuracy. Before performing this meta-analysis, we expected to find differences in diagnostic performance that favoured studies using a higher percentage of luminal narrowing as arteriographic definition of a hemodynamically significant lesion, studies excluding technical failures or uninterpretable test results from the analysis, studies excluding accessory arteries from the analysis, and studies published more recently (because of technological advances). However, these expectations were not met. Only small and nonsignificant differences were seen among studies with and without these characteristics. Nevertheless, for reasons of comparability, future studies should indicate whether the analyses were based on inclusion or exclusion of accessory arteries and missing observations.

We also evaluated the effect of sample size. Publication bias is a well-known problem in meta-analyses because it may affect study results, probably overestimating test accuracy (6). In particular, small studies with optimistic results may be accepted for publication more frequently than small studies with less favorable results. Contrary to these expectations, our meta-analysis showed that large studies had statistically significant better performance than small studies. This may be because authors publishing large studies have more expertise in the performance or evaluation of the studied test.

A large part of the heterogeneity of study results remained unexplained. One source of heterogeneity was the lack of standardization of criteria used to define a positive test result. This problem pertains especially to ultrasonography and captopril renal scintigraphy. For both modalities, many variables, as well as different combinations of variables, were used to define a positive test result. In addition, threshold values for these variables differed between studies. This is a less serious problem because summary ROC analyses adjust for differences in threshold values.

Accuracy estimates may have varied greatly among the ultrasonography studies because ultrasonography is notoriously operator-dependent. However, only 4 of the 24 included ultrasonography studies report a sensitivity and specificity of ≥ 90% (Table); this corroborates the finding that CTA and gadolinium-enhanced MRA are superior to ultrasonography.

Unexplained heterogeneity may also be related to difference in case mix. In diagnostic studies, estimates of sensitivity and specificity are known to depend on the distribution of severity of disease in the studied sample (64). We minimized the variation in case mix among studies by restricting our analysis to studies that only evaluated patients with clinical suspicion of renovascular hypertension. Despite this restriction, the included studies varied greatly in prevalence of renal artery stenosis (range, 7.6% to 69.7%). Therefore, researchers must design and analyse future diagnostic studies in a way that facilitates comparison of results. Future diagnostic studies should adequatly describe inclusion and exclusion criteria and present estimates of sensitivity and specificity for subgroups of patients in whom clinical suspicion of renovascular hypertension varies.

Our key finding is that MRA and CTA have better diagnostic accuracy than ultrasonography, captopril renal scintigraphy, and the captopril test. However, with respect to the comparison of these tests, additional methodological issues must be discussed. First, anatomical tests were compared with functional tests. The use of intra-arterial x-ray angiography as the gold standard may raise concern about possible underestimation of the diagnostic performance of functional tests (for example, captopril renal scintigraphy). Intra-arterial x-ray angiography provides only anatomical information and does not evaluate the hemodynamic consequences of stenosis. Results of tests that provide functional information may be incorrectly judged false-negative when a moderate but hemodynamically insignificant stenosis is seen on intra-arterial angiography. The specificity of functional tests may have been underestimated compared with the specificity of anatomical tests.

As an alternative, the blood pressure response to a revascularization procedure has been proposed as the gold standard. However, as described elsewhere by Mann and Pickering (6), incorrect interpretation is still possible. In a small minority

of captopril renal scintigraphy studies (52, 55, 56, 58), researchers attempted to evaluate the sensitivity and specificity of captopril renal scintigraphy with blood pressure response to intervention as the gold standard. Sensitivity ranged from 58% to 95%, and specificity ranged from 17% to 100%. The results of these analyses, however, pertained to highly selected subgroups of patients, namely those who had had an intervention, and the decision to intervene was based on positive results on angiography. Therefore, these results are difficult to interpret.

Second, most MRA and CTA studies used arteries as the unit of analysis, while most captopril renal scintigraphy studies used patients. This difference in analysis might have led to overestimation of the specificity of CTA and MRA compared with captopril renal scintigraphy. For example, if 10 patients (with 20 renal arteries) were studied and MRA yielded a false-positive result for 2 arteries in separate patients, the false-positive rate for arteries would be 10% (2 of 20) with a test specificity of 90%, whereas the false-positive rate for patients would be 2 of 10 (20%) with a test specificity of only 80%. Therefore, it is recommended that future studies perform by-patient analyses as well by-artery analyses (if possible) in order to improve comparability of studies.

Our meta-analysis indicates that CTA and gadolinium-enhanced MRA are superior to the other studied diagnostic tests for the detection of renal artery stenosis. Careful selection based on clinical evaluation, which can increase the pre-test probability to 20% to 40%, is a prerequisite for cost-effective use of these tests in the work-up strategy for patients with possible renovascular hypertension. Because only a limited number of published studies on CTA and gadolinium-enhanced MRA could be included in our meta-analysis, further research is recommended.

Appendix

In a conventional ROC curve, the true-positive rate is plotted against the corresponding false-positive rate. As described by Irwig and co-workers (8) and Moses and associates (9), a summary ROC curve can be constructed by converting each true-positive rate and false-positive rate to its logistic transform. For each study, the following variables were calculated:

$$D = \text{logit (true positive rate)} - \text{logit (false positive rate)}$$
$$S = \text{logit (true positive rate)} + \text{logit (false positive rate)}$$

where D represents the natural logarithm of the diagnostic odds ratio (and is therefore a measure of discriminatory power of the test) and S is a function of test threshold.

Next, the relationship between D and S can be estimated by the linear regression model:

$$D = a + b0*S$$

The regression coefficient for S determines the asymmetry of the summary ROC curves. If the coefficient equals zero, the curve is symmetrical (65).
For our study, we extended this model by adding five dummy variables representing the tests, which were compared with a reference test. Because the largest number of studies was available for ultrasonography, ultrasonography was used as the reference test.

$$D = a + b0*S + b1*\text{test 1} + b2*\text{test 2} + b3*\text{test 3} + b4*\text{test 4} + b5*\text{test 5}$$

After we fitted this model to the data, the intercept and regression coefficients were estimated. The regression coefficient for S was small (0.02) and not statistically significant ($P > 0.2$); therefore, this term was omitted from the model.
The intercept defines the odds ratio of the reference test and the regression coefficients of the other terms in the model added to the intercept define the odds ratios of the comparative diagnostic modalities. We determined the areas under the summary ROC curve by integrating algebraically the functions, as defined by the odds ratios, corresponding with the different tests. In this way, differences between areas under the summary ROC curve were calculated. We derived the 95% CIs by using the delta method (66).

References

1. Derkx FH, Schalekamp MA. Renal artery stenosis and hypertension. Lancet. 1994;344:237-9.
2. Eardley KS, Lipkin GW. Atherosclerotic renal artery stenosis: is it worth diagnosing? J Hum Hypertens. 1999;13:217-20.
3. Working Group on Renovascular Hypertension. Detection, evaluation, and treatment of renovascular hypertension. Final report. Arch Intern Med. 1987;147:820-9.
4. van Jaarsveld BC, Krijnen P, Pieterman H, Derkx FH, Deinum J, Postma CT, et al. The effect of balloon angioplasty on hypertension in atherosclerotic renal-artery stenosis. N Engl J Med. 2000;342(14):1007-14.
5. Dunnick NR, Sfakianakis GN. Screening for renovascular hypertension. Radiol Clin North Am. 1991;29:497-510.
6. Mann SJ, Pickering TG. Detection of renovascular hypertension. State of the art: 1992. Ann Intern Med. 1992;117:845-53.
7. Pedersen EB, Egeblad M, Jorgensen J, Nielsen SS, Spencer ES, Rehling M. Diagnosing renal artery stenosis: a comparison between conventional renography, captopril renography and ultrasound Doppler in a large consecutive series of patients with arterial hypertension. Blood Press. 1996;5:342-8.
8. Irwig L, Tosteson AN, Gatsonis C, Lau J, Colditz G, Chalmers TC, et al. Guidelines for meta-analyses evaluating diagnostic tests. Ann Intern Med. 1994;120:667-76.
9. Moses LE, Shapiro D, Littenberg B. Combining independent studies of a diagnostic test into a summary ROC curve: data-analytic approaches and some additional considerations. Stat Med. 1993;12:1293-316.
10. Equine O, Beregi JP, Mounier-Vehier C, Gautier C, Desmoucelles F, Carre A. [Importance of the echo-doppler and helical angioscanner of the renal arteries in the management of renovascular diseases. Results of a retrospective study in 113 patients]. Arch Mal Coeur Vaiss. 1999;92:1043-5.
11. Galanski M, Prokop M, Chavan A, Schaefer C, Jandeleit K, Olbricht C. [Accuracy of CT angiography in the diagnosis of renal artery stenosis]. Rofo Fortschr Geb Rontgenstr Neuen Bildgeb Verfahr. 1994;161:519-25.
12. Kaatee R, Beek FJ, de Lange EE, van Leeuwen MS, Smits HF, van der Ven PJ, et al. Renal artery stenosis: detection and quantification with spiral CT angiography versus optimized digital subtraction angiography. Radiology. 1997;205:121-7.
13. Olbricht CJ, Paul K, Prokop M, Chavan A, Schaefer-Prokop CM, Jandeleit K, et al. Minimally invasive diagnosis of renal artery stenosis by spiral computed tomography angiography. Kidney Int. 1995;48:1332-7.
14. Wittenberg G, Kenn W, Tschammler A, Sandstede J, Hahn D. Spiral CT angiography of renal arteries: comparison with angiography. Eur Radiol. 1999;9:546-51.
15. Arlart IP, Guhl L, Hausmann R. [The evaluation of 2D- and 3D-"time of flight" magnetic resonance angiography (MRA) in the diagnosis of renal artery stenoses]. Rofo Fortschr Geb Rontgenstr Neuen Bildgeb Verfahr. 1992;157:59-64.
16. Bongers V, Bakker J, Beutler JJ, Beek FJ, De Klerk JM. Assessment of renal artery stenosis: comparison of captopril renography and gadolinium-enhanced breath-hold MR angiography. Clin Radiol. 2000;55:346-53.
17. Borrello JA, Li D, Vesely TM, Vining EP, Brown JJ, Haacke EM. Renal arteries: clinical comparison of three-dimensional time-of-flight MR angiographic sequences and radiographic angiography. Radiology. 1995;197:793-9.

18. De Cobelli F, Venturini M, Vanzulli A, Sironi S, Salvioni M, Angeli E, et al. Renal arterial stenosis: prospective comparison of color doppler US and breath-hold, three-dimensional, dynamic, gadolinium-enhanced MR angiography. Radiology. 2000;214:373-80.
19. De Cobelli F, Mellone R, Salvioni M, Vanzulli A, Sironi S, Manunta P, et al. Renal artery stenosis: value of screening with three-dimensional phase-contrast MR angiography with a phased-array multicoil. Radiology. 1996;201:697-703.
20. De Haan MW, Kouwenhoven M, Thelissen RP, Koster D, Kessels AG, de Leeuw PW, et al. Renovascular disease in patients with hypertension: detection with systolic and diastolic gating in three-dimensional, phase-contrast MR angiography. Radiology. 1996;198:449-56.
21. Fellner C, Strotzer M, Geissler A, Kohler SM, Kramer BK, Spies V, et al. Renal arteries: evaluation with optimized 2D and 3D time-of-flight MR angiography. Radiology. 1995;196: 681-7.
22. Korst MB, Joosten FB, Postma CT, Jager GJ, Krabbe JK, Barentsz JO. Accuracy of normal-dose contrast enhanced MR angiography in assessing renal artery stenosis and accessory renal arteries. AJR Am J Roentgenol. 2000;174:629.-34.
23. Laissy JP, Benyounes M, Limot O, Cinqualbre A, Benamer H, Kenouch S, et al. Screening of renal artery stenosis: assessment with magnetic resonance angiography at 1.0 T. Magn Reson Imaging. 1996;14:1033-41.
24. Leung DA, Pelkonen P, Hany TF, Zimmermann G, Pfammatter T, Debatin JF. Value of image subtraction in 3D gadolinium-enhanced MR angiography of the renal arteries. J Magn Reson Imaging. 1998;8:598-602.
25. Loubeyre P, Trolliet P, Cahen R, Grozel F, Labeeuw M, Minh VA. MR angiography of renal artery stenosis: value of the combination of three-dimensional time-of-flight and three-dimensional phase-contrast MR angiography sequences. AJR Am J Roentgenol. 1996;167: 489-94.
26. Postma CT, Joosten FB, Rosenbusch G, Thien T. Magnetic resonance angiography has a high reliability in the detection of renal artery stenosis. Am J Hypertens. 1997;10:957-63.
27. Rieumont MJ, Kaufman JA, Geller SC, Yucel EK, Cambria RP, Fang LS, et al. Evaluation of renal artery stenosis with dynamic gadolinium-enhanced MR angiography. AJR Am J Roentgenol. 1997;169:39-44.
28. Smith HJ, Bakke SJ. MR angiography of in situ and transplanted renal arteries. Early experience using a three-dimensional time-of-flight technique. Acta Radiol. 1993;34:150-5.
29. Strotzer M, Fellner CM, Geissler A, Gmeinwieser J, Kohler SM, Kramer BK, et al. Noninvasive assessment of renal artery stenosis. A comparison of MR angiography, color Doppler sonography, and intraarterial angiography. Acta Radiol. 1995;36:243-7.
30. Thornton J, O'Callaghan J, Walshe J, O'Brien E, Varghese JC, Lee MJ. Comparison of digital subtraction angiography with gadolinium-enhanced magnetic resonance angiography in the diagnosis of renal artery stenosis. Eur Radiol. 1999;9:930-4.
31. Bardelli M, Jensen G, Volkmann R, Aurell M. Non-invasive ultrasound assessment of renal artery stenosis by means of the Gosling pulsatility index. J Hypertens. 1992;10:985-9.
32. Baxter GM, Aitchison F, Sheppard D, Moss JG, McLeod MJ, Harden PN, et al. Colour Doppler ultrasound in renal artery stenosis: intrarenal waveform analysis. Br J Radiol. 1996;69:810-5.
33. Breitenseher M, Kainberger F, Hubsch P, Trattnig S, Baldt M, Barton P, et al. [The screening of renal artery stenoses. The initial results with the value of color Doppler sonography]. Rofo Fortschr Geb Rontgenstr Neuen Bildgeb Verfahr. 1992;156:228-31.
34. Claudon M, Plouin PF, Baxter GM, Rohban T, Devos DM. Renal arteries in patients at risk of renal arterial stenosis: multicenter evaluation of the echo-enhancer SH U 508A at color and spectral Doppler US. Levovist Renal Artery Stenosis Study Group. Radiology 2000;214:739-46.

35. Dondi M, Fanti S, Barozzi L, De Fabritiis A, Losinno F, Pavlica P, et al. Evaluation by captopril renal scintigraphy and echo-Doppler flowmetry of hypertensive patients at high risk for renal artery stenosis. J Nucl Biol Med. 1992;36:309-14.
36. Handa N, Fukanaga R, Ogawa S, Matsumoto M, Kimura K, Kamada T. A new accurate and non-invasive screening method for renovascular hypertension: the renal artery Doppler technique. J Hypertens Suppl. 1988;6:S458-S460.
37. Kaplan-Pavlovcic S, Nadja C. Captopril renography and duplex Doppler sonography in the diagnosis of renovascular hypertension. Nephrol Dial Transplant. 1998;13:313-7.
38. Karasch T, Strauss AL, Grun B, Worringer M, Neuerburg-Heusler D, Roth FJ, et al. [Color-coded duplex ultrasonography in the diagnosis of renal artery stenosis]. Dtsch Med Wochenschr. 1993;118:1429-36.
39. Kliewer MA, Tupler RH, Carroll BA, Paine SS, Kriegshauser JS, Hertzberg BS, et al. Renal artery stenosis: analysis of Doppler waveform parameters and tardus-parvus pattern. Radiology. 1993;189:779-87.
40. Lucas P, Blome S, Roche J. Intra-renal Doppler wave-form analysis as a screening test for renal artery stenosis. Australas Radiol. 1996;40:276-82.
41. Miralles M, Santiso A, Gimenez A, Riambau V, Saez A, Daumal J, et al. Renal duplex scanning: correlation with angiography and isotopic renography. Eur J Vasc Surg. 1993;7:188-94.
42. Miralles M, Cairols M, Cotillas J, Gimenez A, Santiso A. Value of Doppler parameters in the diagnosis of renal artery stenosis. J Vasc Surg. 1996;23:428-35.
43. Olin JW, Piedmonte MR, Young JR, DeAnna S, Grubb M, Childs MB. The utility of duplex ultrasound scanning of the renal arteries for diagnosing significant renal artery stenosis. Ann Intern Med. 1995;122:833-8.
44. Oliva VL, Soulez G, Lesage D, Nicolet V, Roy MC, Courteau M, et al. Detection of renal artery stenosis with Doppler sonography before and after administration of captopril: value of early systolic rise. AJR Am J Roentgenol. 1998;170:169-75.
45. Postma CT, van Aalen J, de Boo T, Rosenbusch G, Thien T. Doppler ultrasound scanning in the detection of renal artery stenosis in hypertensive patients. Br J Radiol. 1992;65:857-60.
46. Postma CT, Bijlstra PJ, Rosenbusch G, Thien T. Pattern recognition of loss of early systolic peak by Doppler ultrasound has a low sensitivity for the detection of renal artery stenosis. J Hum Hypertens. 1996;10:181-4.
47. Spies KP, Fobbe F, El-Bedewi M, Wolf KJ, Distler A, Schulte KL. Color-coded duplex sonography for noninvasive diagnosis and grading of renal artery stenosis. Am J Hypertens. 1995;8:1222-31.
48. Strunk H, Jaeger U. [Duplex ultrasonographic diagnosis of renal artery stenosis by intrarenal acceleration determination and recognition of the tardus- parvus phenomenon with special regard to multiple renal arteries]. Rofo Fortschr Geb Rontgenstr Neuen Bildgeb Verfahr. 1995;162:420-8.
49. Vigna C, Pacilli MA, Testa M, Langialonga T, Salvatori MP, Lanna P, et al. Comparison of steerable continuous-wave versus pulsed-wave Doppler ultrasonography to renal artery angiography in diagnosing renal artery stenosis. Am J Cardiol. 1998;81:365-7.
50. Zoller WG, Hermans H, Bogner JR, Hahn D, Middeke M. Duplex sonography in the diagnosis of renovascular hypertension. Klin Wochenschr. 1990;68:830-4.
51. Dondi M, Levorato M, Corbelli C, Zagni P, Zuccala A, Gaggi R, et al. Detection of renal artery stenosis by means of captopril renography with 99mTc-DTPA. Contrib Nephrol 1990;79:181-5.
52. Fommei E, Ghione S, Hilson AJ, Mezzasalma L, Oei HY, Piepsz A, et al. Captopril radionuclide test in renovascular hypertension: a European multicentre study. European Multicentre Study Group. Eur J Nucl Med 1993;20(7):617-233.

53. Gezici A, Ersay A, Antevska E, Heidental GK, Schreij G, Demirtas OC. Quantitative residual cortical activity measurement: appropriate test for diagnosis of renal artery stenosis? Urol Int. 1999;62:1-7.
54. Kahn D, Ben-Haim S, Bushnell DL, Madsen MT, Kirchner PT. Captopril-enhanced 99Tcm-MAG3 renal scintigraphy in subjects with suspected renovascular hypertension. Nucl Med Commun. 1994;15:515-28.
55. Mann SJ, Pickering TG, Sos TA, Uzzo RG, Sarkar S, Friend K, et al. Captopril renography in the diagnosis of renal artery stenosis: accuracy and limitations. Am J Med. 1991;90: 30-40.
56. Mittal BR, Kumar P, Arora P, Kher V, Singhal MK, Maini A, et al. Role of captopril renography in the diagnosis of renovascular hypertension. Am J Kidney Dis. 1996;28:209-13.
57. Nitzsche E, Grosser G, Rump C, Strauss E, Meyer E, Keller E, et al. [Captopril-renal function scintigraphy in the clarification of arterial hypertension]. Radiologe. 1991;31:141-6.
58. Setaro JF, Chen CC, Hoffer PB, Black HR. Captopril renography in the diagnosis of renal artery stenosis and the prediction of improvement with revascularization. The Yale Vascular Center experience. Am J Hypertens. 1991;4:698S-705S.
59. Svetkey LP, Wilkinson Jr R, Dunnick NR, Smith SR, Dunham CB, Lambert M, et al. Captopril renography in the diagnosis of renovascular disease. Am J Hypertens 1991;4: 711S-715S.
60. Tremel F, Caravel JP, Siche JP, Chevallier M, Mallion JM. [Diagnostic value of renal scintigraphy with MAG 3 and DTPA in the diagnosis of renal artery stenosis]. Arch Mal Coeur Vaiss. 1996;89:1035-9.
61. Postma CT, van der Steen PH, Hoefnagels WH, de Boo T, Thien T. The captopril test in the detection of renovascular disease in hypertensive patients. Arch Intern Med. 1990;150: 625-8.
62. Schreij G, van Es PN, Schiffers PM, Lavrijssen AT, de Leeuw PW. 'Captopril test', with blood pressure and peripheral renin as response variables in hypertensive patients with suspected renal artery stenosis. J Hum Hypertens. 1995;9:741-6.
63. Stephan D, Welsch M, Decker N, Brule JM, Jahn C, Grima M, et al. [Captopril test for detecting renal artery stenosis: changes in plasma renin concentration]. Arch Mal Coeur Vaiss. 1993;86:1249-52.
64. Halpern EJ, Rutter CM, Gardiner GAJ, Nazarian LN, Wechsler RJ, Levin DB, et al. Comparison of Doppler US and CT angiography for evaluation of renal artery stenosis. Acad Radiol. 1998;5:524-32.
65. Kester AD, Buntinx F. Meta-analysis of ROC curves. Med Decis Making 2000;20(4):430-9.
66. Efron B, Tibshirani RJ. An introduction to the bootstrap. New York: Chapman & Hall; 1993: 313-5.

Computed tomographic angiography and magnetic resonance angiography for the diagnosis of renal artery stenosis: a comparative study with digital subtraction angiography.

Results of the Renal Artery Diagnostic Imaging Study In Hypertension (RADISH).

Submitted for publication.

G.B.C. Vasbinder, P.J. Nelemans, A.G.H. Kessels, A.A. Kroon, J.H. Maki, T. Leiner, F.J.A. Beek, M.B.J.M. Korst, K. Flobbe, M.W. de Haan, W.H. van Zwam, C.T. Postma, M.G.M. Hunink, P.W. de Leeuw, J.M.A. van Engelshoven, for the Renal Artery Diagnostic Imaging Study in Hypertension (RADISH) study group*.

*The names of the other investigators and research coordinators who participated in the RADISH study are listed in the Appendix.

Abstract

Context
Timely detection of renal artery stenosis is important as it may cause a potentially curable form of hypertension and renal impairment.

Objective
To determine the validity of computed tomographic angiography (CTA) and magnetic resonance angiography (MRA) as compared to the reference standard digital subtraction angiography (DSA) for the detection of renal artery stenosis in patients suspected of having renovascular hypertension.

Design
Prospective multicenter comparative study between CTA, MRA, and DSA, conducted from 1998 to 2001. Two panels of three observers each judged the CTA and MRA exams, blinded to all other results. Four vascular radiologists judged the DSA exams.

Setting
Three large teaching hospitals and three university hospitals in the Netherlands.

Patients
A total of 402 hypertensive patients between 18 and 75 years of age with one or more clinical clues suggestive for the presence of renal artery stenosis were included. A group of 356 patients who underwent all three diagnostic modalities was used for analysis.

Main outcome measures
Reproducibility was assessed by calculating interobserver agreement using linear weighted kappa statistics. Diagnostic accuracy was evaluated in terms of sensitivity, specificity, likelihood ratios, and other diagnostic parameters. Atherosclerotic stenoses of 50% or greater, as well as all cases of fibromuscular dysplasia, were considered clinically relevant.

Results
The prevalence of clinically relevant renal artery stenosis was 20%. For the detection of renal artery stenosis, moderate interobserver agreement was found with kappa values ranging from 0.59 to 0.64 for CTA and 0.40 to 0.51 for MRA. Overall, sensitivity ranged from 61% to 69% for CTA and 57% to 67% for MRA. Specificity ranged from 89% to 97% for CTA and 77% to 90% for MRA. Additional analyses revealed that selecting a subgroup of patients with a high prevalence of renal artery stenosis could substantially increase the diagnostic accuracy of both tests, but sensitivity remained below 90%.

Conclusion
At present, both CTA and MRA are not reproducible or sensitive enough to rule out renal artery stenosis in a population of hypertensive patients with clinical clues suggestive for the presence of renal artery stenosis. Therefore, DSA remains the method of choice in the detection of renal artery stenosis.

Introduction

Renal artery stenosis may cause renovascular hypertension and renal impairment. Timely detection and treatment of clinically relevant stenoses may result in cure or improvement of hypertension and preservation of renal function. Current treatment options include surgery, percutaneous transluminal renal angioplasty with or without stent placement, or medical therapy. Despite the availability of several other diagnostic tests, intra-arterial digital subtraction angiography (DSA) is still the reference standard for making the anatomical diagnosis of renal artery stenosis. DSA, however, is an invasive procedure that carries a non-negligible risk for serious complications and is burdensome for patients (1,2). For this reason, less invasive diagnostic alternatives for DSA such as computed tomographic angiography (CTA) and three-dimensional contrast-enhanced magnetic resonance angiography (MRA) are widely used for the diagnostic workup in patients suspected of having renal artery stenosis.

In a recent meta-analysis, it was shown that CTA and MRA are significantly better than non contrast-enhanced magnetic resonance angiographic techniques, ultrasonography, captopril renal scintigraphy, and the captopril test in identifying the presence of renal artery stenosis when using DSA as the reference standard (3). To date, however, only a limited number of small, well-designed studies have been published on the diagnostic accuracy of either CTA or MRA for the detection of renal artery stenosis in patients suspected of renovascular hypertension (4, 5, 6, 7, 8, 9, 10, 11, 12, 13, 14).

Because CTA and MRA seemed promising techniques with the potential to reduce the number of patients requiring conventional angiography, we set up a large scale multicenter study to investigate the diagnostic performance of CTA and MRA (using DSA as reference standard) in hypertensive patients clinically deemed at risk for renal artery stenosis. Purpose of this study was to determine the interobserver agreement and diagnostic accuracy of CTA and MRA in comparison with DSA and to explore whether CTA or MRA can be used as initial test for the detection of renal artery stenosis.

Methods

We performed a prospective comparative study between CTA, MRA, and the reference standard DSA for the detection of renal artery stenosis. Accordingly, each patient included was subjected to all three diagnostic modalities.

Subjects

Over a three-year period, subjects were prospectively recruited from the Internal Medicine outpatient clinics of three large teaching hospitals and three university hospitals in the Netherlands. At the two hospitals that recruited the great majority of participating patients enrollment was consecutive, while the other participating hospitals included patients arbitrarily. The ethical review board of each hospital approved of the study, and written informed consent was obtained from all subjects. All hypertensive patients between 18 and 75 years of age with diastolic blood pressure of >95 mm Hg were eligible for participation if, in addition, they exhibited

Table 1. Frequency of Inclusion Criteria for the 356 subjects with all three tests

Inclusion Criterion*	No	(%)
Subcostal bruit present†	14	(4)
Malignant hypertension†	20	(6)
Accelerated hypertension†	49	(14)
Hypertensive retinopathy grade III or IV†	22	(6)
Sudden development or worsening of hypertension†	23	(7)
Signs of atherosclerosis		
-in 1 vascular region	25	(7)
- in 2 or more vascular regions	42	(12)
Unexplained worsening of renal function†	38	(11)
(increase of serum creatinine >20 μmol/l within 12 months)		
Hypertension refractory to appropriate 2-drug regimen	188	(53)
Combination of age <30 years or >60 years old and DBP >110 mmHg	34	(10)
Combination of smoking and		
-DBP >95 to 110 mmHg	25	(7)
-DBP >110 mmHg	41	(12)
Impairment of renal function in response to ACE-inhibition†	20	(6)
Suspicion of restenosis following successful intervention	5	(1)
Unilateral small kidney discovered by ultrasonography†	7	(2)
(>10% difference in right and left kidney length)		
Raised serum cholesterol concentration (>7mmol/l)	15	(4)
Lowered serum potassium concentration (<3.6 mmol/l)	3	(1)
(not associated with diuretics)		
Presence of left ventricular hypertrophy	172	(48)
Captopril renography suggesting renal artery stenosis	2	(1)

*In addition to the presence of hypertension, patients also had to fulfill at least one inclusion criterion in order to participate in the study.
The fact that subjects could meet more than one criterion explains that the sum of each column exceeds the total number of included subjects.
† Clinical clues as defined by the Working Group on Renovascular Hypertension (15).

at least one of the clinical clues for the presence of renal artery stenosis (Table 1)(15, 16, 17). Exclusion criteria were: known allergy to iodinated contrast-agents; pregnancy; contra-indications to MRA, CTA, or DSA (18, 19); contra-indications for intervention; and previous participation in the study. All included patients were scheduled to have CTA, MRA and DSA within a three-month window. The case record forms for all patients were collected at the coordinating center (Maastricht University Hospital) and all data were entered in a database.

Imaging techniques

Each participating hospital was equipped with state-of-the art MR scanners (1.0 or 1.5 Tesla), helical CT scanners (single or multiple detector-row systems), and DSA equipment. Due to the variety of manufacturers and models of imaging equipment,

each hospital was allowed to use the scan protocols, which it considered optimal. Also, hospitals were allowed to change scan protocols during the study when new insights emerged or in case of equipment upgrades. Information about manufacturers, scan protocols, and contrast agents is presented in the Appendix. All imaging was either performed or supervised by experienced radiologists and radiological technologists. Renal CTA, MRA and DSA had already been part of clinical routine prior to the start of the study.

Image evaluation

At the conclusion of the study enrollment, two panels of three observers evaluated the CTA exams (GBCV, FJAB, WHVZ) and the MRA exams (JHM, TL, MBJMK) at the coordinating center. All observers had more than three years of experience evaluating such data at a regular basis, and for each modality one observer had more than six years of experience. The evaluations were independently performed by each observer, which were blinded to all other results including clinical information. Digital image data of all CTA and MRA exams were evaluated using a workstation equipped with all commonly used post-processing modalities (EasyVision, release 4.2.1, Philips Medical Systems, Best, the Netherlands). An electronic caliper with 0.1 mm accuracy was available for measurements. The observers were allowed to use any desired post-processing technique, but source images had to be examined in all cases before a final diagnosis could be made.

The DSA exams were evaluated by four vascular radiologists, all with more than ten years experience in this particular field. The first observer was the radiologist who actually performed the DSA and evaluation took place during the DSA procedure. The second and third observer judged each DSA exam, having knowledge of the first observer's judgment. In case discrepancies existed with respect to the number of renal arteries or the nature, location, and severity of pathology (differences of >10% in the degree of stenosis), a fourth radiologist (who had access to the diagnoses of the other observers) made the final diagnosis.

To determine the degree of stenosis, the diameter of the most severely affected part of a renal artery was measured and related to the reference diameter, which was defined as the diameter of the non-affected portion of the artery immediately distal to the stenosis (i.e. beyond the site of post-stenotic dilatation (if present)). In instances where no representative distal renal artery segment was available, the diameter of the non-involved portion of the artery proximal to the stenosis, or a corresponding segment of a comparable contralateral renal artery was measured instead, with a preference for the former. Finally, the degree of stenosis was calculated by the following formula: (1-(diameter of stenosis/reference diameter))*100%. For CTA, MRA, and DSA luminal narrowing of ≥50% as well as all cases of fibromuscular dysplasia were defined as clinically relevant renal artery stenosis. The rationale for choosing these thresholds is the fact that patients with either ≥50% luminal narrowing (equals ≥75% of vessel area reduction) or FMD are generally considered to benefit most from revascularization procedures with respect to blood pressure and renal impairment (6, 20). Therefore, these thresholds are used in the majority of current literature (3).

For each subject, the observers first recorded the number of renal arteries. Subsequently, the renal arteries were divided into two parts. The first part begins

at the aortic ostium and ends 1 mm distally from the outer aortic wall (for CTA) or 4 mm distally from the aortic ostium (for MRA and DSA); this part is referred to as the 'origin' (21). The second part, compromising the remainder of the renal artery, is referred to as the 'truncus'. Both parts were judged with respect to the presence or absence of a stenosis (expressed as percentage of luminal narrowing), as well as the nature of the stenosis (atherosclerotic or fibromuscular dysplasia). In addition, the observers noted the level of confidence in the diagnosis on a 3-point scale: (high (1), moderate (2), and poor (3). In cases where an exam was considered non-diagnostic, this was noted on the standardized form that was used to collect all relevant data.

Statistical analysis

The severity of the stenoses as seen on CTA and MRA was categorized on a five point scale (0% to 19% (grade 1); 20% to 49% (grade 2); 50% to 74% or fibromuscular dysplasia (grade 3); 75% to 99% (grade 4); and total occlusion (100% stenosis; grade 5)). Reproducibility was evaluated by determining interobserver agreement for CTA and MRA images, which was calculated using the linear weighted kappa statistic. Unless stated differently, all analyses on the diagnostic accuracy (sensitivity, specificity, and ROC analysis) of CTA and MRA as compared to DSA reported in the text and tables are based on patients as unit of analysis. The most severe stenosis per patient was used for analysis. In case an observer judged a CTA or MRA exam to be non-diagnostic, this exam was considered as a positive test result in the analyses. This approach was chosen since (in a clinical setting) patients with non-diagnostic test results will most likely be referred to DSA. Receiver-operating characteristics (ROC) curves, areas under the ROC curves and their standard errors were obtained assuming a nonparametric distribution. For the construction of ROC curves, the five-point scale for the severity of stenosis was used. Differences between areas under the ROC curves were calculated taking into account the paired nature of the data (22). P-values <0.05 were considered statistically significant. Ninety-five percent confidence interval (CI) limits were calculated using a binomial distribution.

Subgroup analyses were either defined based on clinical characteristics or stepwise logistic regression analyses.

Results

Between October 28th, 1998, and October 30th, 2001, a total of 402 patients met the inclusion criteria and were included in the study. The distribution of the subjects across the participating hospitals is shown in the Appendix. For reasons described in Table 2, 46 patients were excluded from the analyses because they did not undergo all three diagnostic tests. Claustrophobia prior or during MRA was the most frequent cause for non-completion. Thus, for a total of 356 subjects the results of CTA, MRA, and the reference standard DSA were available. The median time interval between DSA and the index tests CTA and MRA was 1 day (range from 1 to 60 days).

The distribution of the inclusion criteria for these patients is shown in Table 1. Refractory hypertension and the presence of target organ damage were the most frequently used criteria for inclusion. The distribution of clinical characteristics of the 356 patients is shown in Table 3. There were no statistically significant differences between the characteristics of the 356 patients included in the analysis and the 46

Table 2. Reasons for not undergoing or completing exams of one or more of the three studied modalities (n=46 patients)*

	CTA	MRA	DSA
Death†	0	0	1
Allergic reaction to iodinated contrast agent or gadolinium	0	2	1
Extravasation of contrast agent	1	0	0
Claustrophobia before or during CTA or MRA	1	17	0
Withdrawal from participation in the study‡	4	3	4
Lost to follow-up	3	4	4
Miscellaneous§	5	7	5
Unknown	3	1	0

*The numbers in columns represent exams. Since patients could miss more than one exam due to one specific reason, the sum of not performed or incomplete exams exceeds the number of patients.
†Only death which occurred from the time of inclusion to 30 days after the last diagnostic test are reported.
‡Reasons for withdrawal from participation in the study were unrelated to complications to one of the studied tests. Informed consent was not withdrawn.
§ In this group two serious adverse events occurred; one patient had a stroke prior to undergoing any of the studied tests; another patient had dissection of the left renal artery during DSA (selective cathererization) which resulted in nephrectomy. All other patients in this group did not undergo one or more tests either due to physical inability (for instance too big, unable to sustain supine position for over 5 minutes), or psychological inability (fear for needles).

patients who were excluded. In the patients who underwent all three tests, DSA showed clinically relevant renal artery stenoses in 72 patients (96 kidneys), resulting in an overall prevalence of 20%. Twenty-seven patients (38% of all patients with renal artery stenosis) had fibromuscular dysplasia (Table 3). Bilateral significant atherosclerotic renal artery stenosis was present in 12 patients (17% of all patients with renal artery stenosis), while bilateral fibromuscular dysplasia was seen in 11 patients (15%). One patient (1%) had fibromuscular dysplasia and atherosclerotic renal artery stenosis. Of the 58 kidneys demonstrating atherosclerotic renal artery stenosis, the location of pathology was ostial in 35 (60%) and truncal in 23 (40%). Supernumerary renal arteries were seen in 140 out of the 356 patients (39%).

Diagnostic performance

The number of non-diagnostic exams ranged from 0 to 2 for the various CTA observers, while all three MRA observers judged one exam (of the same patient) as such. Linear weighted kappa values indicating the interobserver agreement for the observers ranged from 0.59 to 0.64 for CTA and 0.40 to 0.51 for MRA. For each observer, diagnostic parameters including the positive and negative predictive value for a prevalence of 20% are shown in Table 4. For the CTA and MRA observers with the best diagnostic performance (defined as the highest area under the ROC curve) sensitivities were 69% for CTA observer A and 57% for MRA observer F (95% CI limits: 57% to 80% and 45% to 69%, respectively). The corresponding specificities

Table 4. Demographic, clinical, and ia-DSA characteristics of the 356 included patients with all three tests

Characteristic	No.*	Result
Female sex - no. (%)	356	169 (48)
Age - yr	356	
Mean±SD		52±12
Range		20-75
Systolic blood-pressure at baseline† - mmHg	356	
Mean±SD		183±25
Range		128-280
Diastolic blood-pressure at baseline† - mmHg	356	
Mean±SD		107±15
Range		40-170
Years with known hypertension‡	348	
Mean±SD		8±9
Range		0-43
Smoking habit	353	
Smoker - no. (%)		121 (34.3)
Body mass index	347	
Mean±SD		28±5
Range		17-46
Creatinine (µmol/liter)	356	
Mean±SD		105±44
Range		51-476
Cholesterol (mmol/liter)	349	
Mean±SD		5.7±1.1
Range		2.4-9.1
Fundoscopy	135	
No retinopathy - no. (%)		19 (14)
Grade I & II - no. (%)		94 (70)
Grade III & IV- no (%)		22 (16)
ECG	311	
Left ventricular hypertrophy - no. (%)		172 (55)
Time interval between CTA and DSA - days		
Median - days		1
Range - days		1 - 62
Time interval between MRA and DSA - days		
Median - days		1
Range - days		1 - 62
Intra-arterial DSA	356	
Renal artery stenosis - no. (% of all patients)		72 (20)
-Atherosclerotic RAS - no. (% of all RAS)		45 (63)
-Fibromuscular dysplasia - no. (% of all RAS)		26 (36)
-Both atherosclerotic RAS and FMD - no (% of all RAS)		1 (1)
Distribution of pathology on DSA (five point scale)		
-Grade I (0 - 19% stenosis) - no. (% of all patients)		249 (70)
-Grade II (20 - 49% stenosis) - no. (% of all patients)		35 (10)
-Grade III (50 - 74% stenosis and all FMD) - no. (% of all patients)		49 (14)
-Grade IV (75 - 99% stenosis) - no. (% of all patients)		10 (3)
-Grade V (occlusion) - no. (% of all patients)		13 (4)

RAS= renal-artery stenosis. FMD= fibromuscular dysplasia

*Clinical data or test results were not available for all patients. The number of patients mentioned in the columns may represent a subgroup; calculations provided for a particular characteristic (as well as percentages) are based on this subgroup of patients.

† All patients were included based on mean outpatient diastolic blood pressure of >95 mm Hg. Blood pressures presented here were measured under resting conditions in the hospital.

‡ Criteria for hypertension at the time of initial diagnosis may differ from the criteria currently used.

Table 4a: Overall diagnostic accuracy and areas under the ROC curves for all observers.

Test	CTA	CTA	CTA	MRA	MRA	MRA
Observer	A	B	C	D	E	F
Sensitivity (%)	69	61	61	67	63	57
Specificity (%)	91	89	97	77	84	90
Positive predictive value (%)	67	59	83	42	50	59
Negative predictive value (%)	92	90	91	90	90	89
Likelihood ratio for positive test result	7.9	5.8	19.1	2.9	4.0	5.6
Likelihood ratio for negative test result	0.3	0.4	0.4	0.4	0.4	0.5
Area under the ROC curve	0.84*	0.76†	0.84*	0.75	0.76	0.81

*Areas under the ROC curves for CTA observer A and CTA observer C were 0.843 and 0.836, respectively. Therefore, CTA observer A is considered the best CTA observer.
†Area under the ROC curve of CTA observer B is statistically significant lower than the areas under the ROC curves of CTA observers A and C (p=0.03 and p=0.05, respectively).

were 91% (95% CI limits: 87% to 94%) and 90% (95% CI limits: 86% to 93%), respectively. Figure 1 shows ROC curves for CTA observer A (AUC=0.84; 95% CI limits: 0.78 to 0.90) and MRA observer F (AUC=0.81; 95% CI limits: 0.74 to 0.87). No statistically significant difference between the areas under the ROC curves was found (p=0.41).

Additionally, Table 5 shows the results of analyses performed to explore whether diagnostic performance of CTA and MRA improved when studying subgroups of patients or using different approaches for data analysis. The selection of subgroups of patients with a high pre-test likelihood of renal artery stenosis resulted in the most substantial rise in diagnostic accuracy of both tests.

Discussion

This study is the largest prospective study comparing the diagnostic performance of CTA and MRA with DSA. Our results show that both CTA and MRA have a poor sensitivity but an adequate specificity for detecting renal artery stenoses. These findings are contrary to the results of nearly all other published studies on the validity of CTA and MRA, which report high estimates for both sensitivity and specificity (up to 100%) (3). As a consequence of the favorable results in the literature, both CTA and MRA are widely used in clinical routine practice to rule out renal artery disease in hypertensive patients. Based upon our results, this strategy needs to be reconsidered. Before doing so, however, we must consider potential causes of error in both our study and the other studies in the literature in order to find an explanation for the observed discrepancy.

A first possibility is that the poor diagnostic accuracy reported in this study was due to inadequate technique of the CTA and MRA image acquisition. However, during the entire study duration all participating centers had at their disposal state-

Table 4b Cross tabulations of the CTA observer and MRA observer with the highest area under the ROC curve*

	Positive DSA	Negative DSA	
Positive CTA	50 (69%)	25 (9%)	75
Negative CTA	22 (31%)	259 (91%)	281
Total	72	284	356
	Positive DSA	Negative DSA	
Positive MRA	41 (57%)	29 (10%)	70
Negative MRA	31 (43%)	255 (90%)	286
Total	72	284	356

* The observers with the highest areas under the ROC curve were CTA observer A and MRA observer F

of-the-art equipment and scan protocols. Moreover, in cases where technological improvements became available, each center was allowed to adjust its scan protocol to take advantage of equipment upgrades. An associated advantage of this protocol flexibility is the fact that this allowed for a realistic reflection of clinical practice and implementation of technological developments. Consequently, one might expect CTA and MRA to have performed better in the second half of the study. However, as shown in Table 5, diagnostic accuracy observed for the second half of the study was no better than that found for the entire study period. Another assumption might be that the coordinating center team, which enrolled 61% of the patients, had more experience with renal CTA and MRA and, therefore, could acquire higher quality examinations. This hypothesis was, however, not corroborated (Table 5). These findings indicate that neither new technologic developments nor magnitude of expertise regarding the acquisition of CTA and MRA images resulted in better diagnostic performance of CTA or MRA.

Secondly, the discrepant diagnostic accuracy as found in our study may be the result of a lack of expertise on the part of the observers. This explanation, however, does not appear well founded as some of the CTA and MRA observers participating in this study also have participated in studies reporting sensitivity and specificity estimates up to 100% (6, 14). Moreover, some of the observers are internationally considered as experts in the field of renal CTA or MRA research, and they all have multiple years of experience evaluating such exams.

Thirdly, the lower sensitivity in this study could be related to the fact that the prevalence of clinically relevant renal artery stenosis was lower than in other studies. In practice, severity of stenosis may be related to both the sensitivity and specificity of a test and to prevalence (23). In this study, the prevalence was 20%, a figure close to that reported by another large study (17). Other studies often reported a prevalence exceeding 40%, suggesting differences in patient selection (4, 5, 6, 11, 13). Table 5 illustrates that sensitivity rises with increasing prevalence. Especially, within a risk group with a prevalence of 42%, the sensitivity for CTA and MRA was 88% and 78%, respectively, suggesting that only patients with a high clinical suspicion of having renal artery stenosis should be subjected to the diagnostic workup by CTA or MRA. Severity of stenosis in this high-risk subgroup was statistically significantly higher ($p<0.05$).

Table 5: Additional analyses on diagnostic accuracy for the CTA and MRA observers with the best overall performance

Analysis	No. of patients	Prevalence RAS (%)	Observer A (CTA) Sensitivity / Specificity / AUC	Observer F (MRA) Sensitivity / Specificity / AUC
Overall performance as shown in Table 4	356	20	69 / 91 / 0.84	57 / 90 / 0.81
Analyses on time and location of data acquisition:				
Only patients included in the 2nd half of the study period	195	15	67 / 91 / 0.83	50 / 90 / 0.82
Only patients included at the coordinating center*	218	23	71 / 91 / 0.87	57 / 88 / 0.80
Analyses on patient selection:				
Only patients included according to ≥1 criteria of the Working Group on renovascular hypertension	265	22	72 / 92 / 0.86	64 / 90 / 0.83
Only patients with organ damage†	145	26	78 / 87 / 0.89	65 / 88 / 0.86
Only patients of age ≥60 years	93	32	80 / 87 / 0.89	67 / 76 / 0.80
Only patients with organ damage and age ≥60 years†	61	36	82 / 82 / 0.86	68 / 74 / 0.79
Only patients with a high clinical suspicion of RAS‡	76	42	88 / 89 / 0.94	78 / 82 / 0.89
Change in definition of disease				
Only atherosclerotic RAS considered as disease	356	13	78 / 95 / 0.94	67 / 93 / 0.93
Definition of clinically relevant RAS on DSA ≥70%	356	15	71 / 87 / 0.81	62 / 88 / 0.78
Image evaluation:				
Defensive approach: defining all diagnoses that were not made with a high level of confidence as positive test results	356	20	86 / 54 / 0.73	82 / 58 / 0.75
Only patients without supernumerary arteries	216	21	73 / 92 / 0.86	62 / 90 / 0.82

AUC= area under the ROC curve; RAS= renal-artery stenosis.
*The coordinating center was Maastricht University Hospital.
†Inclusion criteria referring to organ damage were: subcostal bruit present; hypertensive retinopathy grade III/IV; signs of atherosclerosis in one or more vascular regions; unexplained worsening of renal function; unilateral small kidney; and left ventricular hypertrophy.
‡ Logistic regression analysis was used to identify patients with high clinical suspicion of having RAS. The four predictor variables used in the model were: (1) number of clinical clues present (as defined by the Working Group on Renovascular Hypertension), (2) age, (3) body mass index, and (4) duration of hypertension (onset within 2 years versus onset longer than two years ago).

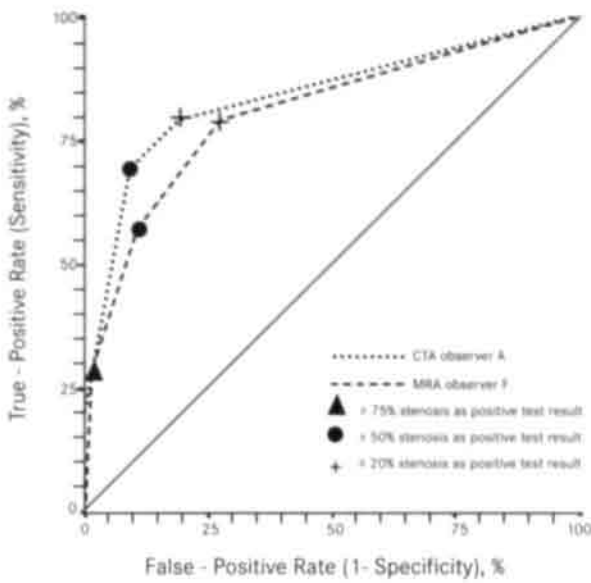

Figure 1: Receiver-operating characteristic (ROC) curves.
For the CTA observer and the MRA observer with the highest overall diagnostic accuracy, ROC curves are shown. Areas under the ROC curve are 0.84 and 0.81 for CTA and MRA, respectively; difference between the areas is 0.03; $z=0.83$; $p=0.41$.

Fourth, additional analyses with respect to the definition of significant renal artery stenosis show that the diagnostic accuracies of both CTA and MRA improved when only atherosclerotic renal artery stenoses, usually located in the more proximal part of the renal artery, were considered as disease. This approach excludes fibromuscular dysplasia, which typically affects the more distal renal artery. In the literature, many authors have already indicated that both CTA and MRA have limited ability for visualizing pathology of the distal (segmental) renal arteries due to the limited spatial resolution of these techniques (5, 11, 23, 24, 25).

A striking difference between the current and other studies is the relatively high proportion of patients with fibromuscular dysplasia (38% of all patients with renal artery stenosis). Although previous studies report the proportion of fibromuscular dysplasia among patients with renal artery stenosis as varying between 16% and 40% (20, 27), in most studies that reported CTA and MRA sensitivities of up to 100%, either the prevalence of fibromuscular dysplasia was quite low or patients with fibromuscular dysplasia were excluded from the analyses. Recently, the results of a MR study demonstrating the presence of linear cranial motion of the kidney and distal renal artery during sustained breath-hold were reported (28). The observed motion degraded distal renal artery image quality and resulted in incorrect diagnoses on MRA for the patients with DSA-proven fibromuscular dysplasia. This phenomenon may similarly affect image quality of the distal renal artery on CTA, and could be an additional factor for the poor depiction of fibromuscular dysplasia by both techniques.

Analyses exploring the effects of changing the threshold for a clinically relevant renal artery stenosis on DSA to (70% did not show a significant increase in sensitivity and did not confirm the expectation that more severe stenoses can be more easily detected.

Fifth, with respect to image evaluation, it was assessed whether a very defensive approach, defining all diagnoses not made with a high level of confidence as positive test results, might have resulted in an acceptable sensitivity. Sensitivity increased, but not to values exceeding 90% as were reported by other studies. Moreover, the increase in sensitivity was associated with much lower specificity estimates than in the other studies.

Furthermore, since many studies analyse only the 'main' renal arteries, calling all supernumerary (smaller) arteries 'accessory' and not clinically relevant, we also studied a subgroup of patients without supernumerary arteries (3). No significant changes in diagnostic accuracy were observed with this approach.

Finally, it can be argued that DSA is an imperfect reference standard due to its two-dimensional nature. Moreover, reported kappa values on interobserver agreement for the detection of significant renal artery stenosis by DSA range from 0.65 to 0.78 (29, 30, 31), while another study showed that the poor interobserver agreement on DSA was due to variations in estimating both the minimum and reference diameter (32). These findings support the notion that DSA is not the perfect reference test. However, imperfection of the reference standard does not seem a plausible explanation for the poor performance of CTA and MRA in the current study. Both CTA and MRA showed only moderate interobserver agreements (kappa values ranging from 0.59 to 0.64 for CTA and 0.40 to 0.51 for MRA), suggesting that poor reproducibility is a more likely explanation for the poor accuracy results.

While some of the additional analyses (Table 5) resulted in higher sensitivity, estimates still remain well below the 90% to 100% values reported in other studies. Although publication bias may have resulted in overrepresentation of studies with favorable results in the literature, this is the first large study showing poor sensitivity for both CTA and MRA.

Based on our study results, we conclude that both CTA and MRA are neither reproducible nor sensitive enough to rule out renal artery stenosis in patients with a pre-test likelihood for the presence of renal artery stenosis of approximately 20%. Even after careful selection of a patient group with a high pre-test probability of stenosis, the sensitivity remained below 90%. Other authors have emphasized that CTA and MRA are not suitable for identifying fibromuscular dysplasia, but postulated that these modalities may be useful for evaluation of patients with a high suspicion of atherosclerotic renal artery stenosis (25, 33). The results of the current study do not confirm this hypothesis.

It can be expected that both CTA and MRA will improve with the advent of new technologic developments, such as more rapid acquisition by multi detector-row CTA and faster MR hardware and software (34, 35). These developments may necessitate new prospective diagnostic studies. Until that time, both the moderate interobserver agreements as well as the low sensitivity of CTA and MRA suggest that DSA is still the method of choice in the diagnostic workup of hypertensive patients with suspected renal artery stenosis.

Protocols for CTA, MRA, and DSA

	's Hertogenbosch	Maastricht†	Nijmegen†	Tilburg	Utrecht	Veldhoven
No. of subjects included / remaining for analysis	26 / 21	242 / 218	89 / 75	19 / 16	15 / 15	11 / 11
No. of subjects scanned with SENSE / MD-CTA*	0 / 0	97 / 0	0 / 21	0 / 0	0 / 0	0 / 0
CT imaging						
Manufacturer CT scanner‡	GE	Elscint	Siemens	Philips	Philips	Philips
CTA						
Collimation - mm / pitch	3 / 1.5	2.5 / 0.7	3 / 1 (4*1 / 1.25)	3 / 1	3 / 1	3 / 1
Name contrast agent§	Omnipaque 300	Omnipaque 350	Omnipaque 350	Omnipaque 300	Ultravist	Iomeron 300
ml of contrast agent / injection rate (ml/second)	120/ 3.0	140/4.0	120/ 3.0	120/4.5	130/3.0	140/4.0
MR imaging						
Manufacturer MR scanner and field strength‡	GE 1.5T	Philips 1.5T	Siemens 1.5T	Philips 1.0T	Philips 1.5T	Philips 1.0T
MRA						
FOV - mm	480*288	512*302 (400*400)	420*263	420*315	400*320	450*338
Matrix	512*192	512*155 (400*296)	512*192	512*163	512*196	384*160
acquisition slice thickness - mm / no. of slices	3.0/ 28	2.2/29 (1.9/35)	2.8/32	3.0/25	3.0/20	2.4/28
TR - msec /TE - msec /FA - degrees	5.6/1.2/40	5.6/1.6/40 (5.0/1.5/40)	4.6/1.8/30	6.4/1.8/40	7.1/1.9/45	6.3/1.7/40
Profile ordering technique	centric	centric	linear	linear	centric	centric
Acquisition voxel size - mm3	4.2	4.3 (2.6)	3.1	4.7	3.8	5.9
Scan duration - seconds	30	25 (26)	28	26	28	28
Name contrast agent§	Magnevist	Magnevist	Magnevist	Omniscan	Magnevist	Prohance
ml of contrast agent / injection rate - ml/second	30/ 2.5	30/3.0 (30/2.5)	14/2.5	20/2.5	30/2.0	30/2
DSA imaging						
Manufacturer DSA equipment‡	GE	Philips	Siemens	Philips	Philips	Philips
Image intensifier (cm)	35	38	40	38	38	38
Matrix	1024	1024	1024	512	512	1024
Name contrast agent§	Omnipaque 300	Omnipaque 300	Omnipaque 240	Omnipaque 300	Ultravist	Iomeron 300
Approximate amount of contrast agent - ml	90	60	160	40	90	60
Injection rate (aorta) - ml/second	15	15	20	20	15	10 to 15
No. of patients with selective renal ia-DSA	8	208	3	0	3	2

* MR-technique SENSE (SENSitivity Encoding) and MD-CTA (MultiDetector row CTA) are recent technical development for MRA and CTA, respectively (34, 35). In a subgroup of the included patients (all remaining for analysis), Maastricht used the SENSE technique and Nijmegen used MD-CTA

† Numbers in parenthesis represent the scanparameters used for the subgroup of patients that either underwent SENSE MRA or MD-CTA.

‡ GE Medical Systems, Milwaukee, Wisconsin, USA. Elscint Ltd., Haifa, Israel. Philips Medical Systems, Best, the Netherlands. Siemens Medical Systems, Erlangen, Germany.

§ Omnipaque and Omniscan are products of Amersham Health, Oslo, Norway. Magnevist and Ultravist are products of Schering AG, Berlin, Germany. Iomeron and Prohance are products of Bracco Byk Gulden, Constanz, Germany.

The numbers refer to the amount of included patients remaining for analysis.

Acknowledgments

Participants

The names of the other participants in the study are as follows: Amsterdam- M. Boers; 's Hertogenbosch- J.J. Beutler, A.A.M.J. Hollander, L. Obertop, H.J. Teertstra; Maastricht- C.D. Dirksen, P. Habets, B.K. Janevski, D. Koster, M.M.E. Krekels, E.E.M.T. Lemaire, T.K. Oei, D. Postulart, R.J.M.W. Rennenberg, M.C.E.F. Wijffels; Nijmegen- J.O. Barentsz, S.J.H. Bredie, M. Hogenkamp, F.B.M. Joosten, E.M. Roumen-Klappe, Th. Thien; Tilburg- L. Lampmann, P. Lohle, W. Rensma; Utrecht- L. Bax, B. Braam, A.E.M. Hamersma, H.A. Koomans, W.P.Th.M. Mali; Veldhoven- P.G.G. Gerlag, H.L.M. Pasmans, A.W. van den Wall Bake, P.F.F. Wijn.

References

1. Young N, Chi KK, Ajaka J, McKay L, O'Neill D, Wong KP. Complications with outpatient angiography and interventional procedures. Cardiovasc Intervent Radiol 2002; 25(2):123-6.
2. Waugh JR, Sacharias N. Arteriographic complications in the DSA era. Radiology 1992; 182(1):243-6.
3. Vasbinder GB, Nelemans PJ, Kessels AG, Kroon AA, de Leeuw PW, van Engelshoven JM. Diagnostic tests for renal artery stenosis in patients suspected of having renovascular hypertension: a meta-analysis. Ann Intern Med 2001; 135(6):401-11.
4. Equine O, Beregi JP, Mounier-Vehier C, Gautier C, Desmoucelles F, Carre A. [Importance of the echo-doppler and helical angioscanner of the renal arteries in the management of renovascular diseases. Results of a retrospective study in 113 patients]. Arch Mal Coeur Vaiss 1999; 92(8):1043-5.
5. Galanski M, Prokop M, Chavan A, Schaefer C, Jandeleit K, Olbricht C. [Accuracy of CT angiography in the diagnosis of renal artery stenosis]. Rofo Fortschr Geb Rontgenstr Neuen Bildgeb Verfahr 1994; 161(6):519-25.
6. Kaatee R, Beek FJ, de Lange EE, et al. Renal artery stenosis: detection and quantification with spiral CT angiography versus optimized digital subtraction angiography. Radiology 1997; 205(1):121-7.
7. Olbricht CJ, Paul K, Prokop M, et al. Minimally invasive diagnosis of renal artery stenosis by spiral computed tomography angiography. Kidney Int 1995; 48(4):1332-7.
8. Wittenberg G, Kenn W, Tschammler A, Sandstede J, Hahn D. Spiral CT angiography of renal arteries: comparison with angiography. Eur Radiol 1999; 9(3):546-51.
9. De Cobelli F, Venturini M, Vanzulli A, et al. Renal arterial stenosis: prospective comparison of color doppler US and breath-hold, three-dimensional, dynamic, gadolinium-enhanced MR angiography. Radiology 2000 Feb;214 (2):373 -80.
10. Leung DA, Pelkonen P, Hany TF, Zimmermann G, Pfammatter T, Debatin JF. Value of image subtraction in 3D gadolinium-enhanced MR angiography of the renal arteries. J Magn Reson Imaging 1998; 8(3):598-602.
11. Rieumont MJ, Kaufman JA, Geller SC, et al. Evaluation of renal artery stenosis with dynamic gadolinium-enhanced MR angiography. AJR Am J Roentgenol 1997; 169(1):39-44.
12. Thornton J, O'Callaghan J, Walshe J, O'Brien E, Varghese JC, Lee MJ. Comparison of digital subtraction angiography with gadolinium-enhanced magnetic resonance angiography in the diagnosis of renal artery stenosis. Eur Radiol 1999; 9(5):930-4.
13. Bongers V, Bakker J, Beutler JJ, Beek FJ, De Klerk JM. Assessment of renal artery stenosis: comparison of captopril renography and gadolinium-enhanced breath-hold MR angiography. Clin Radiol 2000; 55(5):346-53.
14. Korst MB, Joosten FB, Postma CT, Jager GJ, Krabbe JK, Barentsz JO. Accuracy of normal-dose contrast-enhanced MR angiography in assessing renal artery stenosis and accessory renal arteries. AJR Am J Roentgenol 2000; 174(3):629-34.
15. Detection, evaluation, and treatment of renovascular hypertension. Final report. Working Group on Renovascular Hypertension. Arch Intern Med 1987; 147(5):820-9.
16. Anderson GH, Jr., Blakeman N, Streeten DH. Prediction of renovascular hypertension. Comparison of clinical diagnostic indices. Am J Hypertens 1988; 1(3 Pt 1):301-4.
17. Krijnen P, van Jaarsveld BC, Steyerberg EW, Man in 't Veld AJ, Schalekamp MA, Habbema JD. A clinical prediction rule for renal artery stenosis. Ann Intern Med 1998; 129(9):705-11.
18. Shellock FG, Kanal E. Policies, guidelines, and recommendations for MR imaging safety and patient management. SMRI Safety Committee. J Magn Reson Imaging 1991; 1(1):97-101.

19. Lufft V, Hoogestraat-Lufft L, Fels LM, et al. Contrast media nephropathy: intravenous CT angiography versus intraarterial digital subtraction angiography in renal artery stenosis: a prospective randomized trial. Am J Kidney Dis 2002; 40(2):236-42.
20. Safian RD, Textor SC. Renal artery stenosis. N Engl J Med 2001; 344(6):431-42.
21. Kaatee R, Beek FJ, Verschuyl EJ, et al. Atherosclerotic renal artery stenosis: ostial or truncal? Radiology 1996; 199(3):637-40.
22. Hanley JA, McNeil BJ. A method of comparing the areas under receiver operating characteristic curves derived from the same cases. Radiology 1983; 148(3):839-43.
23. Fletcher RH, Fletcher SW, Wagner EH. Clinical epidemiology: the essentials. 3rd ed. Baltimore (MD): Williams and Wilkins; 1996. p. 54-5.
24. Farres MT, Lammer J, Schima W, et al. Spiral computed tomographic angiography of the renal arteries: a prospective comparison with intravenous and intraarterial digital subtraction angiography. Cardiovasc Intervent Radiol 1996; 19(2):101-6.
25. Kim TS, Chung JW, Park JH, Kim SH, Yeon KM, Han MC. Renal artery evaluation: comparison of spiral CT angiography to intra-arterial DSA. J Vasc Interv Radiol 1998; 9(4): 553-9.
26. Schoenberg SO, Knopp MV, Londy F, et al. Morphologic and functional magnetic resonance imaging of renal artery stenosis: a multireader tricenter study. J Am Soc Nephrol 2002; 13(1):158-69.
27. Pohl MA, Novick AC. Natural history of atherosclerotic and fibrous renal artery disease: clinical implications. Am J Kidney Dis 1985; 5(4):A120-A130.
28. Vasbinder GB, Maki JH, Nijenhuis R.J., Leiner T., Wilson GJ, Kessels AG et al. Motion of the distal renal artery during 3D contrast-enhanced breath-hold MRA. J Magn Reson Imaging 2002; 16:985-96.
29. de Vries AR, Engels PH, Overtoom TT, Saltzherr TP, Geyskes BG. Interobserver variability in assessing renal artery stenosis by digital subtraction angiography. Diagn Imaging Clin Med 1984; 53(6):277-81.
30. Schreij G, de Haan MW, Oei TK, Koster D, de Leeuw PW. Interpretation of renal angiography by radiologists. J Hypertens 1999; 17(12 Pt 1):1737-41.
31. van Jaarsveld BC, Pieterman H, van Dijk LC, et al. Inter-observer variability in the angiographic assessment of renal artery stenosis. DRASTIC study group. Dutch Renal Artery Stenosis Intervention Cooperative. J Hypertens 1999; 17(12 Pt 1):1731-6.
32. Paul JF, Cherrak I, Jaulent MC, et al. Interobserver variability in the interpretation of renal digital subtraction angiography. AJR Am J Roentgenol 1999; 173(5):1285-8.
33. Rieumont MJ, Kaufman JA, Geller SC, et al. Evaluation of renal artery stenosis with dynamic gadolinium-enhanced MR angiography. AJR Am J Subsecond multi-slice computed tomography: basics and applications. Eur J Radiol 1999; 31(2):110-2Roentgenol 1997; 169(1):39-44.
34. Pruessmann KP, Weiger M, Scheidegger MB, Boesiger P. SENSE: sensitivity encoding for fast MRI. Magn Reson Med 1999; 42(5):952-62.
35. Klingenbeck-Regn K, Schaller S, Flohr T, Ohnesorge B, Kopp AF, Baum U. Subsecond multi-slice computed tomography: basics and applications. Eur J Radiol. 1999; 31(2):110-2.

Motion of the proximal renal artery during the cardiac cycle

Journal of Magnetic Resonance Imaging: 2000;12:924-928.

D.W. Kaandorp, G.B.C. Vasbinder, M.W. de Haan, G.J. Kemerink,
J.M.A. van Engelshoven

Abstract

In 48 hypertensive patients, the motion of the proximal renal artery during the cardiac cycle was quantified using two-dimensional Quantitative Flow measurements and automatic contour detection. Substantial translational motion was observed with an amplitude ranging from 1 to 4 mm. Since motion effectively reduces spatial resolution, the use of motion suppression techniques should strongly be considered for renal MR angiography.

Introduction

Contrast Enhanced MR Angiography (CE-MRA) is quickly gaining clinical acceptance in radiological practices throughout the world (1). This imaging technique has been applied successfully to arteries which are relatively motionless, like the peripheral arteries (2) or the cerebral arteries (3,4). However, the arteries in the human trunk demonstrate a substantial amount of motion due to a combination of respiration and heartbeat, which makes the accurate depiction of thoracic and abdominal arteries much more demanding. The diaphragm moves down during inspiration, pushing the abdominal organs caudally, and subsequently moves up during expiration (5). The beating heart generates a pulsatile blood pressure and flow, which causes the compliant arteries to dilate and translate, respectively. As a result, many different motion suppression techniques have been developed over the years in to reduce the imaging artifacts associated with motion like ghosting and blurring.

Gating is one of the earliest approaches to avoid respiratory motion and is based on the acquisition of data exclusively during the relatively motionless period at end expiration. The trigger moment is provided by an external respiratory device or by using the more accurate navigator technique (5-7). When scan-times decreased to under 30 seconds, breath holding during the entire acquisition became possible. This initially seemed to be the ultimate way to avoid respiratory motion. However, breath holding does not completely eliminate motion of the diaphragm. During a 20-second breath hold, the mean displacement of the diaphragm is still on the order of 25% of that during normal breathing (8). In our experience, the diaphragm gradually moves cranially during a breath hold. In addition, breath holding requires a certain patient cooperation, and in multiple breath-hold techniques, slice registration errors may occur. It has early been shown that by using navigators, basically any form of motion can be corrected retrospectively with the adaptive three-dimensional phase multiplication technique (9). A more recent development is the combination of navigator gating during free breathing with adaptive real-time correction of the imaged volume position (10). This may be followed by retrospective correction of the residual motion (11). Finally, there are so called 'autocorrection' post processing methods, which iteratively correct for motion artifacts based on the optimization of a particular image metric (12).

For the same reasons, the repetitive contraction and motion of the heart also requires triggering or gating. Here, ECG-leads or a Peripheral Pulse Unit (PPU) provide the trigger moment. The major difference between the cardiac and the respiratory cycle is that the cardiac frequency is higher and more constant, which enables the use of retrospective triggering techniques. Even simultaneous temporally resolved cardiac and respiratory motion has been described, although this technique requires excessively long scan times (13).

Motion during both the respiratory and the cardiac cycle is probably most pronounced for the coronary arteries. The translational motion of the left anterior descending artery during one respiratory cycle can be as large as 7.5 mm (14). During a breath hold, the motion pattern and amplitude for coronary arteries due to the heart action have also shown to vary substantially from patient to patient (15). The mean proximal displacement of the right coronary artery during one cardiac cycle was measured to be 13 mm, whereas the distal motion of this artery averaged 20

mm (16). While coronary artery motion during the cardiac cycle has been described in detail, we found no reports in literature on renal artery motion. However, in our experience, motion during the cardiac cycle is not restricted to the coronary arteries. The aorta, the renal, mesenteric, and even the iliac arteries clearly demonstrate a substantial amount of motion at the cardiac frequency due to the heart action.

In current contrast-enhanced renal MR angiography, breath holding is essential to eliminate the artifacts caused by respiratory motion. Due to the available scan-time in a single breath hold (±25 sec) and the relatively short time between arterial and venous contrast arrival (±10 sec), cardiac synchronization is usually not employed. However, we have observed a substantial motion of the renal arteries at the cardiac frequency due to the pulsating blood pressure and flow. Respiratory motion has shown to affect mainly the distal part of the renal arteries (17), whereas this secondary motion mainly affects the proximal renal arteries. The goal of this study was to provide objective arguments for the improvement of renal MR angiography. Therefore, the motion of the proximal renal arteries during the cardiac cycle was quantified in a representative group of hypertensive patients using retrospectively triggered two-dimensional quantitative flow measurements and automatic contour detection. The quantitative information presented here can subsequently be used to decide on issues of spatial resolution and the need for cardiac synchronization in renal MR angiography.

Materials and methods

This study was part of an ongoing multi-center trial called RADISH (Renal Artery Diagnostic Imaging Study in Hypertension) in which conventional angiography, CTA, and MRA of the renal arteries are being compared in patients suspected of renovascular hypertension (18). Here, the MR data from 48 consecutive patients (32 men, age 57±10; 16 women, age 49±13) were used to obtain the motion of the proximal renal artery. The study was approved by the hospital's committee on medical ethics and all patients gave informed consent.

In chronological order, the MR imaging protocol consisted of a survey, an untriggered three-dimensional phase contrast angiogram (PCA) (19), four two-dimensional quantitative flow (QF) measurements that provided both vessel position and blood flow, and finally a three-dimensional gadolinium-enhanced MR angiogram. Two of the QF measurements were planned perpendicular to the proximal left and right renal arteries, as illustrated in Figure 1. Often, the slice orientation of these scans was double oblique. The other two QF measurements were performed perpendicular to the aorta just above and just below the renal arteries. All measurements were carried out on a 1.5 T Philips Gyroscan ACS-NT scanner (Powertrak 6000, Philips Medical Systems, Best, The Netherlands) using the body coil for signal reception. The scan parameters for the two-dimensional QF acquisitions were: RF-spoiled gradient echo, FOV 300 x 210 mm, acquisition matrix 256 x 108, slice thickness 6 mm, TR/TE/α = 14/6/20°, and venc = 120 cm/s. The scans were retrospectively triggered using a Peripheral Pulse Unit (PPU) yielding 25 heart-phases at a frequency of 65 beats/min within a scan-time of about 2 minutes.

Standard image reconstruction produced phase difference and modulus images for all heart phases covering the complete cardiac cycle. The cross-sectional area

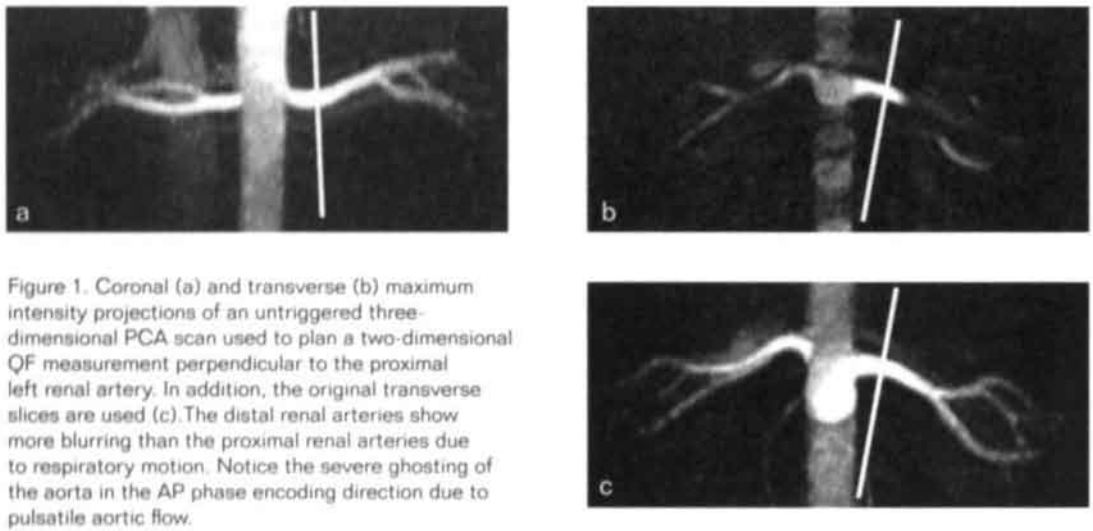

Figure 1. Coronal (a) and transverse (b) maximum intensity projections of an untriggered three-dimensional PCA scan used to plan a two-dimensional QF measurement perpendicular to the proximal left renal artery. In addition, the original transverse slices are used (c).The distal renal arteries show more blurring than the proximal renal arteries due to respiratory motion. Notice the severe ghosting of the aorta in the AP phase encoding direction due to pulsatile aortic flow.

of the renal artery was *determined in the modulus image* by using a closed contour model tracking the maximum gradient in signal intensity (20, 21). Figure 2 shows a representative QF measurement with an example of a detected contour, defined on a grid which doubled the reconstruction resolution. The center position of each renal artery contour was determined in two perpendicular directions. Due to the slightly oblique sagittal slice orientation, these directions were oblique anterior-posterior (AP) and oblique cranio-caudal (CC). This directional separation of motion was done because we expect the AP motion to be caused by the dilatation of the aorta due to the pressure pulse, and the CC motion to be caused by the kinetic energy transfer of the pulsatile blood flow. Compared to the aorta, the renal artery showed almost no dilatation during systole but merely translation. Therefore, motion of the renal artery (and of its vessel wall) was defined as the difference between the minimum and the maximum center positions throughout all heart-phases. Because renal artery motion was found to be approximately in a straight line, the full motion was calculated as the square root of the sum of the variances of the motions in the above two perpendicular directions.

Due to the 2-minute scan time, all quantitative flow measurements were performed during normal breathing. As a result, a systematical error was introduced in the flow measurement since the respiratory motion of the proximal renal artery can be in the order of a few mm, as already reported by Debatin et al. (17). To determine whether this respiratory motion affects the motion during the cardiac cycle as observed in the modulus images, two additional measurements were performed on a healthy volunteer. For this purpose, a standard two-dimensional gradient echo sequence was used (FOV 256 x 204 mm, acquisition matrix 256 x 144, slice thickness 7 mm, TR/TE/α = 9.8/5.8/20°, flow compensation on). The scan was cardiac gated using a peripheral pulse unit (PPU) yielding 10 heart-phases at a frequency of 65 beats/minute within a scan time of 38 seconds. The slice was positioned perpendicular to

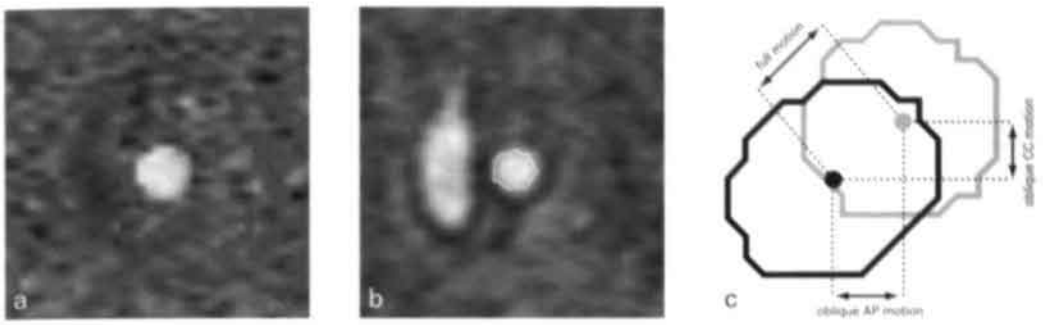

Figure 2. One of the phase difference (a) and modulus images (b) of a retrospect-ively triggered two-dimensional QF measurement. Contours are detected in all modulus images and the maximum translational motion of the proximal renal artery is determined (c).

the left proximal renal artery and one measurement was performed within a breath hold, while the other was performed during normal breathing.

Results

The first important result of the two additional measurements on a healthy volunteer is that the 38-second breath hold scan clearly showed a substantial translational motion of the proximal renal artery during the cardiac cycle of approximately 1.5 mm, thereby confirming the presence of motion due solely to the heart action. As expected, the images obtained from the second scan during normal breathing showed some blurring of the margins of the renal artery and vein and an artifactual enlargement of the vessel areas. However, they still showed the same translational motion of the renal artery during the cardiac cycle of about 1.5 mm, which implies that the artifacts due to respiratory motion do not alter the center position of the vessel.

Of all 48 quantitative flow scans on the left renal artery, 17 (35%) showed insufficient image quality for the automatic contour detection due either to improper slice positioning or to flow voids during systole caused by proximal stenoses. These scans were therefore excluded from the analysis. Of all 48 scans on the right renal artery, 9 (26%) were discarded. The remaining scans that were analyzed showed the renal arteries clearly delineated with approximately circular cross-sections. It should be noted that the level of blurring due to respiratory motion differed between patients, but never hampered automatic contour detection.

The measured motion of the proximal left and right renal arteries during the cardiac cycle is depicted in Figure 3 and Figure 4, respectively. The average motion of the left renal artery in the oblique AP direction is 1.1 $\pm$ 0.4 mm, which is significantly smaller than its average motion in the oblique CC direction of 1.7 $\pm$ 0.6 mm (paired t-test, $P < 0.001$). A less significant difference was found for the right renal artery, which showed an oblique AP motion of 1.5 $\pm$ 0.5 mm and an oblique CC motion of 1.7 $\pm$ 0.5 mm (paired t-test, $P = 0.006$). The motional amplitudes in the CC direction for the left and right renal arteries are equal. In the AP direction, however, the average motion of the right renal artery was significantly larger than that of the left artery (two sample t-test, $P = 0.001$).

Figure 5 shows the calculated full motion of both the left renal artery (2.1 ± 0.5 mm) and the right renal artery (2.3 ± 0.6 mm), which were not significantly different (two sample t-test, P = 0.23). The full motion ranges from 1 to 4 mm. Note that values between 0 and 1 mm were not observed.

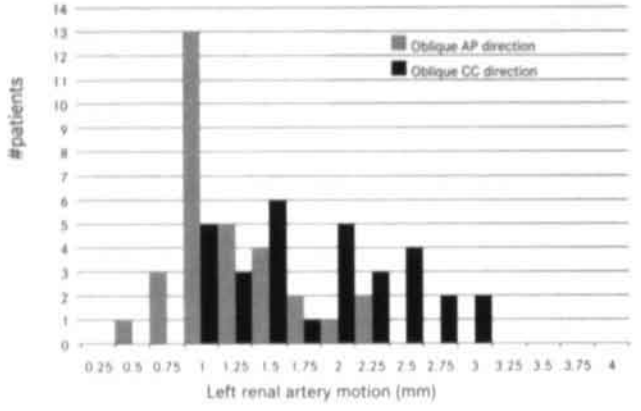

Figure 3. Histogram of the motion of the proximal left renal artery. The total number of arteries depicted in this plot is 31.

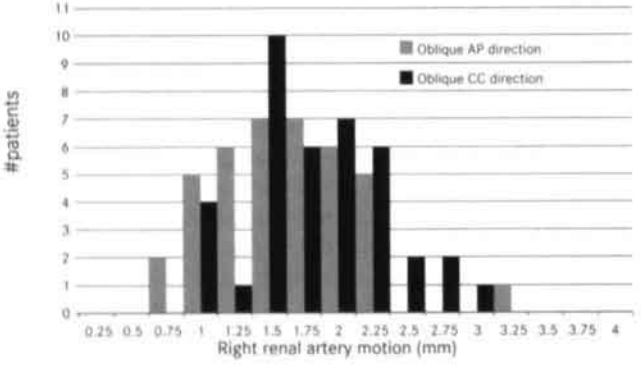

Figure 4. Histogram of the motion of the proximal right renal artery. The total number of arteries depicted in this plot is 39.

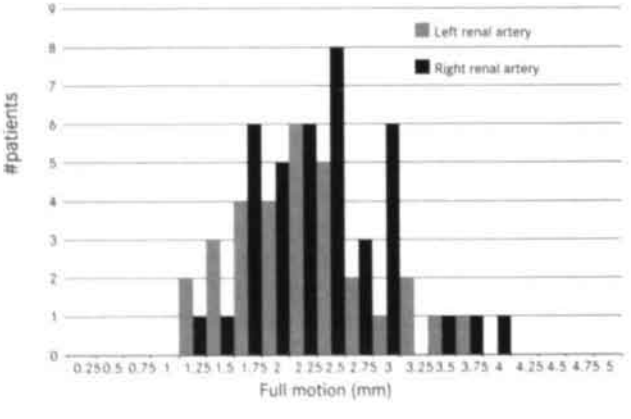

Figure 5. Histogram of the full motion of the proximal renal arteries. The total number of arteries depicted in this plot is 70.

Discussion

The reason that respiratory motion does not affect the center position of a vessel is found by considering the number of breathings during a scan. A single breathing period is about 5 seconds. Therefore, a 38-second scan contains almost 8 breathings, while a 2-minute scan contains as many as 24 breathings. Based on our results, this number of breathings is obviously sufficient to obtain an effective averaging of the vessel position, although the vessel margins become less sharp. The above argument can also be applied to all different phases in a cardiac triggered scan, resulting in the vessel purely showing its motion during the cardiac cycle.

A small but significant difference in amplitude between CC and AP motion of the proximal renal artery was found. This observation supports our expectation that the motion in these two orthogonal directions originates from different causes. CC motion is primarily caused by the repetitive force exerted onto the renal artery wall by the pulsatile blood flow, which is strongly deflected from longitudinal in the aorta to transverse in the renal artery. The left and right renal arteries are likely to experience equal longitudinal forces, as confirmed by our measurements which show the equality of left and right CC motion. AP motion is induced by the pressure pulse from the heart which causes the aorta to dilate during systole. Because the posterior aortic wall is nearly immobilized by the spinal cord, the anterior wall shows the largest motional amplitude, as visually confirmed by our additional two-dimensional QF measurements on the aorta. The renal arteries originate laterally from the aorta, and thereby obtain their AP motion, although with smaller amplitude than the anterior aortic wall. However, the right renal artery often originates antero-laterally, whereas the left renal artery origin tends to be located postero-laterally (22) (see also Figure 1B). This immediately explains the observed difference in amplitude between left and right AP motion. The more anterior the origin of the renal artery is located, the larger the motion, in agreement with our results (left AP motion 1.1 $\pm$ 0.4 mm, right AP motion 1.5 $\pm$ 0.5 mm).

It should be emphasized that none of the renal arteries showed zero or almost negligible motion. This can partly be attributed to image noise which slightly affects the center position of all contours and thereby creates a small minimum amount of motion. However, the influence of image noise on the center position is much less than on each individual section of the contour. The minimum amount of motion due to noise roughly equals the smallest observed motional amplitude of 1 mm. The much larger range in measured motion up to 4 mm can thus only be explained by an actual physiological motion of the proximal renal artery. Moreover, at higher amplitudes of the translational motion, the additional effect of image noise becomes smaller. Visual inspection of the modulus images in fast cine mode confirmed that renal artery motion at the cardiac frequency due to the heart action is always present. Another source of error in the contour position might be the left-right (LR) motion of the renal arteries due to aortic dilatation, which cannot be determined with our two-dimensional QF measurements. However, since these QF measurements were positioned perpendicular to the renal arteries in a slightly oblique sagittal orientation, the error induced by LR motion may expected to be small.

Under the likely assumption that the observed motion of the proximal renal artery due to the heart action during normal respiration equals that during a breath hold,

it is clear from Figure 5 that a submillimeter resolution for renal MR angiography without any cardiac synchronization is not very effective, as all patients showed a full motion of at least 1 mm. Current untriggered examinations use a spatial resolution of about 1 to 2 mm, which is smaller than or close to the average renal artery motion. Since all our patients also underwent three-dimensional contrast-enhanced MR angiography, the degradable effect of motion on image quality (14, 17) could be judged. Our untriggered MRA scan was performed in a 25 second breath hold using a coronal slice orientation with an acquisition resolution of 1 x 2 x 2.2 mm (CC x LR x AP). Surprisingly, after careful examination of all MR angiograms, including original slices and maximum intensity projections, we could not identify any image quality parameter that correlated with the measured translational motion. Neither vessel edge sharpness (blurring) nor vessel diameter (relative to the conventional angiogram) revealed any relationship with vessel motion. This is in agreement with a remark of Holland et al. (8) that when motion is continuous and smooth, image artifacts will not be readily identifiable, but resolution will effectively be reduced. As a consequence, only studies that directly compare cardiac triggered and untriggered contrast enhanced renal MRA can be used to quantify the effects of motion during the cardiac cycle on image quality and clinical outcome.

Our findings apply to relatively undiseased renal arteries of hypertensive patients. Normotensive patients might reveal different motion patterns, especially in the AP direction, as the blood pressure is the major cause of this motion. In future studies it would be interesting to correlate physiological parameters such as vessel compliance, blood pressure, distal resistance, and age with the observed renal artery motion. Principally, our findings do not apply to stenotic renal arteries, since in these cases the measurement of motion using a two-dimensional QF scan was practically impossible. This implies that the image quality of stenotic vessels could not be correlated with vessel motion. Nevertheless, we expect that for the accurate depiction of renal artery stenoses, a higher spatial resolution in the order of 1 mm is required. Therefore, implementing some form of motion correction technique in future renal MR angiography studies should be given serious consideration.

Conclusions

The major conclusion of this study is that substantial motion of the proximal renal arteries due to pulsations of the blood pressure and flow during the cardiac cycle is always present. In a representative group of hypertensive patients, the average CC motion is slightly larger than the AP motion. In addition, the AP motion of the right renal artery is larger than that of the left renal artery due to the more antero-lateral location of the right renal artery origin. More important, with respect to contrast-enhanced renal MR angiography, is that the average full motion of the proximal renal arteries is comparable to or larger than the voxel dimensions in currently used scan protocols. As motion effectively reduces spatial resolution, implementing some form of motion correction technique should be considered when the accurate depiction of renal artery stenoses is required.

Acknowledgments

The Flow software package was kindly provided to us by the Division of Image Processing, Department of Radiology, Leiden University Medical Center, The Netherlands.

References

1. Prince MR, Grist TM, Debatin JF. 3D contrast MR Angiography. Berlin: Springer-Verlag; 1999.
2. Ho KYJAM, Leiner T, van Engelshoven JMA. MR Angiography of run-off vessels. Eur Radiol 1999;9:1285-1289.
3. Yucel EK, Anderson CM, Edelman RR, et al. Magnetic Resonance Angiography: Update on applications for extracranial arteries. Circulation 1999;100:2284-2301.
4. Kaandorp DW, Kopinga K, Wijn PFF. Venous signal suppression in three-dimensional dynamic Gd-enhanced carotid artery imaging using the eigenimage filter. Magn Reson Med 1999;42:307-313.
5. Taylor AM, Jhooti P, Wiesmann F, Keegan J, Firmin DN, Pennell DJ. MR navigator-echo monitoring of temporal changes in diaphragm position: Implications for MR coronary angiography. J Magn Reson Imaging 1997;7:629-636.
6. McConnell MV, Khasgiwala VC, Savord BJ, Chen MH, Chuang ML, Edelman RR, Manning WJ. Comparison of respiratory suppression methods and navigator locations for MR coronary angiography. Am J Roentgenol 1997;168:1369-1375.
7. Sachs TS, Meyer CH, Hu BS, Kohli J, Nishimura DG, Macovski A. Real-time motion detection in spiral MRI using navigators. Magn Reson Med 1994;32:639-645.
8. Holland AE, Goldfarb JW, Edelman RR. Diaphragmatic and cardiac motion during suspended breathing: preliminary experience and implications for breath-hold MR imaging. Radiology 1998;209:483-489.
9. Korin HW, Felmlee JP, Ehman RL, Riederer SJ. Adaptive technique for three-dimensional MR imaging of moving structures. Radiology 1990;177:217-221.
10. Stuber M, Botnar RM, Danias PG, Kissinger KV, Manning WJ. Submillimeter three-dimensional coronary MR angiography with real-time navigator correction: Comparison of navigator locations. Radiology 1999;212:579-587.
11. Wang Y, Ehman RL. Retrospective adaptive motion correction for navigator-gated three-dimensional coronary MR angiography. J Magn Reson Imaging 2000;11:208-214.
12. McGee KP, Manduca A, Felmlee JP, Riederer SJ, Ehman RL. Image metric-based correction (autocorrection) of motion effects: Analysis of image metrics. J Magn Reson Imaging 2000;11:174-181.
13. Fredrickson JO, Wegmüller H, Herfkens RJ, Pelc NJ. Simultaneous temporal resolution of cardiac and respiratory motion in MR imaging. Radiology 1995;195:169-175.
14. Wang Y, Riederer SJ, Ehman RL. Respiratory motion of the heart: Kinematics and the implications for the spatial resolution in coronary imaging. Magn Reson Med 1995;33:713-719.
15. Wang Y, Vidan E, Bergman GW. Cardiac motion of coronary arteries: Variability in the rest period and implications for coronary MR Angiography. Radiology 1999;213:751-758.
16. Foo TKF, Ho VB, Hood MN. Vessel tracking: Prospective adjustment of section-selective MR angiographic locations for improved coronary artery visualization over the cardiac cycle. Radiology 2000;214:283-289.
17. Debatin JF, Ting RH, Wegmüller H, et al. Renal artery blood flow: Quantitation with phase-contrast MR imaging with and without breath holding. Radiology 1994;190:371-378.
18. Renal Artery Diagnostic Imaging Study in Hypertension (RADISH). Sponsored by the Dutch healthcare insurance board OG97-003, November 1999 - November 2001.
19. de Haan MW, Kouwenhoven M, Thelissen GRP, et al. Renovascular disease in patients with hypertension: Detection with systolic and diastolic gating in three-dimensional phase contrast MR angiography. Radiology 1996;198:449-456.

20. Flow software package, version 1.01, LKEB, Leiden University Medical Center, The Netherlands, 1999.
21. van der Geest RJ, Niezen RA, van der Wall EE, de Roos A, Reiber JHV. Automated measurement of volume flow in the ascending aorta using MR velocity maps: Evaluation of inter- and intraobserver variability in healthy volunteers. J Comp Assist Tomogr 1998;20: 904-911.
22. Verschuyl E-J, Kaatee R, Beek FJA, et al. Renal artery origins: Best angiographic projection angles. Radiology 1997;205:115-120.

Motion of the distal renal artery during three-dimensional contrast-enhanced breath-hold MRA

Journal of Magnetic Resonance Imaging 2002;16:685-696.

G.B.C. Vasbinder, J.H. Maki, R.J. Nijenhuis, T. Leiner, G.J. Wilson, A.G.H. Kessels, E. Lemaire, D.W. Kaandorp, K.Y.J.A.M. Ho, J.M.A. van Engelshoven.

Abstract

Purpose

To study the potential detrimental effects of renal motion on breath-hold three-dimensional contrast-enhanced (CE) MRA.

Materials and Methods

A computer model simulating linear motion was applied to MRA pulse sequences. Subsequently, to study whether renal motion is present, 24 patients being evaluated for possible renovascular hypertension underwent a breath-hold non-enhanced single slice two-dimensional dynamic turbo field-echo magnetic resonance imaging (MRI) scan with a typical duration of 32 seconds. This sequence was followed by breath-hold three-dimensional CE renal MRA. CE-MRA images were evaluated by two independent observers.

Results

The computer model revealed linear renal motion to cause artifacts. The severity of these artifacts correlated with velocity. Significant ($P < 0.001$) near linear cranial motion of the kidneys and diaphragm during a sustained breath-hold was found for the right kidney, left kidney, right diaphragm, and left diaphragm (0.26 ± 0.21 mm/second, 0.25 ± 0.23 mm /second, 0.43 ± 0.43 mm/second, and 0.29 ± 0.33 mm/second [mean ± SD], respectively). CE-MRA images showed artifacts of the distal renal artery that corroborated the computer model findings.

Conclusions

The observed cranial motion of the kidneys during a breath-hold adversely affects distal renal artery image quality on three-dimensional CE-MRA and jeopardizes reliable clinical evaluation. Shortening scan time may be beneficial for decreasing image degradation caused by this phenomenon.

Introduction

Three-dimensional contrast-enhanced (CE) renal MRA is gaining increased acceptance as a reliable test for the detection of renal artery stenosis. It has high sensitivity and specificity estimates when compared to the generally accepted gold standard of intra-arterial digital subtraction angiography (ia-DSA), and it overcomes many of the drawbacks of ia-DSA and spiral computed tomography angiography (CTA), as patients are not exposed to radiation or iodinated contrast media (1-7). The two most common indications for renal MRA are the pre-operative screening of potential kidney donors and the evaluation of suspected renal artery stenosis. Because the correction of renal artery stenosis may improve blood pressure and preserve renal function in patients with renovascular hypertension, early detection and treatment is desirable (8, 9). Although renal MRA is generally considered a valid diagnostic test for the detection of proximal renal arterial disease, the reliability of MRA for the detection of pathology located in the more distal part of the renal artery, as is often seen in fibromuscular dysplasia, is at least controversial at this time (10-12). State-of-the-art magnetic resonance imaging (MRI) scanner hardware and software is now capable of achieving ultra-high spatial resolution within a single breath-hold. However, at our institute, we routinely encounter variable degrees of blurring and ringing artifacts in the distal renal arteries and kidneys, hampering clinical evaluation. Initially, we attributed the observed artifacts to respiratory motion during three-dimensional MRA acquisition. Respiration causes translation of the kidneys, and is known for its detrimental effect on image quality (13-16). However, most of the patients demonstrating blurring or ringing artifacts on three-dimensional CE renal MRA were convinced they sustained a breath-hold for the entire scan. In the majority of the cases, this claim was confirmed by a respiratory monitoring device. Other than respiratory motion, additional motion sources that may adversely affect image quality in renal MRA are gross patient motion, bowel peristalsis, and vessel pulsation during the cardiac cycle (17). However, because these types of motion also affect the proximal part of the renal artery, it is unlikely that they are responsible for the observed distal blurring and ringing.

The aim of this study was two-fold. First, computer modeling was performed to better understand the effects of motion on three-dimensional MRA image quality. Second, a clinical study was devised to test the hypotheses that: 1) renal motion occurs during a breath-hold, and 2) this motion correlates with three-dimensional CE renal MRA image quality. In addition, the results of three-dimensional CE renal MRA were compared with ia-DSA, which was considered to be the standard-of-reference test.

Materials and methods

Computer modeling

To simulate the effects of motion on three-dimensional CE renal MRA images, computer modeling was performed using MATLAB (MathWorks, Inc., Natick, MA) based on the technique described by Maki et al. (18, 19). A baseline three-dimensional data set simulating four six-mm diameter vessels, one without stenosis and three with 66% stenoses (2.0 mm lumen; oriented left-right, superior-inferior

[SI], and 45° oblique) was first created. This dataset was then Fourier transformed in three dimensions to yield a true k-space representation of the motionless simulated image. Each line of k-space in the frequency (k_x) direction (simulated echo) was considered to be obtained instantaneously. The appropriate phase shift was then applied to each simulated echo (for a particular left-right [k_y] and slice [k_z] phase encoding value) based on the displacement at the time that echo was obtained. This modeling was performed for linear, linear centric (centric in k_y, linear in k_z), and elliptical centric profile ordering (20). The model allows any matrix size, TR, number of slices, rectangular field of view (FOV), and sensitivity encoding (SENSE) factor (21). Parameters were chosen identical to those used in the clinical data acquisition: FOV = 400 x 400 mm; matrix = 400 x 296; TR = 5.0 msec; 35 slices 1.90 mm thick, zero filled to 70 slices of 0.95 mm; SENSE factor 2 (left-right [y] phase-encoding direction); acquisition time = 26 seconds. Homodyne reconstruction for partial echo acquisition was built into the model.

Modeling was performed for read-out (x) direction constant velocities ranging from 0 to 1 mm/second to simulate linear cranio-caudal motion during a coronal acquisition. Qualitative evaluation was made regarding the type and degree of artifact caused by motion. Line profiles through stenotic and non-stenotic portions of the simulated vessels were then analyzed to determine vessel lumen caliber and degree of stenosis. Non-stenotic vessel width was measured as the full width half maximum (FWHM) of the line profile through the non-stenotic vessel, and the width of the stenosis was measured as the full width of the line profile through the stenosis at one half of the maximum of the line profile through the motionless stenosis.

Patient study

Patient recruitment

From September 2000 to February 2001, 30 consecutive patients with a median age of 52 years (15 men and 15 women; age range 22-74 years) referred for evaluation of possible renovascular hypertension were included in the study. All patients underwent MRA followed by ia-DSA the next day, as they were a subgroup of a larger multicenter study evaluating the accuracy of MRA and spiral CTA vs. ia-DSA (22). The study protocol for both the large trial and the current study was approved by the local institutional review board, and written informed consent allowing for the evaluations performed in the current study was obtained for all patients.

MRI

Imaging was performed on a Philips Intera 1.5T MR scanner (release 8.1.1; Philips Medical Systems, Best, The Netherlands). For all imaging, a surface phased array body coil was used.

Balanced fast field-echo (B-FFE) and three-dimensional phase-contrast angiography survey sequences were used for renal and renal artery localization. All breath-hold examinations were performed at end expiration.

In order to quantify renal motion during a breath-hold, a breath-hold cardiac triggered dynamic two-dimensional turbo field-echo (TFE) MRI was performed. Cardiac triggering was utilized to minimize the contribution of motion from cardiac pulsation, and was performed in the usual fashion using vector cardiography signals.

Single slices were planned in the coronal (all patients, N = 30) and transverse (subset of 10 patients) planes through the kidneys to measure motion of the kidneys during a breath-hold. The coronal scans also enabled measurement of diaphragmatic motion. Scan parameters for the two-dimensional TFE sequences were: FOV = 400 x 320 mm, matrix = 256 x 205 (interpolated to 512 x 512), TR/TE (msec) = 5.2/ 2.5, flip angle = 25°, slice thickness = 7.00 mm, 36 dynamic phases for an average scan duration of 32 seconds (one phase per heartbeat).

Following this, coronal three-dimensional CE breath-hold renal MRA using SENSE was performed using the following scan parameters: FOV = 400 x 400 mm, matrix = 400 x 296 (zero interpolated to 512 x 512), TR/TE (msec) = 5.0/ 1.5, flip angle = 40°, number of slices = 35, slice thickness = 1.90 mm (interpolated to 70 slices of 0.95 mm), partial echo factor = 62.5%, CENTRA (Contrast ENhanced Timing Robust Angiography; Philips terminology for an elliptical centric profile ordering variant) (23), SENSE factor 2 (phase-encoding [y] direction), acquisition voxel size = 2.54 mm^3, scan duration = 26 seconds. Twenty-eight mL of gadolinium (Magnevist, Schering, Berlin, Germany) followed by 20 mL of saline were injected at a rate of 3.0 mL/second. The use of this standardized volume of contrast agent is routine clinical practice at our institution, and is designed to speed workflow. Appropriate timing for the three-dimensional CE MRA sequence was obtained using a coronal two-dimensional dynamic timing sequence with a temporal resolution of 0.9 seconds (2 mL of gadolinium followed by 46 mL of saline, all at a rate of 3.0 mL per second). The scan delay (time interval between the start of the injection of contrast agent and the start of acquisition) for the three-dimensional CE MRA scan was determined from the timing sequence as the elapsed time from contrast injection to enhancement of the iliac bifurcation. To better facilitate breath-holding, oxygen was administered to all subjects at a rate of 3 liters per minute via a nasal cannula during the entire examination. To exclude any motion caused by early relaxation of the inspiratory muscles (e.g., diaphragm, which typically occurs a few seconds after end inspiration has been achieved), a 2-second delay after the patient initiated the breath-hold was used before scan initiation (24). To verify the patients' ability to sustain a breath-hold, a respiratory monitoring device was used as a supplement to visual inspection of the abdomen and thorax by a technologist. Additionally, all patients were queried as to whether they successfully sustained breath-hold over the entire acquisition.

Ia-DSA imaging

Ia-DSA was performed using Philips Integris V5000 digital angiography equipment (Philips Medical Systems, Best, The Netherlands). In all cases, a 31-cm FOV with an image matrix of 1024 x 1024 was used. A mean total of 60 mL of contrast medium (iohexol, Omnipaque 300; Nycomed, Oslo, Norway) was injected through a 4-F universal flush catheter (Cordis Europe N.V., Roden, The Netherlands) using a remotely triggered power injector (Medrad Spectris, Indianola, PA). Images were obtained in anteroposterior projections; in addition, 20° right oblique projections or 40° left anterior oblique projections were obtained in cases where the most proximal part of the renal arteries was not clearly visualized. Moreover, selective renal ia-DSA was performed in all patients using an 4-F cobra catheter (Cordis Europe N.V., Roden, NL). All DSA images were acquired during inspiratory breath-hold.

Image Evaluation

The dynamic two-dimensional TFE examinations were evaluated by one investigator with the aid of dedicated software (EasyVision, release 4.2.1, Philips Medical Systems, Best, The Netherlands). Cranial or caudal translation of both kidneys and diaphragm (coronal scans), as well as anterior or posterior kidney motion (transverse scans) during a sustained breath-hold, was measured using an electronic caliper with a 0.1 mm accuracy. To prevent inclusion of translation due to an incomplete breath-hold, the analysis was terminated following the first image acquired at the onset of cranio-caudal cyclical motion. Two independent experienced observers, both blinded from the results of the ia-DSA outcome as well as each other's results, evaluated the three-dimensional CE renal MRA examinations. Each renal artery segment was evaluated with respect to the presence or absence of renal artery stenosis (expressed as % of luminal narrowing), using a 5-point scale for image quality (non-evaluable = 1; poor = 2; fair = 3; good = 4; excellent = 5) and a 4 point scale for artifacts (severe = 0; moderate = 1; mild = 2; and none = 3). The presence and nature of all artifacts were registered (blurring, ringing, other). Renal artery segments were defined as follows: 1) aortic ostium to four mm distally, 2) more than four mm from the aortic ostium to the first branching of the renal artery, 3) distal to the beginning of branching to the level where the renal artery enters the renal parenchyma, and 4) the intra-parenchymal portion of the renal artery. Results of the ia-DSA evaluation (which were reached in consensus by three experienced vascular radiologists) were available for each patient. No motion measurements were performed for ia-DSA because this modality has a very short acquisition time (in the order of milliseconds), requires only very brief breath-holds, and its two-dimensional images are not affected by typical MRA artifacts such as ringing and blurring. A standardized form was used to collect all relevant data.

Statistical Analysis

All statistical calculations were performed using SPSS (SPSS, Inc., Chicago, Illinois). Renal and diaphragm motion were calculated by linear regression of the translation vs. time data. The regression coefficient of the regression line can be interpreted as the velocity (in mm/second). To assess the presence of motion and to enable comparison of motion between both kidneys and diaphragm, one-way t-tests or Wilcoxon signed-rank tests were used. Possible correlations between motion, image quality, and artifacts were analyzed by calculating Spearman's correlation coefficients (for non-parametric distribution). P values < 0.05 were considered statistically significant.

Results

Computer Modeling

Source coronal and reformatted sagittal and transverse computer modeled images through the mid-point of the stenoses with no motion, and for a constant velocity cranio-caudal translation of 0.25 mm/second using linear, linear centric, and elliptical centric k-space acquisition orders are shown in Figure 1. Orthogonal line profiles obtained from the coronal partition through both normal and stenotic portions of the horizontal and 45° oblique vessel are shown in Figure 2. Stenosis measurements for

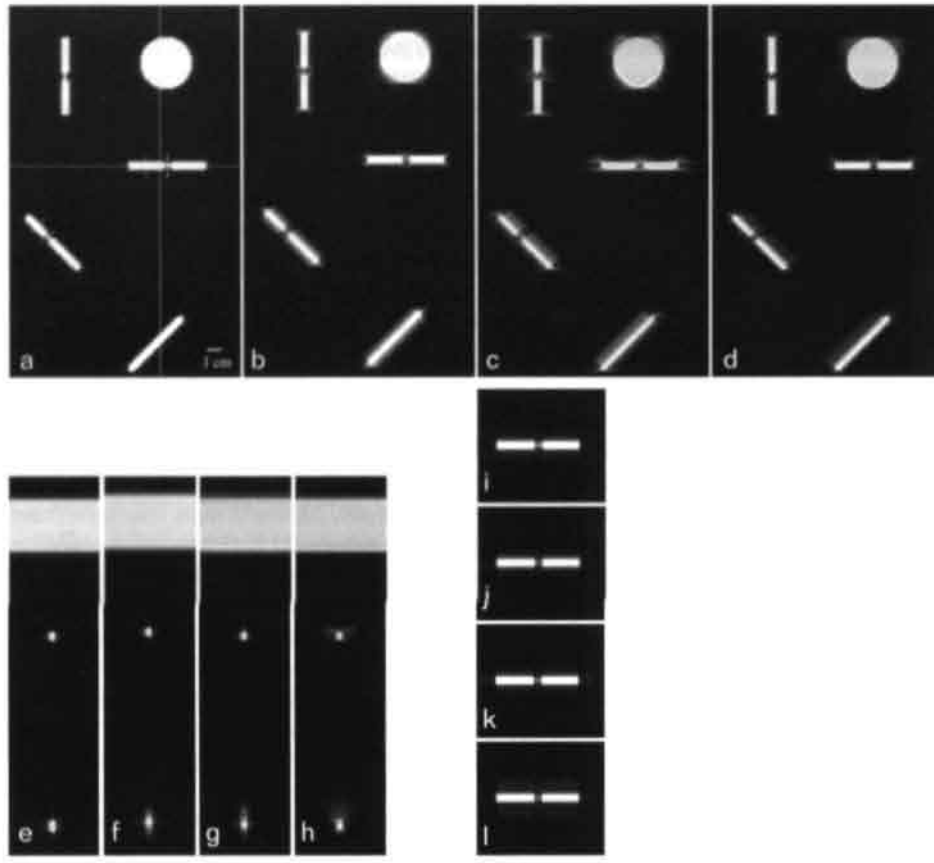

Figure 1. Three-dimensional phantom coronal simulations for cranial linear translation of 0.25 mm/second in a 26-second, 400 x 400 x35 matrix, SENSE factor 2 (left-right [y] direction) acquisition simulating a renal MRA. Source coronal images showing no motion (a), motion with linear (b), motion with linear centric (c), and motion with elliptical centric profile ordering (d) for a velocity of 0.25 mm/second. Sagittal reformats (vertical white line in Figure [a]) showing no motion (e), motion with linear (f), motion with linear centric (g), and motion with elliptical centric profile ordering (h) for a velocity of 0.25 mm/second. Transverse reformats (horizontal white line in Figure a) showing no motion (i), motion with linear (j), motion with linear centric (k), and motion with elliptical centric profile ordering (l) for a velocity of 0.25 mm/second. The four shortlines in Figure a represent the line plot trajectories for Figure 2. Windowing and leveling are identical for all scans.

all profile ordering variants based on coronal source images

(horizontal and 45° oblique vessel) and transverse reformats (horizontal vessel only) are shown in Figure 3 for velocities of 0 and 0.25 mm/second. Figure 4 demonstrates coronal slices and sagittal reformats as velocities range from 0 to 1 mm/second (elliptical centric profile ordering). In Figure 5, measured stenosis (coronal plane, elliptical centric profile ordering) for the horizontal and 45° angled vessel are plotted vs. velocity.

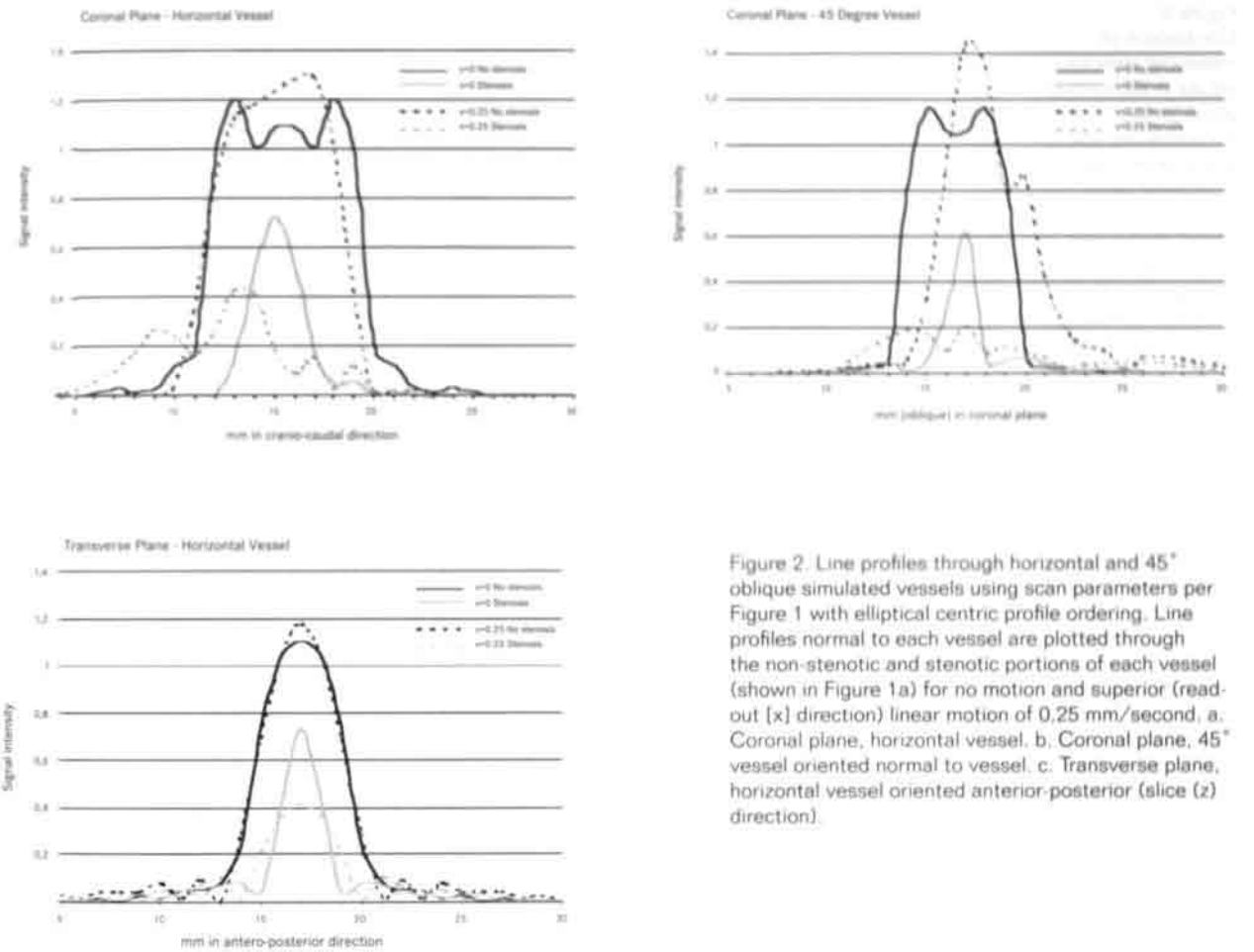

Figure 2. Line profiles through horizontal and 45° oblique simulated vessels using scan parameters per Figure 1 with elliptical centric profile ordering. Line profiles normal to each vessel are plotted through the non-stenotic and stenotic portions of each vessel (shown in Figure 1a) for no motion and superior (read-out [x] direction) linear motion of 0,25 mm/second. a. Coronal plane, horizontal vessel. b. Coronal plane, 45° vessel oriented normal to vessel. c. Transverse plane, horizontal vessel oriented anterior-posterior (slice (z) direction).

Patient Study

Of the 30 patients included in this study, six were excluded from analysis. Based on a previous study showing that for typical three-dimensional MRA scan parameters a minimum of 50% of the three-dimensional CE MRA scan duration (assuming centric k-space ordering) should be performed in breath-hold to minimize artifacts caused by breathing, five of these six patients were excluded because they exhibited one or more respiratory-like cycles of the diaphragm within 15 seconds of starting the dynamic two-dimensional acquisition (19). We consider these patients most likely to have more generalized respiratory artifacts, which could be falsely attributed to kidney motion during a sustained breath-hold, and therefore exclusion of these patients seems justified. The sixth patient was excluded from analysis because of inaccurate planning of the coronal dynamic two-dimensional scan, resulting in poor visualization of both kidneys.

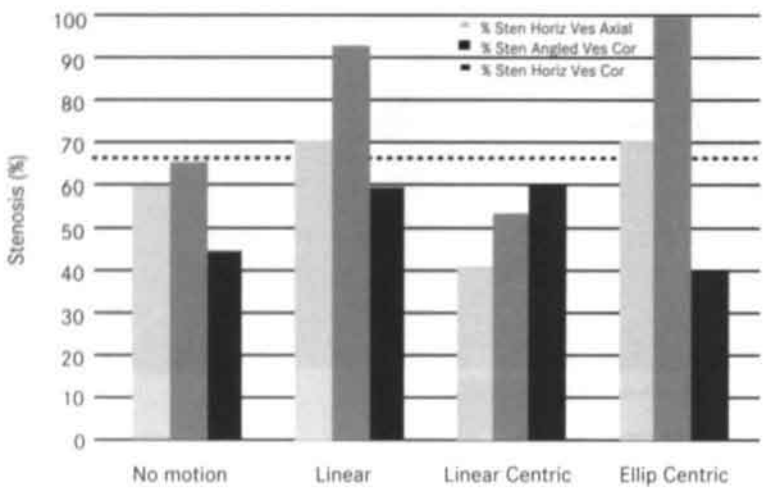

Figure 3. Comparison of measured stenosis values in the coronal plane for the horizontal and 45° vessel, and in the transverse plane for the horizontal vessel. Performed for no motion, and for a superior linear translation of 0.25 mm/second using linear, linear centric, and elliptical centric profile ordering. The dotted line indicates the true stenosis.

Motion

Analysis of motion in the transverse plane revealed no anterior/posterior or left-right renal motion during the breathhold. Statistically significant cranio-caudal motion was found for both the kidneys and the diaphragm (both $P < 0.001$). This motion followed a definite linear trend (Figure 6), with 36 of 48 kidneys having a R^2 value >0.9 (goodness of fit value for a linear model), and 40 of 48 kidneys having a R^2 value >0.8. The same linear trend was found for the diaphragm; 17 of 24 right diaphragms and 17 of 24 left diaphragms had a R^2 value >0.9, while 20 of 24 right diaphragms and 21 of 24 left diaphragms had a R^2 value >0.8. Mean velocities for the right kidney, left kidney, right diaphragm and left diaphragm were 0.26 ± 0.21 mm/second, 0.25 ± 0.23 mm/second, 0.43 ± 0.43 mm/second, and 0.29 ± 0.33 mm/second (mean ± SD), respectively. There was no significant difference between the right and left renal velocities ($P = 0.67$); however, a significant difference was found between velocities of the right and left diaphragm ($P = 0.01$). Strong correlations were found between renal velocities and velocity of the ipsilateral diaphragm, where Spearman's correlations coefficients were 0.80 and 0.81 ($p<0.01$) for the right and left side, respectively.

Image Quality and Artifacts

Figure 7 shows maximum intensity projections (MIP) of the renal arteries and kidneys in two patients, both of whom completed a full breath-hold during the three-dimensional CE MRA acquisition. One of these patients (Figure 7a) demonstrates the typical artifacts we initially attributed to respiratory motion.

Evaluation of renal artery segments 1 through 4, as depicted by three-dimensional CE MRA, showed progressive significant worsening of image quality when comparing any segment with its adjacent more distal segment. No significant correlations were found between velocity and image quality of the renal artery segments in all but one renal artery segment (observer 2; segment 2 of the right renal artery; Table 1). In contrast to this, statistically significant correlation coefficients were found with

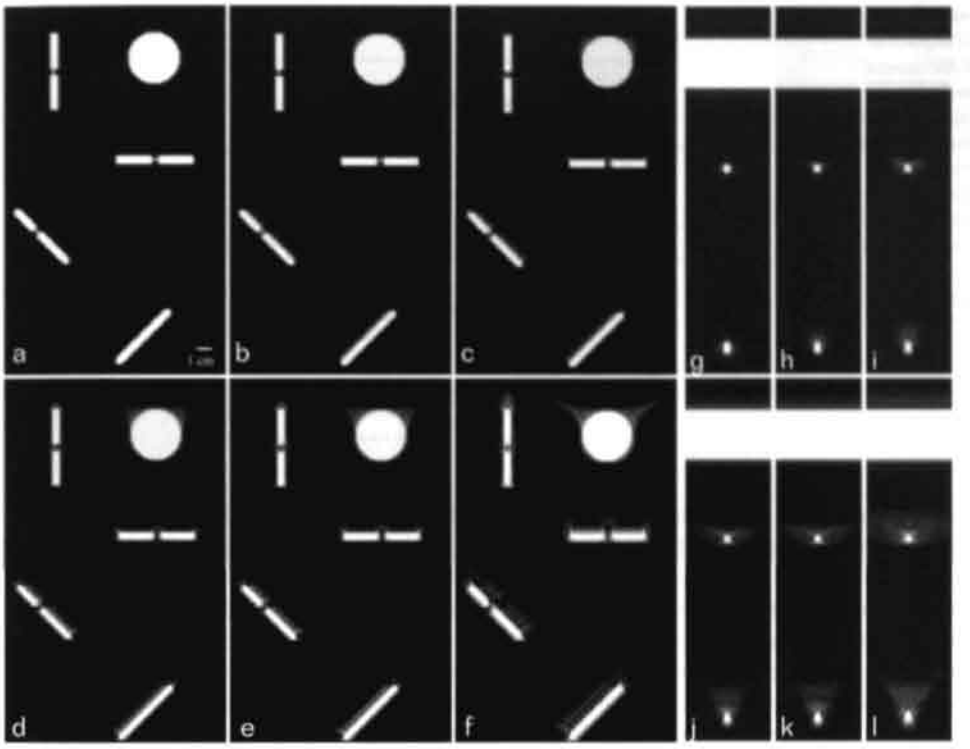

Figure 4. Simulated elliptical centric profile ordered coronal source images versus cranial linear translation velocity for no motion (a), 0.125 mm/second (b), 0.25 mm/second (c), 0.375 mm/second (d), 0.5 mm/second (e), and 1 mm/second (f). Simulated elliptical centric sagittal reformats for same velocities of no motion (g), 0.125 mm/second (h), 0.25 mm/second (i), 0.375 mm/second (j), 0.5 mm/second (k), and 1 mm/second (l). Windowing and leveling are identical for all velocities.

respect to velocity vs. the mean artifact score of both observers (0.46 and 0.41, right and left kidney, respectively; $P < 0.01$). The artifact scores between both observers were significantly correlated (correlation coefficients of 0.77 and 0.41 for the right [$P < 0.01$] and left kidney [$P < 0.05$], respectively).

The artifact scores for observer 1 were 1.4 ± 1.4 and 1.3 ± 1.2, while the concurrent values for observer 2 were 2.2 ± 1.0 and 1.9 ± 0.5 (mean $\pm$ SD; right and left kidney, respectively). Both observers indicated that artifacts primarily consisted of blurring, and (to a lesser degree) ringing, of renal artery segments 3 and 4, as well as the kidney itself. These findings were distributed equally over the right and left kidney.

Comparison with Ia-DSA

Ia-DSA revealed a total of 62 renal arteries (34 right and 28 left) in the 24 patients remaining for analysis. In this group, three patients had fibromuscular dysplasia (bilateral in two patients; unilateral [right] in one patient) that was located in segment 3 of the renal artery, and 2 patients had $\geq$ 50% atherosclerotic luminal narrowing

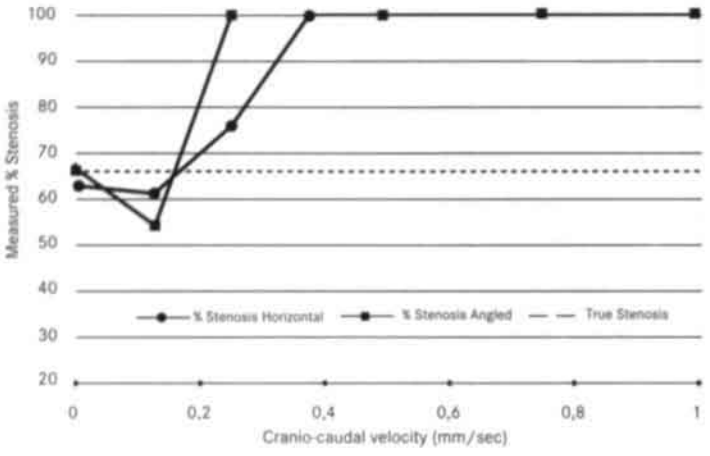

Figure 5. Stenosis measurements from simulated data in the coronal plane for horizontal and 45° vessel using elliptical centric profile ordering. Stenosis measured as full width of the moving stenotic vessel at one half the maximum of the no motion stenosis divided by the full width half maximum of the non-stenotic portion of the vessel x 100. Data are shown for both vessels vs. superior (read-out [x]) linear translation velocity (mm/second). True stenosis is 66.6% (2-mm stenosis, 6-mm lumen).

of the proximal (segment 2) renal artery (bilateral in one patient, unilateral [left] in the other patient). Observers 1 and 2 of the three-dimensional CE MRA scans *both detected 33 right renal arteries and 29 vs. 31 left renal arteries*, respectively. Re-evaluation of both the ia-DSA and MRA exams in cases discordant with respect to the number of arteries revealed that the right renal artery not seen by the MRA observers was a branch of the superior mesenteric artery, and due to overlap, was erroneously mistaken as a renal artery on ia-DSA. One small left renal artery, originating at the same level as the main renal artery, was not seen by ia-DSA, while multiplanar reformation of the MRA data enabled good visualization of the separate origin of this vessel; both observers found this vessel to be a left renal artery. The two left renal arteries only depicted by MRA observer 2 (not seen by MRA observer 1 or on ia-DSA) were most likely tiny lumbar arteries; however, due to the small vessel size and poor distal image quality, no clear-cut decision in these two cases could be made. Both observers failed to detect all three patients with fibromuscular dysplasia, while the patients with proximal atherosclerotic stenoses were correctly interpreted (Figure 8). No false-positive diagnoses were made by either observer.

Discussion

The computer simulation data provide insight into the type and magnitude of artifacts generated by constant velocity motion of the type encountered when performing CE renal MRA. First, note that for linear and linear centric profile ordering (Figures 1b, 1c, 1f, 1g, 1j, and 1k), the artifacts generated are confined to the x and y direction (coronal plane), whereas for elliptical centric profile ordering (Figures 1d, 1h, and 1l), artifacts propagate in all three axes. This occurs because for both linear and linear centric profile ordering, each line of k-space in the kz direction is traversed relatively rapidly (35 slices times TR of 5 msec = 175 msec). Thus to first order, the displacement during any line of kz acquisition is negligible, there is no phase modulation across k_z, and hence no artifacts propagate in the z direction. Note from

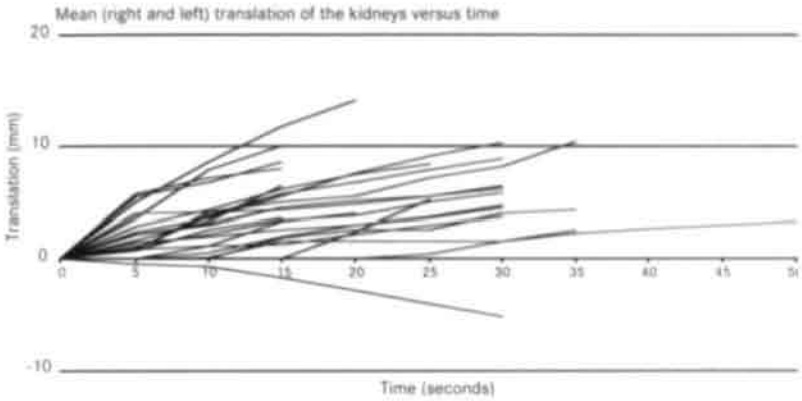

Figure 6. Mean (of left and right) cranio-caudal kidney translation versus time for the period of analysis (range 15-50 seconds) of each patient (n=24). Note the linearity of the translation in most cases.

Figure 1 that the mild artifacts present in the slice (z) direction with linear and linear centric profile ordering are present in the motionless simulation as well- these are caused by finite spatial resolution and Gibbs phenomenon (25). Elliptical centric profile ordering differs in that it is designed such that phase modulation occurs symmetrically relative to both phase encoding directions ky and kz (based on the radial distance from the k-space center), and hence artifacts propagate relatively uniformly in the y and z direction.

As demonstrated in Figure 1, the artifacts generated by linear profile ordering consist of blurring in the xy plane (Figures 1b and 1f), while linear centric causes a more severe ringing in the xy plane originating from edges in the direction of the motion (Figures 1c and 1g). Elliptical centric profile ordering, on the other hand, tends to produce milder ringing radiating diagonally in the xy and yz planes, again originating from edges, oriented outward in the direction of motion (Figures 1d and 1h and Figure 4). This type of artifact is often seen in renal MRA, most noticeably originating from the kidney and propagating superiorly in a diagonal direction (Figure 9). Qualitatively assessing image quality, linear centric profile ordering appears the least satisfactory. Even though transverse image quality is good (Figure 1k), note how the stenoses become deformed in the coronal plane (Figure 1c). Linear profile ordering seems somewhat better than elliptical centric in the transverse plane (as expected due to elliptical centric producing artifacts in the z direction - compare Figures 1j and 1l), although edges in the coronal plane appear sharper with elliptical centric profile ordering (Figures 1b vs. 1d). Examining the accuracy of stenosis measurement (Figure 3), both linear profile ordering and elliptical centric profile ordering are somewhat limited, particularly for the 45o angled vessel. Note that both techniques in the simulation markedly overcall stenosis in the 45o vessel. Realize also that the definition of vessel diameter becomes quite arbitrary, particularly for a 2-mm stenosis, where the line profile is quite broadened and deformed by even small amounts of motion (Figure 2). These simulations demonstrate just how much degradation in stenosis (or small vessel) visualization occurs due to the approximate

Table 1 Image quality per renal artery segment correlated with motion

Renal artery segment	Median IQ observer 1	IQ p-value observer 1*	Median IQ observer 2	IQ p-value observer 2*	Motion vs IQ cor coef observer 1	Motion vs IQ p-value observer 1**	Motion vs IQ cor coef observer 2	Motion IQ p-value observer
1R	4	NA	5	NA	-0.24	0.20	-0.31	0.08
2R	4	<0.01	4	<0.01	-0.21	0.25	-0.40	0.02
3R	3	<0.01	4	<0.01	-0.30	0.10	-0.26	0.15
4R	1	<0.01	1	<0.01	-0.08	0.68	-0.14	0.42
1L	4	NA	5	NA	0.05	0.80	0.02	0.92
2L	4	<0.01	4	<0.01	0.13	0.52	-0.08	0.67
3L	3	<0.01	3	<0.01	-0.25	0.19	-0.16	0.40
4L	1	<0.01	1	<0.01	0.00	1.00	-0.21	0.26

Renal artery segment: number indicates segment; R=right renal artery; L=left renal artery. Median IQ: IQ = image quality; median of image quality score. IQ P-value: P-value (Wilcoxon signed-rank test) of comparisons between image quality of a segment with the segment located more proximally; * P values <0.05 indicate statistically significant worsening of IQ;
NA=not applicable. Motion vs IQ cor coef and P-value: Spearman's correlation coefficients of image quality per renal artery segment versus kidney motion with the concurrent P-values of the correlation coefficients; ** P-values <0.05 indicates statistically significant correlation.

average 0.25 mm/second motion seen in our study patient population.

While at first glance linear profile ordering may appear to be the best choice (Figure 3), it has other limitations when used with CE MRA. First, centric techniques are much more forgiving for short (incomplete) breath-holds; note that five of 24 patients in our study held their breath for less than 20 seconds (19, 26). Second, given that much three-dimensional CE MRA today uses automated bolus detection (e.g. BolusTrak, Philips Medical Systems, Best, The Netherlands), some type of centric profile ordering is requisite. Hence, we focused further on elliptical centric profile ordering as the most practical profile ordering scheme. Figure 4 demonstrates coronal and sagittal simulation images for velocities up to 1 mm/second (slightly greater than the maximum seen in the patient study). Artifacts clearly become more severe for increasing velocity, with the true stenotic lumen not visualized beyond velocities of approximately 0.25 mm/second. This is demonstrated in Figure 5, which shows how inaccurately stenosis is measured (overestimated). For velocities much greater than 0.25 mm/second, these 66% simulated stenoses appear 100% occluded.

The clinical part of this study reveals the presence of significant renal and diaphragmatic cranial motion during sustained breath-hold at end inspiration, ranging from -5.2 to 23.1 mm and -16.6 to 32.5 mm, respectively (for a scan duration of 26 seconds). The distal renal artery typically has a close anatomic relation to the kidney; for that reason, the assumption of similar motion in the distal renal artery to that found in the kidneys seems justified. In this study, a strong correlation was found between renal motion and ipsilateral diaphragmatic motion. Diaphragmatic movement is well known to cause motion of the intra-abdominal organs and kidneys

during respiration. Therefore, renal motion during sustained breath-hold almost certainly relates to diaphragmatic motion. The underlying mechanism(s) that result in the observed linear cranial translation, however, remains unclear. Holland et al. (24) postulated progressive inspiratory muscle relaxation and a change in lung volume as an explanation for cranial diaphragmatic translation during an inspiratory breath-hold.

The observed average net renal displacement during breath-hold three-dimensional CE MRA is greater than the typically used voxel size, and thus jeopardizes the reliability of three-dimensional CE MRA for interpretation of the distal renal arteries. This is corroborated in this study, where minor to severe blurring and ringing artifacts were found to affect both segments 3 and 4 of the renal artery, as well as the kidney itself, adding to diagnostic uncertainty. The severities of artifacts in this study were found to correlate with motion. Image quality of segments 3 and 4 of the renal artery, however, had no clear correlation with motion. This can be explained by the fact that image quality becomes quite degraded by even minimal

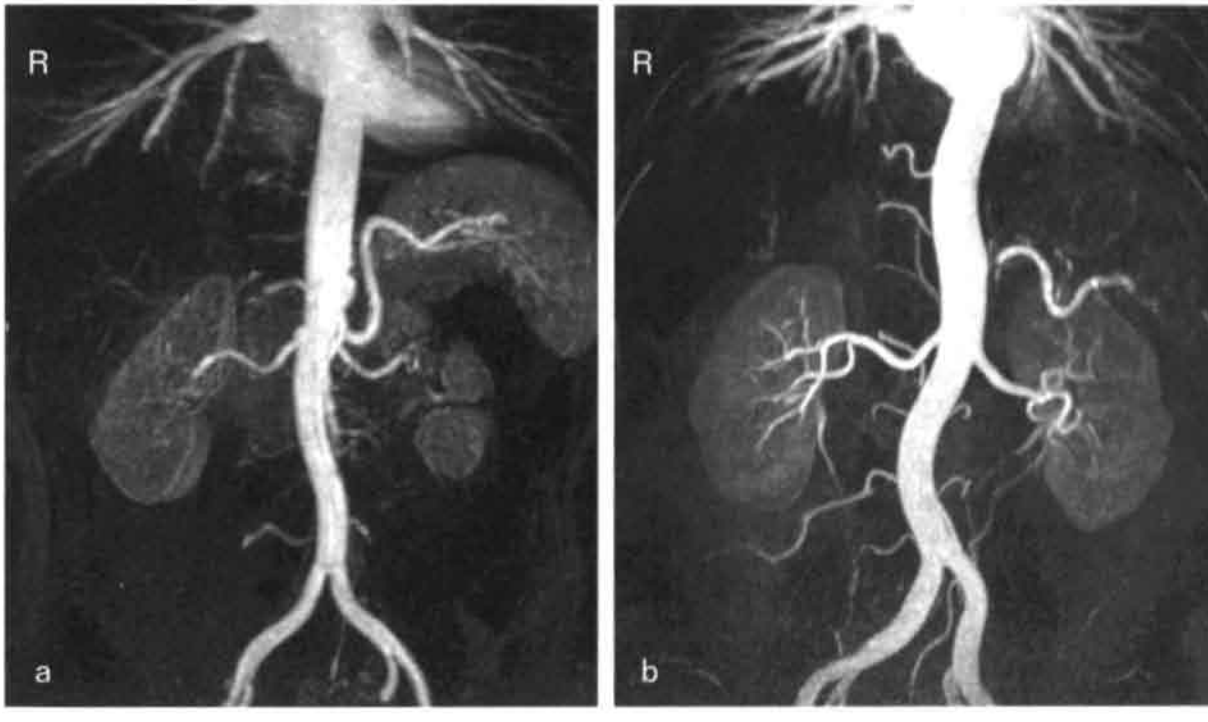

Figure 7. MIPs of two patients who sustained a breath-hold during the entire three-dimensional CE MRA acquisition. a: Segment 3 renal arteries are poorly visualized and the kidneys show respiratory-like artifacts resulting in image degradation of the distal renal artery. Kidney translation in this patient was 0.25 mm/second for the right kidney and 0.41 mm/second for the left kidney. b: Sharp delineation of segment 3 renal arteries and kidneys resulting in good distal image quality in a patient with no kidney translation during a breath-hold.

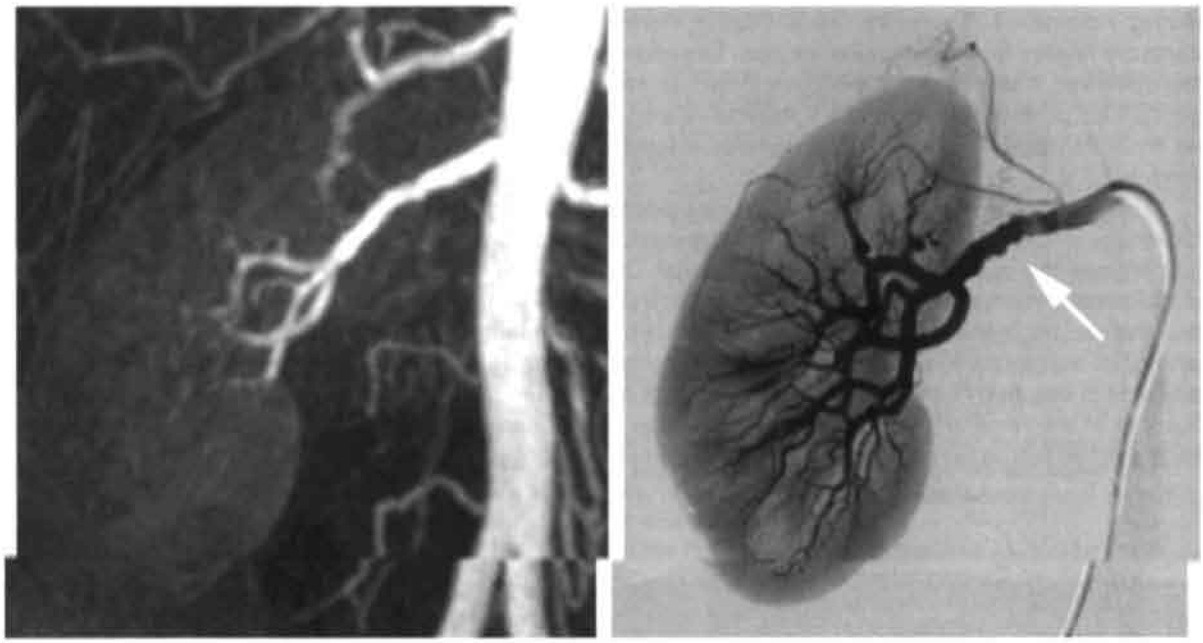

Figure 8. MIP (a) of a right renal artery and kidney as seen on 3D CE MRA compared with the corresponding selective ia-DSA image in a patient with unilateral fibromuscular dysplasia. MRA was unable to visualize the 'string of beads' which is clearly shown on selective ia-DSA (b).

kidney motion (≥ 0.25 mm/second; see computer modeling discussion and Figure 4). Moreover, segment 4 (the intra-parenchymal parts of the renal artery) is not typically visualized by three-dimensional CE MRA due to its small size and surrounding enhanced parenchyma.

To put the modeling findings (above) into context for the type of linear motion seen in this patient group, the most relevant parameter appears to be the net displacement over the scan duration. For example, based on Figures 4b and Figure 5, a velocity of 0.125 mm/second is likely acceptable in terms of image degradation. For our 26-second scan, this translates to a net displacement of 3.25 mm over the image acquisition. For an "average" patient with a velocity of 0.25 mm/sec, this would therefore require a scan time of under 13 sec. One approach to decreasing scan time to such a large degree is through using a smaller FOV, a shorter TR, an increased SENSE factor, or a combination of these. All of these techniques step through k-space more rapidly, either by decreasing the interval between successive k-space samples (shorter TR), or by taking larger steps through k-space (smaller FOV, SENSE). These techniques all alter the temporal relationship between displacement (motion) and k-space acquisition such that less displacement evolves within the same k-space radius (radial distance from the center of k-space) (19). An alternative, but almost certainly less acceptable approach is to decrease spatial

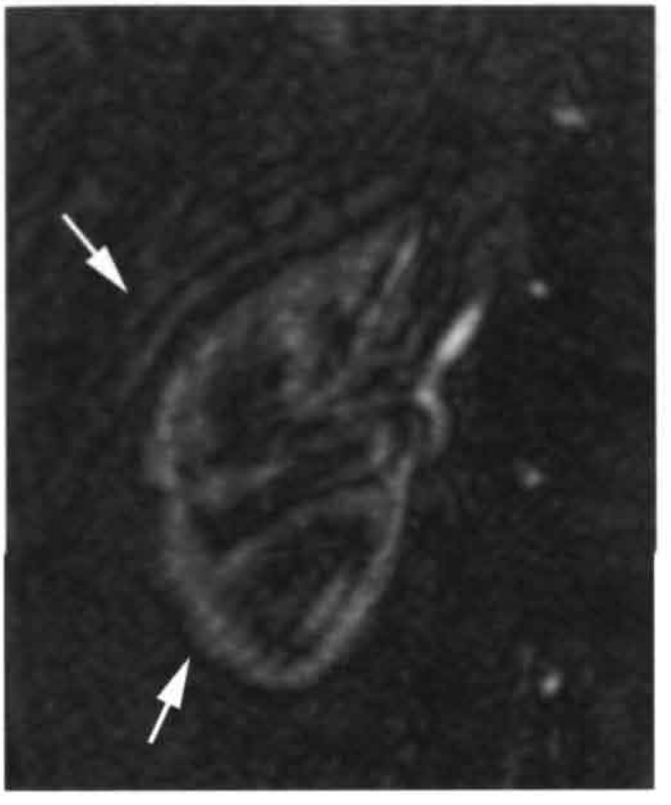

Figure 9. Original slice (coronal) of the right kidney from an MRA examination showing the typical artifacts also seen with the computer simulation (arrows).

resolution. This reduces scan time by decreasing the overall extent (size) of k-space collected, not collecting the higher frequency (more peripheral) k-space lines in order to reduce acquisition time. This, however, does not change the temporal relationship between displacement and k-space acquisition (i.e., Δkz, Δky, and TR do not change), and therefore any displacement impacts the critical central k-space lines in a manner identical to that occurring without decreased spatial resolution (19). Thus, approaches that propagate more rapidly through k-space should decrease the detrimental effects of the motion type described here. Of these techniques, decreasing TR typically requires upgraded hardware. Decreasing FOV, on the other hand, is an easy, viable option (provided vessels can be adequately localized and aliasing can be tolerated), and SENSE simply requires the appropriate software and a quick reference scan (2, 27).

Holland and co-workers found less diaphragmatic translation using an end-expiratory breath-hold (24). At our institution, we found end-expiratory breath-hold essentially impossible to sustain for a scan duration of 26 seconds (clinical observations). End-expiratory breath-hold, however, becomes more feasible with the shorter scan durations that can be achieved using the techniques mentioned above.

Because the aorta does not move significantly with respiration, the linear breath-hold drift reported here for the kidney must taper to near zero at the renal ostium.

This likely explains why renal MRA does better at defining stenoses than would be predicted based on Figure 5; most stenoses are quite proximal and therefore unaffected by this type of motion. As we attempt to better define the more peripheral renal arteries (for example to reliably diagnose fibromuscular dysplasia), this type of motion becomes more relevant, as clearly illustrated in this study, where both observers missed all three patients with fibromuscular dysplasia (Figure 8). Thus, we must either ensure that the kidneys do not undergo significant displacement during a breath-hold, or we must decrease acquisition time according to how much breath-hold displacement is expected. This rationale has been proven effective in a recent comparative renal MRA study using SENSE to decrease acquisition time, demonstrating significant improvement in distal renal artery image quality with the shorter SENSE acquisition (28). To those that argue short acquisition time leads to decreased signal-to-noise ratio (SNR), the simulation images as presented here have infinite SNR, and that does not compensate for the motion-related image degradation seen in Figure 7. Recently developed contrast media with higher T_1-reducing properties may help to compensate for acquisition time-related decreases in SNR (29).

In conclusion, this study has demonstrated the presence of significant near linear cranio-caudal renal (and therefore distal renal artery) motion despite sustained breath-holding during three-dimensional CE renal MRA. The (potential) effects of this motion on clinical CE MRA evaluation have been discussed, with particular attention to the small distal renal arteries. Other than some type of motion correction (which is in theory possible for a known motion), reducing scan time by increasing SENSE factor and/or shortening TR (which may also enable end-expiratory breath-holding) currently seems to be the best solution for reducing the detrimental effects of this motion. Implementation of a coronal two-dimensional dynamic TFE scan (or a similar sequence) before three-dimensional CE renal MRA enables quantification of breath-hold drift from which a patient-tailored three-dimensional CE MRA protocol can subsequently be created. Future studies will elucidate whether this method results in more reliable distal renal artery assessment.

References

1. Vasbinder GB, Nelemans PJ, Kessels AG, Kroon AA, de Leeuw PW, van Engelshoven JM. Diagnostic tests for renal artery stenosis in patients suspected of having renovascular hypertension: a meta-analysis. Ann Intern Med 2001; 135: 401-411.
2. Fain SB, King BF, Breen JF, Kruger DG, Riederer SJ. High-spatial-resolution contrast-enhanced MR angiography of the renal arteries: a prospective comparison with digital subtraction angiography. Radiology 2001; 218: 481-490.
3. Masunaga H, Takehara Y, Isoda H, Igarashi T, Sugiyama M, Isogai S, Kodaira N, et al. Assessment of gadolinium-enhanced time-resolved three-dimensional MR angiography for evaluating renal artery stenosis. AJR Am J Roentgenol 2001; 176: 1213-1219.
4. Mittal TK, Evans C, Perkins T, Wood AM. Renal arteriography using gadolinium enhanced three-dimensional MR angiography--clinical experience with the technique, its limitations and pitfalls. Br J Radiol 2001; 74: 495-502.
5. Qanadli SD, Soulez G, Therasse E, Nicolet V, Turpin S, Froment D, Courteau M, et al. Detection of renal artery stenosis: prospective comparison of captopril-enhanced Doppler sonography, captopril-enhanced scintigraphy, and MR angiography. AJR Am J Roentgenol 2001; 177: 1123-1129.
6. Voiculescu A, Hofer M, Hetzel GR, Malms J, Modder U, Grabensee B, Hollenbeck M. Noninvasive investigation for renal artery stenosis: contrast-enhanced magnetic resonance angiography and color Doppler sonography as compared to digital subtraction angiography. Clin Exp Hypertens 2001; 23: 521-531.
7. Cochran ST, Bomyea K, Sayre JW. Trends in adverse events after IV administration of contrast media. AJR Am J Roentgenol 2001; 176: 1385-1388.
8. Dunnick NR, Sfakianakis GN. Screening for renovascular hypertension. Radiol Clin North Am 1991; 29: 497-510.
9. van Jaarsveld BC, Krijnen P, Pieterman H, Derkx FH, Deinum J, Postma CT, Dees A, et al. The effect of balloon angioplasty on hypertension in atherosclerotic renal-artery stenosis. Dutch Renal Artery Stenosis Intervention Cooperative Study Group. N Engl J Med 2000; 342: 1007-1014.
10. Bakker J, Ligtenberg G, Beek FJ, Reedt Dortland RW, Hene RJ. Preoperative evaluation of living renal donors with gadolinium-enhanced magnetic resonance angiography. Transplantation 1999; 67: 1167-1172.
11. Rieumont MJ, Kaufman JA, Geller SC, Yucel EK, Cambria RP, Fang LS, Bazari H, et al. Evaluation of renal artery stenosis with dynamic gadolinium-enhanced MR angiography. AJR Am J Roentgenol 1997; 169: 39-44.
12. Shetty AN, Bis KG, Kirsch M, Weintraub J, Laub G. Contrast-enhanced breath-hold three-dimensional magnetic resonance angiography in the evaluation of renal arteries: optimization of technique and pitfalls. J Magn Reson Imaging 2000; 12: 912-923.
13. Ahmad NR, Huq MS, Corn BW. Respiration-induced motion of the kidneys in whole abdominal radiotherapy: implications for treatment planning and late toxicity. Radiother Oncol 1997; 42: 87-90.
14. Moerland MA, van den Bergh AC, Bhagwandien R, Janssen WM, Bakker CJ, Lagendijk JJ, Battermann, JJ. The influence of respiration induced motion of the kidneys on the accuracy of radiotherapy treatment planning, a magnetic resonance imaging study. Radiother Oncol 1994; 30: 150-154.
15. Schwartz LH, Richaud J, Buffat L, Touboul E, Schlienger M. Kidney mobility during respiration. Radiother Oncol 1994; 32: 84-86.
16. Wilman AH, Riederer SJ, Grimm RC, Rossman PJ, Wang Y, King BF, Ehman RL. Multiple breathhold three-dimensional time-of-flight MR angiography of the renal arteries. Magn Reson Med 1996; 35: 426-434.

17. Kaandorp DW, Vasbinder GB, de Haan MW, Kemerink GJ, van Engelshoven JM. Motion of the proximal renal artery during the cardiac cycle. J Magn Reson Imaging 2000; 12: 924-928.
18. Maki JH, Prince MR, Londy FJ, Chenevert TL. The effects of time varying intravascular signal intensity and k-space acquisition order on three-dimensional MR angiography image quality. J Magn Reson Imaging 1996; 6: 642-651.
19. Maki JH, Chenevert TL, Prince MR. The effects of incomplete breath-holding on three-dimensional MR image quality. J Magn Reson Imaging 1997; 7: 1132-1139.
20. Wilman AH, Riederer SJ. Improved centric phase encoding orders for three-dimensional magnetization-prepared MR angiography. Magn Reson Med 1996; 36: 384-392.
21. Pruessmann KP, Weiger M, Scheidegger MB, Boesiger P. SENSE: sensitivity encoding for fast MRI. Magn Reson Med 1999; 42: 952-962.
22. Renal Artery Diagnostic Imaging Study in Hypertension (RADISH). Sponsored by the Dutch Healthcare Insurance Board. Grant number OG97-003. November 1999-November 2001.
23. Willinek WA, Gieseke J, von Falkenhausen M, Hoogeveen RM, Textor J, Urbach H, Schild HH, et al. CE-three-dimensional MRA of the supraaortic arteries at 512 and 1024 matrix: the use of randomly segmented central k-space ordering (CENTRA). Abstract in Proc Intl Soc Magn Reson Med 10 (2002).
24. Holland AE, Goldfarb JW, Edelman RR. Diaphragmatic and cardiac motion during suspended breathing: preliminary experience and implications for breath-hold MR imaging. Radiology 1998; 209: 483-489.
25. Hashemi RH, Bradley WG. Artifacts in MRI. In: Hashemi RH, Bradley WG, editors. MRI: the basics, 1st ed. Baltimore, MD: Williams and Wilkins; 1997. p. 181-183.
26. Wilman AH, Riederer SJ. Performance of an elliptical centric view order for signal enhancement and motion artifact suppression in breath-hold three-dimensional gradient echo imaging. Magn Reson Med 1997; 38: 793-802.
27. Weiger M, Pruessmann KP, Kassner A, Roditi G, Lawton T, Reid A, Boesiger P. Contrast-enhanced three-dimensional MRA using SENSE. J Magn Reson Imaging 2000; 12:671-677.
28. Wilson GJ, Maki JH, Evitts M, Eubank W, Hoogeveen RM. A direct comparison study to evaluate the usefulness of sensitivity encoding (SENSE) in evaluating renal artery stenosis using MR angiography. Abstract in the Proceedings of the XIII Annual International Workshop on MRA, Madison, WI. 2001; 30-31.
29. Knopp MV, Tengg-Kobligk H, Floemer F, Schoenberg SO. Contrast agents for MRA: future directions. J Magn Reson Imaging 1999; 10: 314-316.

Pitfalls and limitations of contrast-enhanced renal magnetic resonance angiography for the detection of atherosclerotic renal artery stenosis

G.B.C. Vasbinder, P. J. Nelemans, A.G.H. Kessels, T. Leiner, J.H. Maki, M.W. de Haan, M.B.J.M. Korst, D. Koster, T.K. Oei, P.N. Lohle, J. J. Teertstra, H.M. Pasmans, J.O. Barentsz, J.M.A. van Engelshoven.

Abstract

Purpose

In a recent large multicenter study (Renal Artery Diagnostic Imaging Study in Hypertension [RADISH]), we found three-dimensional, contrast-enhanced magnetic resonance angiography (MRA) to have poor sensitivity for the diagnosis of renal artery stenosis. The purpose of the present study was to identify causes of the poor sensitivity of MRA for the diagnosis of atherosclerotic renal artery stenosis (ARAS).

Methods

In the RADISH study the most severe atherosclerotic stenosis per kidney as seen on MRA and DSA was categorized on a five-point scale: 0% to 19% (grade 1); 20% to 49% (grade 2); 50% to 74% (grade 3); 75% to 99% (grade 4); and total occlusion (grade 5). Out of the 710 kidneys (356 patients) analyzed, kidneys with discrepant findings between MRA and DSA with respect to the severity of ARAS were evaluated. For analysis, kidneys with discrepancies of two or more grades were selected. Retrospectively, a non-blinded reviewer analyzed the selected MRA and DSA images in order to explore the causes of the observed discrepancies.

Results

Seventy-nine kidneys with discrepancies of 2 or more grades were included. Incorrect MRA image evaluation, the limited spatial resolution of MRA, and artifacts caused by distal renal artery motion during MRA data acquisition, were found to be the most frequent causes of discrepancy between MRA and DSA (76% of all discrepancies). DSA was incorrect in 15% of the cases. For 48 kidneys diagnosed with FMD by MRA, incorrect MRA image evaluation (56%) and motion artifacts (29%) were the most frequent causes of false-positive FMD diagnosis.

Conclusions

This study demonstrates that incorrect MRA image evaluation, MRA spatial resolution limitations, and MRA motion artifacts, are the most frequent reasons for discrepancies between MRA and DSA, and therefore contribute most substantially to the poor overall sensitivity of MRA. Future developments that overcome the artifacts and limitations of MRA data acquisition and improve MRA image evaluation may ultimately result in more accurate MRA exams.

Introduction

Renovascular hypertension is the most common form of secondary hypertension, and is caused by renal artery stenosis as a result of either atherosclerosis or fibromuscular dysplasia (FMD) (1). Timely detection of a clinically relevant stenosis is important because current treatment options, such as surgery, percutaneous transluminal renal angioplasty with or without stent placement, and medical therapy may cure or improve hypertension and prevent the associated progressive loss of renal function (2-5). Currently, intra-arterial digital subtraction angiography (DSA) is considered the standard of reference for the detection of renal artery stenosis. This test, however, is invasive and occasionally results in serious complications such as arterial dissection and adverse contrast agent reactions (6-9) .

Recently, several alternative minimally invasive diagnostic imaging tests have become available for the detection of ARAS. In a recent meta-analysis, it was shown that using DSA as a standard of reference, three-dimensional contrast-enhanced magnetic resonance angiography (MRA) performed significantly better than non contrast-enhanced magnetic resonance angiographic techniques, ultrasonography, captopril scintigraphy, and the captopril test for the non-invasive assessment of the presence of a clinically relevant renal artery stenosis in patients suspected of renovascular hypertension (10). The MRA studies that met the inclusion criteria for meta-analysis had sensitivities ranging from 88% to 100% and specificities ranging from 75% to 100%. This meta-analysis, however, was only able to include six studies, and the number of patients per study was small (ranging from 20 to 88 patients).

Because of the favorable results published in the literature, renal artery MRA is now widely used in clinical practice as a non-invasive alternative to DSA to rule out renal artery stenosis in patients suspected of renovascular hypertension. Recently, we reported the results of a prospective multicenter study on the diagnostic accuracy of MRA, using DSA as the reference standard, in a large group of hypertensive patients who exhibited at least one clinical clue suggestive of renal artery stenosis (Renal Artery Diagnostic Study in Hypertension (RADISH)) (11). In direct contradiction to the results of other studies, MRA had poor overall sensitivity for the detection of renal artery stenosis (ranging from 57% to 67% for the three observers), while specificity was acceptable (ranging from 77% to 90%). Additional analyses of RADISH data showed a substantial rise in sensitivity when patients with DSA-proven FMD were excluded from analysis, indicating that this condition was partly responsible for the poor diagnostic performance. FMD is well known for its poor depiction by MRA (12-14). However, omitting FMD from analyses still did not result in sensitivities approaching those reported in literature, which leads to the conclusion that as presently performed, MRA is not sensitive enough to diagnose atherosclerotic renal artery stenosis (ARAS).

The results of the RADISH study, which conflict strongly with those of other studies, require an explanation. Therefore, we performed a retrospective analysis of the RADISH image data to identify factors that explain the poor diagnostic accuracy of MRA for the detection of atherosclerotic renal artery stenosis.

Methods

Subjects and methods

The RADISH study was a prospective multicenter study on diagnostic accuracy of MRA for the detection of renal artery stenosis in a large group of hypertensive patients who exhibited generally accepted clinical clues for the presence of renovascular hypertension. DSA was used as reference test. Detailed information on inclusion and exclusion criteria, demographic and clinical characteristics of the study subjects, diagnostic equipment, scan-protocols, and image evaluation are described in detail elsewhere (11).

In the RADISH study, a panel of three experienced observers (TL, JHM, MBJMK) independently evaluated all MRA data of 356 hypertensive patients (710 kidneys), while the DSA exams were evaluated in consensus by four vascular radiologists. On a standard form, the MRA and DSA observers indicated the image quality of the renal artery segments on a three-point scale, the nature and location of pathology (if present), and the severity of stenosis (for atherosclerotic lesions only - expressed as percentage of luminal narrowing). In instances where an observer judged an exam as a technical failure, this was noted as well. Each renal artery was considered to consist of an ostial segment (from the aortic ostium to 4 mm distally), and a truncal segment (compromising the remainder of the renal artery). Of the 356 patients, DSA showed clinically relevant renal artery stenoses in 72 patients (96 kidneys). Fifty-eight kidneys (60% of all affected kidneys) had ARAS, while 38 kidneys (40%) had FMD.

The present study focuses on ARAS, and for this reason all kidneys with DSA-proven FMD were excluded from analysis. The most severe renal artery stenosis per kidney as judged by each RADISH MRA observer and the DSA consensus was identified and categorized on a five-point scale: 0% to 19% (grade 1); 20% to 49%

Table 1 Distribution of discrepancies with respect to the severity of renal-artery stenosis between MRA and DSA (n=672 kidneys)

MRA Observer	Under estimation of ≥2 grades by MRA	Under estimation of ≥1 grade by MRA	Perfect agreement	Over estimation of ≥1 grade by MRA	Over estimation of ≥2 grades by MRA	Total number of kidneys discrepant ≥2 grades	FMD as diagnosis on MRA
	no.	no.	no.	no.	no.	no.	no.
Observer A	12	38	456	160	44	56	18
Observer B	4	41	507	104	33	37	20
Observer C	6	53	531	72	17	23	16

MRA= three-dimensional contrast-enhanced magnetic resonance angiography. DSA= digital subtraction angiography. FMD= fibromuscular dysplasia Numbers indicate kidneys. All kidneys with DSA-proven FMD are excluded.
A five-point scale was used to classify the severity of renal-artery stenosis; 0% - 19% (grade 1); 20% - 49% (grade 2); 50% - 74% (grade 3); 75% - 99% (grade 4); and occlusion (grade 5).

Table 2 Classification of causes that resulted in discrepancies in observed severity of ARAS between MRA and DSA (n=79 kidneys)*

Causes of discrepancy (in retrospect and unblinded)	Good mra image quality discrepancy by:				Sub-optimal mra image quality discrepancy by:				Total
	1 observer		>1 observer		1 observer		>1 observer		
	under-rated	over-rated	under-rated	over-rated	under-rated	over-rated	under-rated	over-rated	
Related to MRA data acquisition:									
- distal renal artery motion artifacts on MRA	-	1	-	-	-	7	1	5	14
- contrast-timing related artifacts on MRA	-	-	-	-	-	2	-	2	4
- metallic implants artifacts on MRA (including stents)	-	-	-	-	-	1	-	-	1
- technical failure during MRA due to other reasons	-	-	-	-	-	1	-	-	1
- MRA 3D volume did not include the (entire) renal artery	-	-	-	-	-	1	-	-	1
- inadequate spatial resolution of MRA	2	1	1	1	3	4	2	4	18
Related to MRA image evaluation:									
- re-evaluation of MRA shows no discrepancy with DSA	2	15	-	4	1	6	-	-	28
Related to limitations of DSA:									
- re-evaluation of DSA shows no discrepancy with MRA	1	3	1	-	-	1	-	-	6
- MRA 3D postprocessing techniques visualized renal artery not seen on DSA	-	-	1	2	-	2	-	1	6
									79

ARAS= atherosclerotic renal artery stenosis.

*Kidneys that were diagnosed with FMD by MRA are not included in this Table.

(grade 2); 50% to 74% (grade 3); 75% to 99% (grade 4) and total occlusion (grade 5). Because our goal was to focus on factors that resulted in considerable discrepancies between MRA and DSA, differences in stenosis severity of two or more grades were chosen for analysis. This approach assumes that a one-grade discrepancy is most likely due to subtle variations in interpretation. In addition, separate analyses were performed for all kidneys with the false-positive diagnosis FMD as judged by one or more of the MRA observers.

For each MRA observer the distribution of underestimations, overestimations, and perfect agreements between MRA and DSA, as well as the number of kidneys diagnosed with FMD by MRA, for the 672 kidneys without DSA-proven FMD are shown in Table 1.

In the present study, one experienced reviewer who had not previously evaluated the MRA and DSA data (GBCV) performed retrospective evaluation of the MRA and DSA data of the kidneys included for analysis. Image evaluation took place using the same workstation used by the initial observers. The MRA images were

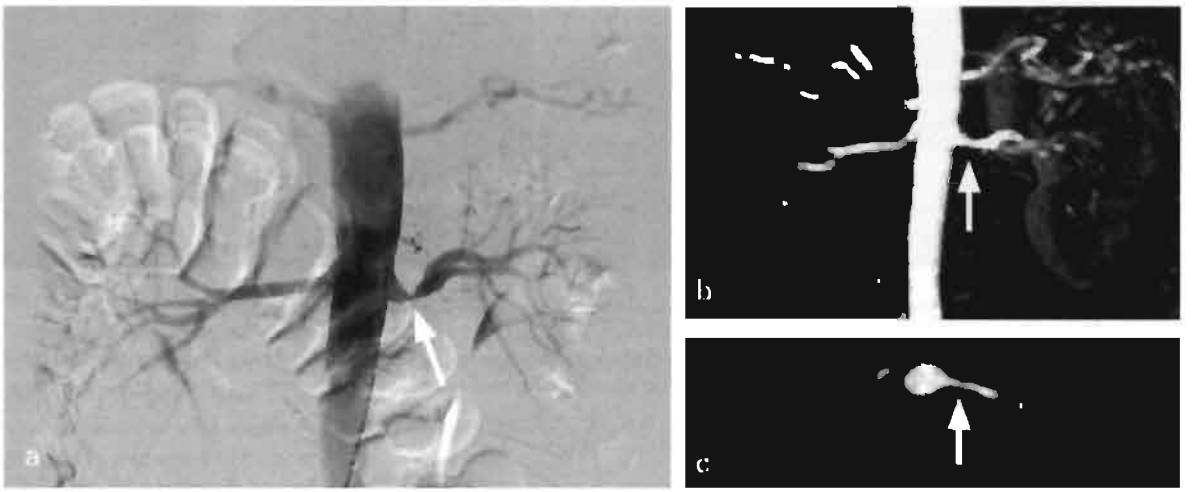

Figure 1: (a)DSA image showing a severe stenosis of the left renal artery (arrow). MRA only showed a slight left renal artery stenosis on both the original slices, (b) a maximum intensitity projection, and (c) a tranverse reformatted image. This discrepancy between MRA and DSA was considered to be caused by limited MRA spatial resolution.

evaluated prior to the DSA images and, at the time of MRA evaluation, the reviewer was unaware of the magnitude of the discrepancy. After making an initial assessment of the most likely reason for the discrepant result, the reviewer examined the evaluations of all MRA and DSA observers. Next, the reviewer assigned a subjective image quality score to the discrepant renal artery segment (using the three-point scale as described earlier), and subjectively assessed the reason for the discrepancy in severity of stenosis. In cases where the reviewer considered the MRA diagnosis instead of the DSA diagnosis to be correct, a consensus was reached by conferring with a DSA observer (MWDH).

Data analysis

The evaluations by the three MRA observers could and often did differ with respect to the magnitude of the discrepancy with DSA and the image quality for a discrepant renal artery segment. In cases where one observer underrated and the other two overrated, the severity of stenosis was considered overrated. In cases where all three observers arrived at different conclusions (for example one observer underrated, one observer overrated, and one observer gave a rating in agreement with DSA), the largest discrepancy was selected. In cases of equal discrepancies in opposite directions, the reviewer made the final judgment with respect to underrating or overrating.

The evaluations of the three RADISH observers and the reviewer (4 evaluations in total) were used to assess the overall MRA image quality. Using the best three scores, image quality was rated as good if at least two observers reported good image quality and none of the three observers reported poor image quality. In all other cases, overall image quality was considered sub-optimal.

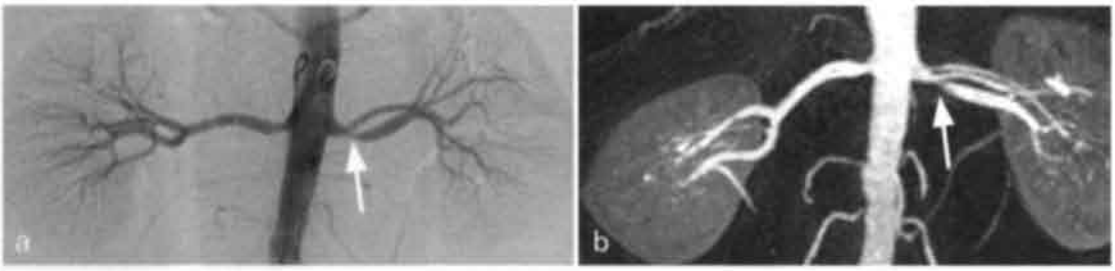

Figure 2: (a) DSA image showing a 50% stenosis of the left caudal segmental renal artery with distal post-stenotic dilatation (arrow). However, (b) a MRA maximum intensity projection depicted an additional segmental renal artery that overprojected on DSA and caused DSA to diagnose a false-positive renal artery stenosis. This example illustrates the addititional value of three-dimensional MRA postprocessing techniques.

Results

A total of 136 kidneys were either discrepant by ≥2 grades or diagnosed with FMD by MRA by one or more observers. Due to problems with digital data transfer at one participating hospital, the image data from 9 kidneys that were eligible for analysis were unavailable, leaving 127 kidneys (70 right kidneys and 57 left kidneys) for analysis. Of the 127 kidneys, 10 kidneys demonstrated discrepancies between MRA and DSA for all three observers, while 20 kidneys and 97 kidneys demonstrated discrepant results by 2 observers and 1 observer, respectively. Twenty-four kidneys had a DSA-proven clinically relevant atherosclerotic renal artery stenosis (grade 3 or greater; 13 ostial stenoses and 11 truncal stenoses). Out of the 127 kidneys included for analysis, 79 kidneys were discrepant based on differences between MRA and DSA with respect to the severity of atherosclerotic lesions, while the remaining 48 kidneys were included because they were false-positively diagnosed to have FMD by MRA. The results of the analysis of the two distinct groups of discrepancies will be presented and discussed separately, and can subjectively be broken down into 1) discrepancies related to MRA data acquisition problems; 2) discrepancies related to incorrect MRA image evaluation; and 3) discrepancies related to limitations of DSA.

The findings upon re-evaluation of the MRA image data for the 79 kidneys discrepant for measured severity of atherosclerotic renal artery stenosis are shown in Table 2. In 39 kidneys (49%), MRA data acquisition problems were considered to have caused the discrepancy.

Distal renal artery motion artifacts were considered the cause of the discrepancy in 14 kidneys, which resulted in overrating of the severity of stenosis for all but 3 kidneys.

Contrast-timing related artifacts on MRA were seen in 4 kidneys ('ringing' in 2 kidneys and insufficient contrast agent present during data acquisition in 2 kidneys). Metallic stent artifact, technical failure, and exclusion of a portion of the renal artery from the acquired image volume, each accounted for one discrepant kidney. Inadequate MRA spatial resolution was the most frequent explanation in this group (18 kidneys - Figure 1). Limited MRA spatial resolution was considered the cause of discrepancy between MRA and DSA when DSA clearly visualized a well delineated renal artery with or without stenosis, while no other MRA artifact was likely to have

Table 3 Classification of causes that resulted in discrepancies between MRA and DSA because of the diagnosis FMD by MRA (n=48 kidneys)*

Causes of discrepancy (in retrospect and unblinded)	Good MRA image quality		Sub-optimal MRA image quality		Total
	discrepancy by:		discrepancy by:		
	1 observer	>1 observer	1 observer	>1 observer	
Related to MRA data acquisition:					
- distal renal artery motion artifacts on MRA	1	-	11	2	14
- inadequate spatial resolution of MRA to depict lesion	2	1	1	-	4
Related to image evaluation:					
- re-evaluation of MRA shows no discrepancy with DSA	14	-	12	1	27
Related to limitations of DSA:					
- re-evaluation of DSA shows no discrepancy with MRA	1	-	-	-	1
- MRA evaluated renal artery not depicted by DSA	1	-	1	-	2
					48

FMD= fibromuscular dysplasia

*Kidneys that were diagnosed with atherosclerotic renal artery stenosis (ARAS) by MRA are not included in this Table.

caused the discrepancy.

In 28 of the 79 kidneys (35%), discrepancies were considered to be related to incorrect MRA image evaluation. For this group, in retrospect and with awareness of the DSA results, similar diagnoses as those that were initially made on DSA could be confirmed on MRA (overrating in 25 kidneys). In all but 4 of the 28 kidneys, a discrepancy was seen for only one of the three MRA observers.

Discrepancies related to limitations of DSA were attributed to 12 of the 79 kidneys (15%). In contrast to discrepancies related to MRA image evaluation, the diagnoses initially made by MRA could retrospectively be confirmed by DSA for 6 kidneys (overrating in 4 kidneys). MRA post-processing techniques depicted a renal artery that was not visible on DSA in another 6 kidneys. For 5 of these 6 kidneys, MRA found a renal artery stenosis in an artery that was missed by DSA. In the remaining kidney, MRA was able to exclude the presence of a DSA-proven stenosis because overprojection of the renal artery that was missed by DSA suggested the presence of a stenosis (Figure 2).

A breakdown of the remaining group of 48 kidneys that were discrepant because MRA diagnosed FMD is shown in Table 3. In the great majority (92%), discrepancies were seen because of FMD being diagnosed by one observer only. In retrospect, 27 kidneys (56% in this group) did not show discrepancies with DSA. Motion artifacts were considered to have caused the incorrect diagnosis by MRA in 14 kidneys (29%). Other causes accounted for the discrepancy in the remaining 7 kidneys (15%).

Discussion

In the present study, we attempted to identify causes that contributed to discrepancies with respect to the severity of atherosclerotic renal artery stenosis between MRA and DSA. Only kidneys without DSA-proven fibromuscular dysplasia were analyzed. Kidneys considered to have FMD by MRA will be discussed separately in this discussion. Three major categories resulting in discrepancies with respect to the measured severity of atherosclerotic lesions were identified; 1) discrepancies related to MRA data acquisition; 2) discrepancies related to MRA image evaluation; and 3) discrepancies related to limitations of DSA.

MRA Data Acquisition

First, a number of discrepancies were found to be related to limitations or failures of MRA data acquisition. This accounted for the discrepancy in 49% of the analyzed kidneys. The most frequently observed limitation in this category was inadequate spatial resolution. The limited voxel size of MRA relative to vessel size and the inherent partial volume effects may result in inaccurate visualization of a renal artery and hamper the correct assessment of the presence or absence of a stenosis (15). In the present study, this limitation was considered the reason for the discrepancy between MRA and DSA when DSA clearly visualized a well delineated renal artery with or without a renal artery stenosis and, in the reviewers opinion, no other artifact (in particular motion) was likely to have contributed substantially to the observed discrepancy. In the study, the limited spatial resolution of MRA more frequently led to overrating a stenosis (10/18 cases - Table 2).

A frequently observed limitation of MRA in this study was motion. Motion is known to cause blurring and ringing artifacts on MRA images (16). This artifact caused sub-optimal image quality in the majority of the kidneys in the group that was considered discrepant because of motion. All discrepancies caused by motion were located in the truncal segment and resulted in a false-positive result in 13 out of 14 kidneys. A recent study described the presence of linear cranial motion (drift) of the kidneys during MRA, despite breath holding, at an average of 0.26 mm/second, and further quantified the detrimental effects of this motion on distal renal artery image quality (17). The motion artifacts seen in the current study corroborate the findings of the aforementioned study, and emphasize the present limitations of renal MRA to assess reliably the distal renal artery in clinical practice.

While current technical developments allow for an increase in the spatial resolution of MRA using techniques such as parallel imaging and ultra-short TR, MRA spatial resolution still falls short of DSA. In addition, high intrinsic spatial resolution cannot be truly realized in the presence of motion. This argues for extremely rapid MR acquisition times substantially shorter than the 20-25 seconds used here and elsewhere, and/or for algorithms that can correct for motion such as cardiac and respiratory triggering- or gating. Other reasons for discrepancies ascribed to MRA data acquisition were occasionally seen, with contrast-timing related artifacts being the most frequent (4 kidneys). With the exception of metallic implants, the remaining artifacts could have been prevented (operator's errors) and, therefore, will not be discussed further.

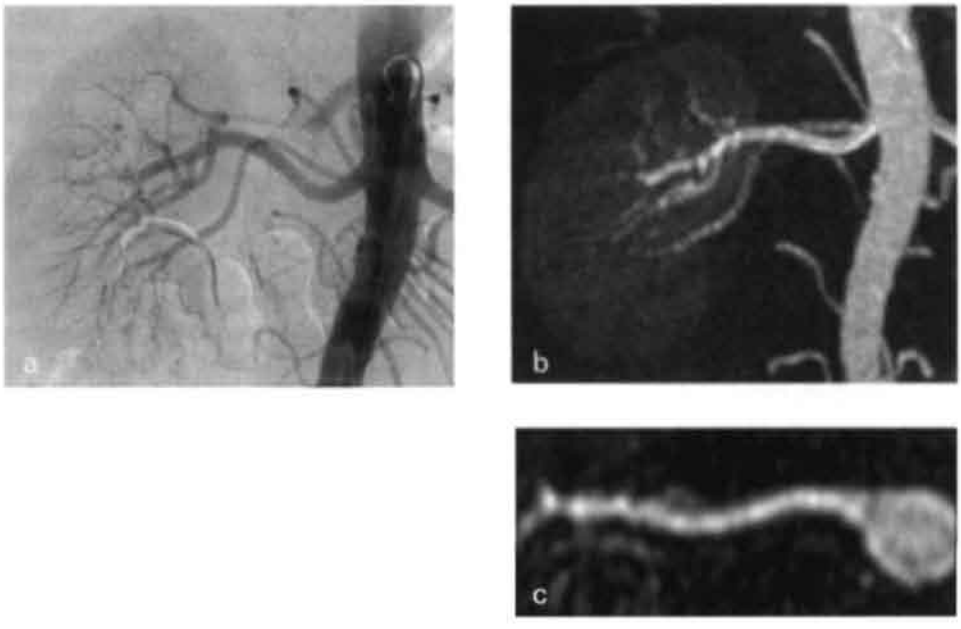

Figure 3: (a) DSA image of the right renal artery showing a patent proximal and distal renal artery. (b) MRA maximum intensity projection, and (c) MRA curved transverse reformatted image, showing the typical signal-to-noise related spiculations of the distal renal artery that may mimic fibromuscular dysplasia.

MRA Image Evaluation

Next, the discrepancies arising from MRA image evaluation must be discussed. This source of error accounted for 35% of all discrepancies (28 of 79 kidneys). For these kidneys, the initial diagnosis by DSA could retrospectively be confirmed on MRA. Overrating by MRA was observed in 25 kidneys (25/28 - 89%). The renal arteries of most kidneys were rated as good MRA image quality, and discrepancies in the majority of cases resulted from misinterpretation by only 1 of the 3 observers (24 out of 28 kidneys - 86%). For the two other observers the MRA diagnosis was in agreement with the DSA diagnosis. This finding suggests that a uniform approach of image evaluation and assessment of RAS may reduce the number of misinterpretations and improve interobserver agreement, which was only moderate in the RADISH study (ranging from 0.40 to 0.51). However, in the RADISH study, all observers evaluated the images using prior defined criteria and a standard form.

Limitations of DSA

Incorrect DSA image evaluation was considered the source of discrepancy in 6 kidneys; the initial MRA diagnosis was confirmed by retrospective evaluation of the DSA images by both the reviewer and one of the DSA observers. For another 6 discrepant kidneys, 3D MRA post-processing techniques enabled the depiction of a renal artery that was not visible on DSA. Due to the two-dimensional nature of DSA, it is often impossible to depict renal arteries that are obscured by a contrast-filled structure located anterior or posterior to an artery. In these cases, the 3D nature of MRA data can be fully exploited.

Although this study excluded kidneys with DSA-proven FMD, MRA diagnosed

48 kidneys with FMD. This finding indicates that MRA, besides missing FMD, also results in false-positive diagnoses of FMD. Retrospective evaluation of these false- positive FMD cases suggests that motion artifacts and incorrect MRA image evaluation were the primary causes for the observed discrepancy. In the great majority of the cases, the discrepancies were the result of a false-positive diagnosis by just one observer. In earlier literature, it has been reported that the 'stair step' artifact due to limited spatial resolution may mimic the typical 'string of beads' appearance of fibromuscular dysplasia (18). In the present study, however, this artifact was not observed. The effects of distal renal artery motion and signal-to-noise related spiculations are the most likely causes that have contributed to the false-positive diagnoses of FMD (Figure 3). Spin dephasing because of turbulence at the level where the main renal artery branches into the segmental renal arteries can potentially result in focal signal loss. This focal signal loss can be interpreted as FMD. However, since the MRA sequences used short TEs (typically under 2 msec) and flow in the distal renal artery should be relatively laminar, the presence of this kind of artifact in our study is unlikely.

In conclusion, this study has shown that the majority of discrepancies between MRA and DSA with respect to the severity of atherosclerotic renal artery stenosis result from MRA data acquisition problems and incorrect MRA image evaluation. These reasons were identified as the main causes of the poor performance of MRA as compared to DSA in the RADISH study.

Future technical developments of MRA should allow for a substantial increase of both spatial and temporal resolution, and may overcome most of the present shortcomings of renal MRA data acquisition. Moreover, recently developed software tools that allow for the automated evaluation of the severity of a renal artery stenosis are potentially capable to replace the subjective evaluations of radiologists. These tools can overcome the poor interobserver agreement for CTA and MRA, which has shown to be a considerable source of error in the present study. If attainable, the combination of all aforementioned developments is likely to improve the accuracy of MRA for the detection of renal artery stenosis.

References

1. Safian RD, Textor SC. Renal artery stenosis. N Engl J Med 2001; 344(6):431-42.
2. Plouin PF, Chatellier G, Darne B, Raynaud A. Blood pressure outcome of angioplasty in atherosclerotic renal artery stenosis: a randomized trial. Essai Multicentrique Medicaments vs Angioplastie (EMMA) Study Group. Hypertension 1998; 31(3):823-29.
3. Ramsay LE, Waller PC. Blood pressure response to percutaneous transluminal angioplasty for renovascular hypertension: an overview of published series. BMJ 1990; 300(6724):569-72.
4. van Jaarsveld BC, Krijnen P, Pieterman H, Derkx FH, Deinum J, Postma CT et al. The effect of balloon angioplasty on hypertension in atherosclerotic renal artery stenosis. Dutch Renal Artery Stenosis Intervention Cooperative Study Group. N Engl J Med 2000; 342(14):1007-14.
5. Webster J, Marshall F, Abdalla M, Dominiczak A, Edwards R, Isles CG et al. Randomised comparison of percutaneous angioplasty vs continued medical therapy for hypertensive patients with atheromatous renal artery stenosis. Scottish and Newcastle Renal Artery Stenosis Collaborative Group. J Hum Hypertens 1998; 12(5):329-35.
6. Rudnick MR, Berns JS, Cohen RM, Goldfarb S. Nephrotoxic risks of renal angiography: contrast media-associated nephrotoxicity and atheroembolism--a critical review. Am J Kidney Dis 1994; 24(4):713-27.
7. Waugh JR, Sacharias N. Arteriographic complications in the DSA era. Radiology 1992; 182(1): 243-46.
8. Young N, Chi KK, Ajaka J, McKay L, O'Neill D, Wong KP. Complications with outpatient angiography and interventional procedures. Cardiovasc Intervent Radiol 2002; 25(2):123-26.
9. Cochran ST, Bomyea K, Sayre JW. Trends in adverse events after IV administration of contrast media. AJR Am J Roentgenol 2001; 176(6):1385-88.
10. Vasbinder GB, Nelemans PJ, Kessels AG, Kroon AA, de Leeuw PW, van Engelshoven JM. Diagnostic tests for renal artery stenosis in patients suspected of having renovascular hypertension: a meta-analysis. Ann Intern Med 2001; 135(6):401-11.
11. Vasbinder GB, Nelemans PJ, Kessels AG, Kroon AA, Maki JH, Leiner T, et al. Computed tomographic angiography and magnetic resonance angiography for the diagnosis of renal artery stenosis: A comparative study with digital subtraction angiography. Results of the Renal Artery Diagnostic Imaging Study in Hypertension (RADISH). Submitted.
12. Shetty AN, Bis KG, Kirsch M, Weintraub J, Laub G. Contrast-enhanced breath-hold three-dimensional magnetic resonance angiography in the evaluation of renal arteries: optimization of technique and pitfalls. J Magn Reson Imaging 2000; 12(6):912-23.
13. Rieumont MJ, Kaufman JA, Geller SC, Yucel EK, Cambria RP, Fang LS et al. Evaluation of renal artery stenosis with dynamic gadolinium-enhanced MR angiography. AJR Am J Roentgenol 1997; 169(1):39-44.
14. Bakker J, Ligtenberg G, Beek FJ, Reedt Dortland RW, Hene RJ. Preoperative evaluation of living renal donors with gadolinium-enhanced magnetic resonance angiography. Transplantation 1999; 67(8):1167-72.
15. Elgavish RA, Twieg DB. Improved depiction of small anatomic structures in MR images using Gaussian-weighted spirals and zero-filled interpolation. Magn Reson Imaging 2003; 21(2):103-12.
16. Maki JH, Chenevert TL, Prince MR. The effects of incomplete breath-holding on 3D MR image quality. J Magn Reson Imaging 1997; 7(6):1132-39.
17. Vasbinder GB, Maki JH, Nijenhuis R.J., Leiner T., Wilson GJ, Kessels AG et al. Motion of the distal renal artery during 3D contrast-enhanced breath-hold MRA. J Magn Reson Imaging 2002;16(6):685-96.
18. Lee VS, Martin DJ, Krinsky GA, Rofsky NM. Gadolinium-enhanced MR angiography: artifacts and pitfalls. AJR Am J Roentgenol 2000; 175(1):197-205.

General discussion

Since treatment of renal artery stenosis (RAS) by percutaneous transluminal renal angioplasty or surgery may result in improvement or cure of renovascular hypertension and may halt the associated deterioration of renal function, several diagnostic tests have been introduced that aim to identify patients with RAS. In this thesis, a number of studies related to the morphologic diagnosis of RAS are reported. For reasons of comparison, chapter 2 includes an evaluation of morphological diagnostic tests versus functional diagnostic tests for RAS.

Diagnostic tests for renal artery stenosis

For many years now, intra-arterial digital subtraction angiography (DSA) has generally been considered the most sensitive test for the detection of RAS. This test, however, is invasive and harbors a small risk for complications such as arterial dissection and adverse contrast media reactions including acute renal failure. Moreover, patients who are subjected to DSA are exposed to ionizing radiation. Over the past decades, several non-invasive or minimally invasive diagnostic tests have been advocated to replace DSA for the diagnostic workup of patients suspected of having RAS. These tests 1) aim to provide morphologic images of a stenosis or 2) aim to give functional information on the effects of a stenosis on renal blood flow or the renin-angiotensin system. Currently, the morphologic tests computed tomographic angiography (CTA) and three-dimensional, contrast-enhanced magnetic resonance angiography (MRA) are generally considered the preferred minimally invasive diagnostic alternatives to DSA. In chapter 2, this opinion is corroborated by a meta-analysis that included studies on CTA, MRA, non contrast-enhanced magnetic resonance angiographic techniques, ultrasonography, captopril renal scintigraphy, and the captopril test using DSA as reference test (1). The meta-analysis found CTA and MRA to have a significantly better diagnostic performance as compared to the other studied tests. However, only 5 studies for CTA and 6 studies for MRA met the inclusion criteria. Many studies that were considered for meta-analysis suffered from shortcomings with respect to study design. Studies were frequently excluded from meta-analysis because they evaluated patients whose reason for referral to the diagnostic tests was not primarily suspicion of RAS, and because selective referral of patients based on the results of previous tests, so-called verification bias, could not be excluded.

The studies that were included showed considerable variation in results. Sources of heterogeneity included the lack of standard criteria used to define a positive test result and differences in data analysis, but a large part of heterogeneity remained unexplained. The most probable source of this unexplained heterogeneity is differences in case-mix. The prevalence of RAS in the included studies varied between 8% and 70%. This finding reflects large differences in patient selection between studies, although the description of the inclusion and exclusion criteria did not provide an explanation for these differences. Adequate description of the studied patient population is a prerequisite for diagnostic studies. Several characteristics of patients, such as stage and severity of disease may be related both to the sensitivity/specificity of a test and to prevalence, because different kinds of patients are found in high- and low-prevalence situations.

In summary, it was concluded that future diagnostic studies should be designed and analyzed in a way that facilitates comparison of results by adequate description

of inclusion and exclusion criteria, and presentation of estimates of sensitivity and specificity within subgroups of patients with variable degrees of clinical suspicion of renovascular hypertension.

The diagnostic accuracy of CTA and MRA

The limitations mentioned above created a need for a large well-designed study on the diagnostic accuracy of CTA and MRA. Numerous other authors have also expressed the need for such a study. The Renal Artery Diagnostic Study in Hypertension (RADISH) aimed to satisfy this need (2). The results of this study are reported in chapter 3. For the 356 patients who were evaluated, poor sensitivity for the several observers (ranging from 61% to 69% for CTA and from 57% to 67% for MRA) was found for the detection of clinically relevant RAS (≥50% atherosclerotic luminal reduction and fibromuscular dysplasia (FMD)). The specificity for both tests was acceptable and ranged from 89% to 97% for CTA and 77% to 90% for MRA. Moderate interobserver agreement was found with kappa values ranging from 0.59 to 0.64 for CTA and 0.40 to 0.51 for MRA. As a result, it was concluded that both CTA and MRA are not sufficiently sensitive and reproducible for the accurate detection of clinically relevant RAS. These findings conflict strongly with the results of other studies in the literature which report sensitivities and specificities up to 100%.

A striking finding in the RADISH was the relative high proportion of patients with fibromuscular dysplasia (38% of all patients with RAS). In a patient population with RAS, the literature reports a prevalence of FMD ranging from 16% to 40% (3, 4). However, in studies on the diagnostic accuracy of CTA and MRA either the prevalence of fibromuscular dysplasia was quite low or patients with fibromuscular dysplasia were excluded from the analyses. As extensively discussed in this thesis and in other literature, FMD is known for its poor detection by CTA and MRA. In the RADISH study, many stenoses due to FMD were missed and an additional analysis of the RADISH data revealed that missing FMD contributed most substantially to the poor overall sensitivity of CTA and MRA.

Additional evaluation of the RADISH data showed that omitting FMD from analysis still did not result in the high sensitivities as reported by other studies, indicating that CTA and MRA are not sensitive enough to diagnose atherosclerotic RAS either. Also, it was observed that diagnostic performance varied between subgroups of patients with different pre-test probabilities of renal artery stenosis. The sensitivity increased to 88% (for CTA) and 78% (for MRA) in a subgroup of patients in whom the predicted probability of disease was more than 25%. In this subgroup, the observed prevalence of renal artery stenosis was 42% and more severe stenoses were observed. This finding is in agreement with the well-known fact that estimates of sensitivity and specificity depend on the distribution of severity of disease in the studied sample (5).
It illustrates that the selection of patients, at least in part, may be an explanation for the discrepant findings on the diagnostic accuracy between RADISH and studies evaluating patient groups with a high prevalence of RAS. Moreover, it stresses the importance of referring for diagnostic work-up only patients with a high pre-test likelihood of disease and the current need for a valid clinical prediction rule in order to raise the pre-test likelihood for the presence of RAS. The generally accepted

clinical clues for the presence of RAS that were used in the RADISH resulted in a mere prevalence of 20%.

Limitations of MRA for the detection of RAS

Although we also reported poor results for CTA as a diagnostic test for RAS, in the thesis we focused on exploring the limitations of MRA that contributed to its' poor diagnostic accuracy. To a certain extent, the limitations found for MRA are likely to have affected CTA as well.

The performance of a MRA exam

Carrying out a high quality MRA exam is a painstaking task. Besides the necessity of up-to-date equipment, well-trained experienced technologists and radiologists are a requisite. Most important, however, is a collaborative patient. The 'perfect' patient should be able to sustain a near motionless supine position in the scanner for at least 15 minutes, which is required for the acquisition of localizer scans, a timing sequence, and the MRA scan itself. During the MRA scan duration (typically 20 to 25 seconds), the patient has to sustain a breath-hold. For many patients this is hard to achieve. Practicing the breath-hold command before the patient enters the scanner and the administration of oxygen by means of a nasal cannula have proven to be effective methods to increase the patient's compliance and breath-holding performance (6).

Even when an initially successful exam has been performed, the final diagnosis made on MRA images is still subject to sources of error. In chapters 4 through 6, the limitations of MRA are investigated and discussed. Three major causes that hamper a correct diagnosis were identified and include 1) artifacts caused by motion of the (distal) renal artery, 2) inadequate spatial resolution, and 3) incorrect MRA image evaluation.

Motion of the renal artery

Two distinct causes of motion of the renal artery were identified and are presented in chapter 4 and 5 (7, 8). First, the beating heart causes motion of the proximal renal artery. This generates a pulsatile blood pressure and flow, which causes the aorta and renal arteries to dilate and translate, respectively. An average full motion of the proximal renal artery was observed of 2.1 mm for the left kidney and 2.3 mm for the right kidney. Second, significant cranial translation of the kidney was observed despite sustained breath holding. This motion was near linear with a mean translation of 0.26 mm/second and 0.25 mm/second for the right and left kidneys, respectively. For typical scan duration of 25 seconds, a net kidney translation of approximately 6 mm takes place. The distal renal artery typically has a close anatomic relation to the kidney; for that reason, the assumption of similar motion in the distal renal artery to that found in the kidneys seems justified.

Currently used voxel sizes are smaller than the observed translation of both the proximal and distal renal artery. As motion effectively reduces spatial resolution and causes artifacts, implementing some form of motion correction technique should be considered for an accurate depiction of RAS. Cardiac triggering may reduce the effects of motion of the proximal renal artery. However, this is currently not feasible during MRA due to limitations with respect to the arterio-venous window and

breath-hold. The observed motion of the distal renal artery can be reduced by using techniques that allow for faster data acquisition, such as a shorter TR, smaller FOV, parallel imaging techniques, or a combination of these (9, 10).

Inadequate spatial resolution

As shown in chapter 6, the limited voxel size of MRA relative to vessel size and the inherent partial volume effects may result in inaccurate visualization of a renal artery and hamper the correct assessment of the presence or absence of a stenosis (11). Nowadays, state-of-the-art MR scanners can achieve sub-millimeter spatial resolution. However, the pixel size of DSA (with an approximate size of 0.2 x 0.2 mm) is still far superior to that of MRA. One might question the usefulness of ultra-high spatial resolution in MRA, when the deleterious effects of renal artery motion are present.

Incorrect image evaluation

As observed in chapter 6, failures during MRA image evaluation was the most frequent reason for discrepancies with respect to the observed severity of stenosis between MRA and DSA (11). Retrospective and non-blinded evaluation of the MRA data did result in similar diagnoses as those that were initially made on DSA. In the majority of the cases, the observed discrepancy resulted from incorrect interpretation by only one out the three MRA observers. For the two other observers the MRA diagnosis was in agreement with the DSA diagnosis, suggesting that a more uniform approach of image evaluation may lead up to a substantial better diagnostic performance. However, in the RADISH study, the observers evaluated the images using prior defined criteria and a standard form

Clinical Utility of CTA and MRA

Diagnostic parameters for CTA and MRA as found in the RADISH study are intermediate outcomes. However, gains in effectiveness and potential cost savings that can result from the use of diagnostic tests are largely determined by the management strategy adopted on the basis of the test results (12).

Detection of renal artery stenosis usually implies treatment by percutaneous transluminal renal angioplasty (PTRA) or stenting. Available evidence indicates that especially patients with FMD benefit from revascularization, but the clinical benefit for patients with detected atherosclerotic renal artery stenosis is still unclear (13). Recent trials that compared the results of PTRA and treatment with antihypertensive drugs in patients with atherosclerotic renal artery stenosis showed little advantage of PTRA over drug therapy with respect to blood pressure control (14, 15, 16). Whether PTRA results in better preservation of renal function is not yet proven by randomized trials. Therefore, missing atherosclerotic renal artery stenoses may have fewer consequences for patient outcome than missing renal artery stenoses due to FMD.

The question whether and when CTA and/or MRA, despite their limitations, can be clinically useful alternatives to DSA will also be addressed by a cost-effectiveness analysis using data from the RADISH study. This analysis compared direct use of DSA in all patients with selective use of DSA, whereby patients are referred for DSA only in case of a positive MRA or CTA test result. Selective use of DSA is expected

to result in cost savings and in fewer complications due to DSA, but these effects should be weighed against the health effects that result from missed diagnoses of renal artery stenosis. The results are expected to be published shortly elsewhere and will provide the information that is needed to answer the question whether and when CTA and/or MRA are clinically useful alternatives to DSA.

Future directions

Recent and future developments in CTA and MRA technology may increase the accuracy of both techniques for the detection of RAS. Promising early experiences are reported for multidetector-row CT scanners and MR parallel-imaging techniques (17, 18). These techniques enable faster data acquisition and, therefore, may reduce the effects of motion artifacts of the distal renal artery and allow for higher spatial resolution. Motion artifacts and inadequate spatial resolution were the most frequently observed limitations of MRA data acquisition that resulted in discrepancies in the measured severity of stenosis between MRA and DSA (50% of all discrepancies). Moreover, a recent study on MRA at 3.0 Tesla reports an objective and subjective better image quality for several vascular regions as compared to 1.5 Tesla (19). Along with these developments, recently developed software tools that allow for the automated evaluation of the severity of a renal artery stenosis are potentially capable to replace the subjective evaluations of radiologists. These tools can overcome the poor interobserver agreement for CTA and MRA, which has shown to be a considerable source of error in the RADISH study.

A further challenge for the diagnosis of RAS is to exploit the ability of MR imaging to obtain functional information of blood flow and perfusion. In this thesis, only morphologic criteria were used for the diagnosis of RAS by CTA and MRA. However, 50% luminal narrowing may not cause renovascular hypertension in some patients while in other patients a 30% RAS may be sufficient to induce renovascular hypertension. Recent studies reported promising results on the functional consequences of a stenosis diagnosed on MRA, using phase-contrast flow measurements, magnetic resonance renography, and computational fluid dynamics (20, 21, 22). CT does not offer the possibility to measure blood flow, but recent studies report promising preliminary results on dynamic electron-beam CT in order to obtain information of renal perfusion (23, 24).

Along with the technological developments that are considered to improve the morphologic assessment of RAS by CTA and MRA, the implementation of the functional assessment of renal blood and perfusion is expected to significantly improve the performance to diagnose clinically relevant RAS. Future, well-designed, large studies will have to elucidate whether this approach can reliably replace DSA for the diagnosis of RAS in patients with clinical suspicion for the presence of RAS.

Conclusions

In direct contradiction to the results of other studies, the RADISH study found poor sensitivity and moderate reproducibility for the detection of clinically relevant RAS by CTA and MRA. These finding were striking, the more so because a meta-analysis found both CTA and MRA to be superior to all other non-invasive or minimally

invasive diagnostic tests for RAS. The inability of CTA and MRA to correctly diagnose FMD in many patients contributed substantially to the poor overall sensitivity. This finding is especially piteous, because PTRA may effectively improve the treatment of hypertension in many patients with this disease. The question whether and when CTA and/or MRA can be clinically useful alternatives to DSA must be addressed by a cost-effectiveness analysis.

New technological developments and the full utilization of the ability of MRA and CTA to obtain functional information on blood flow and renal perfusion may improve the diagnostic accuracy of CTA and MRA to an extent that these techniques can reliably replace DSA in the diagnostic work-up of patients suspected to have RAS.

References

1. Vasbinder GB, Nelemans PJ, Kessels AG, Kroon AA, de Leeuw PW, van Engelshoven JM.Diagnostic tests for renal artery stenosis in patients suspected of having renovascular hypertension: a meta-analysis. Ann Intern Med 2001; 135(6):401-11.
2. Vasbinder GB, Nelemans PJ, Kessels AG, Kroon AA, Maki JH, Leiner T, et al. Computed tomographic angiography and magnetic resonance angiography for the diagnosis of renal artery stenosis: A comparative study with digital subtraction angiography. Results of the Renal Artery Diagnostic Imaging Study in Hypertension (RADISH). Submitted.
3. Textor SC. Epidemiology and clinical presentation. Semin Nephrol 2000; 20(5):426-31.
4. Pohl MA, Novick AC. Natural history of atherosclerotic and fibrous renal artery disease: clinical implications. Am J Kidney Dis 1985; 5(4):A120-A130.
5. Fletcher R.H., Fletcher S.W., Wagner E.H. Diagnosis. Clinical epidemiology. The essentials. Baltimore: Williams and Wilkins, 1996: 54-55.
6. Prince MR, Grist TM, Debatin JF. Basic Concepts. 3D Contrast MR Angiography. Berlin Germany: Springer Verlag, 2003: 3-44.
7. Kaandorp DW, Vasbinder GB, de Haan MW, Kemerink GJ, van Engelshoven JM. Motion of the proximal renal artery during the cardiac cycle. J Magn Reson Imaging 2000; 12(6):924-28.
8. Vasbinder GB, Maki JH, Nijenhuis RJ, Leiner T, Wilson GJ, Kessels AG et al. Motion of the distal renal artery during three-dimensional contrast-enhanced breath-hold MRA. J Magn Reson Imaging 2002; 16(6):685-96.
9. Fain SB, King BF, Breen JF, Kruger DG, Riederer SJ. High-spatial-resolution contrast-enhanced MR angiography of the renal arteries: a prospective comparison with digital subtraction angiography. Radiology 2001; 218(2):481-90.
10. Wilson GJ, Maki JH, Eubank W.B, Vasbinder GB, Kessels AG, Hoogeveen R. A direct comparison study to determine the utility of Sensitivity Encoding (SENSE) for renal MRA. Submitted.
11. Vasbinder GB, Nelemans P.J., Kessels AG, Leiner T, Maki JH, de Haan MW et al. Pitfalls and limitations of contrast-enhanced renal magnetic resonance angiography for the detection of atherosclerotic renal artery stenosis. Submitted.
12. Hunink MG. Outcomes research and cost-effectiveness analysis in radiology. Eur Radiol 1996; 6(5):615-20.
13. Ramsay LE, Waller PC. Blood pressure response to percutaneous transluminal angioplasty for renovascular hypertension: an overview of published series. BMJ 1990; 300(6724):569-72.
14. Plouin PF, Chatellier G, Darne B, Raynaud A. Blood pressure outcome of angioplasty in atherosclerotic renal artery stenosis: a randomized trial. Essai Multicentrique Medicaments vs Angioplastie (EMMA) Study Group. Hypertension 1998; 31(3):823-29.
15. van Jaarsveld BC, Krijnen P, Pieterman H, Derkx FH, Deinum J, Postma CT et al. The effect of balloon angioplasty on hypertension in atherosclerotic renal artery stenosis. Dutch Renal Artery Stenosis Intervention Cooperative Study Group. N Engl J Med 2000; 342(14):1007-14.
16. Webster J, Marshall F, Abdalla M, Dominiczak A, Edwards R, Isles CG et al. Randomised comparison of percutaneous angioplasty vs continued medical therapy for hypertensive patients with atheromatous renal artery stenosis. Scottish and Newcastle Renal Artery Stenosis Collaborative Group. J Hum Hypertens 1998; 12(5):329-35.
17. Weiger M, Pruessmann KP, Kassner A, Roditi G, Lawton T, Reid A et al. Contrast-enhanced 3D MRA using SENSE. J Magn Reson Imaging 2000; 12(5):671-77.

18. Hahn U, Konig CW, Miller S, Brehm B, Heuschmid M, Kopp AF et al. [Multidetector CT Angiography - is it a valuable screening tool to detect significant renal artery stenosis?]. Rofo Fortschr Geb Rontgenstr Neuen Bildgeb Verfahr 2001; 173(12):1086-92.
19. Leiner T, De Vries M, Hoogeveen R, Vasbinder GB, Lemaire E, van Engelshoven JM. Contrast-enhanced peripheral MR angiography at 3.0 Tesla: Initial experience with a whole-body scanner in healthy volunteers. J Magn Reson Imaging 2003; 17(5):609-14.
20. Schoenberg SO, Knopp MV, Londy F, Krishnan S, Zuna I, Lang N et al. Morphologic and functional magnetic resonance imaging of renal artery stenosis: a multireader tricenter study. J Am Soc Nephrol 2002; 13(1):158-69.
21. de Priester JA, Kroon AA, Giele EL, den Boer JA, Vasbinder GB, Kessels AG et al. Automated post-processing and enhancement parameterization in magnetic resonance renography. Patterns in hypertensive patients with and without renal artery stenosis. Submitted.
22. Yim PJ, Vasbinder GB, Ho VB, Choyke PL. A computational model for measurement of arterial distensibility. Submitted.
23. Paul JF, Ugolini P, Sapoval M, Mousseaux E, Gaux JC. Unilateral renal artery stenosis: perfusion patterns with electron-beam dynamic CT--preliminary experience. Radiology 2001; 221(1):261-265.
24. Romero JC, Lerman LO. Novel noninvasive techniques for studying renal function in man. Semin Nephrol 2000; 20(5):456-62.

Summary and conclusions

In a general hypertensive population, the proportion of patients with renovascular hypertension is considered to range from 1% to 5%. Renovascular hypertension is caused by renal artery stenosis (RAS). Treatment of RAS by percutaneous transluminal renal angioplasty with or without stent placement or surgery may improve or cure hypertension and may reverse the associated progressive loss of renal function. Because treatment is possible, it is important to identify patients with RAS. Traditionally, intra-arterial digital subtraction angiography (DSA) has been considered as the best diagnostic test for the detection of RAS. Since DSA is an invasive procedure that subjects patients to intra-arterial catheters, potentially nephrotoxic iodinated contrast agents, and X-rays, many non invasive or minimally invasive diagnostic alternatives for DSA have been proposed.

Diagnostic tests for renal artery stenosis

In chapter 2, we performed a meta-analysis that summarized and compared the validity of computed tomographic angiography (CTA), three-dimensional contrast-enhanced magnetic resonance angiography (MRA), non contrast-enhanced magnetic resonance angiographic techniques, ultrasonography, captopril renal scintigraphy, and the captopril test for the diagnosis of RAS in patients with clinical clues for the presence of renovascular hypertension. DSA was used as reference test. The construction of summary receiver-operating characteristics (ROC) curves and the areas under the ROC curves were used for analysis and comparison.

We found CTA and MRA to perform significantly better as compared to the other non invasive or minimally invasive tests and, based on these findings, we concluded that CTA and MRA seemed to be preferred in patients referred for evaluation of renovascular hypertension. However, because few studies that met the inclusion criteria for the meta-analysis have been published, we recommended further research.

CTA and MRA for the diagnosis of renal artery stenosis

In chapter 3, we report the results of the Renal Artery Diagnostic Imaging Study in Hypertension (RADISH). This large prospective multicenter study on the validity of CTA and MRA for the diagnosis of RAS evaluated 356 patients with clinical clues suggestive for the presence of RAS who all underwent CTA, MRA, and the reference test DSA within a three-month window. Contrary to expectation, we found CTA and MRA to have a poor sensitivity (ranging from 61% to 69% for CTA and from 57% to 67% for MRA) for the detection of clinically relevant RAS (≥50% atherosclerotic RAS and FMD). Specificity ranged from 89% to 97% for CTA and from 77% to 90% for MRA. Moreover, a moderate interobserver agreement was found, ranging from 0.59 to 0.64 for CTA and from 0.40 to 0.51 for MRA. Additional analyses revealed that missing FMD contributed substantially to the poor sensitivity. Selecting a subgroup of patients with a high prevalence of RAS could significantly increase the diagnostic accuracy of CTA and MRA, but sensitivity remained below 90%.

We concluded that CTA and MRA are not sensitive and reproducible enough to reliably diagnose clinically relevant RAS in patients with clinical clues for the presence of RAS. Therefore, DSA remains the method of choice for this purpose.

Limitations of MRA for the detection of RAS

In chapter 4, we quantified the motion of the proximal renal artery during the cardiac cycle in 48 hypertensive patients suspected of having RAS using two-dimensional quantitative flow measurements and automated contour detection. The goal of the study was to provide objective arguments for the improvement of renal MRA. Substantial translational motion was observed with amplitude ranging from 1 to 4 mm. This motion is comparable to or larger than currently used MRA voxel sizes. As motion effectively reduces spatial resolution, we concluded that implementing some form of motion correction should be considered for the accurate depiction of RAS.

In chapter 5, we aimed to find an explanation for the routinely encountered variable degrees of blurring and ringing artifacts in the distal renal arteries and kidneys on MRA, hampering clinical evaluation. Initially, these artifacts were attributed to respiratory motion. However, the majority of patients sustained a breath-hold during the entire MRA scan duration. Therefore, a clinical study was devised to test the hypotheses that renal motion occurs during a breath-hold and this motion correlates with MRA image quality. Moreover, computer simulation was performed to better understand the effects of motion on MRA image quality. Twenty-four patients underwent a breath-hold, non-enhanced single slice two-dimensional dynamic turbo field-echo magnetic resonance imaging scan, followed by MRA and the reference test DSA. We observed significant near linear cranial motion of the kidneys, averaging 0.26 mm/second, during a sustained breath-hold. The computer model revealed linear motion to cause artifacts. The MRA images showed artifacts of the distal renal artery that correlated with velocity and corroborated the computer model findings. These artifacts jeopardized reliable clinical evaluation. We concluded that some kind of motion correction or techniques that allow for reducing scan time should be implemented for decreasing the detrimental effects of the observed motion on MRA image quality.

In chapter 6, we performed a retrospective analysis of the RADISH data in order to identify factors that explain the poor diagnostic accuracy of MRA for the detection of atherosclerotic RAS. We found incorrect MRA image interpretation, MRA spatial resolution limitations, and motion artifacts, to be the most frequent reasons that caused discrepancies between the diagnoses made on MRA and the diagnosis made on DSA. Future developments that overcome the artifacts and limitations of MRA data acquisition and improve MRA image evaluation may ultimately result in more accurate MRA exams.

In chapter 7, the findings of this thesis are placed in perspective and the clinical utility of CTA and MRA as alternatives to DSA in current practice is discussed. Moreover, the limitations of MRA are addressed. Finally, recent developments that may improve the accuracy of CTA and MRA for the detection of renal artery stenosis are discussed and recommendations for future developments are given.

Conclusions

The conclusions of this thesis are:

1. The meta-analysis indicates that computed tomographic angiography and three-dimensional, contrast-enhanced magnetic resonance angiography are superior to other non invasive or minimally invasive tests for the diagnosis of renal artery stenosis in patients suspected of having renovascular hypertension, using intra-arterial digital subtraction angiography as standard of reference. Because only a limited number of CTA and MRA studies were published, further studies were recommended.
2. The meta-analysis found a considerable variation between studies, especially with respect to prevalence, possibly reflecting differences in patient selection.
3. Compared to the reference test DSA, CTA and MRA are not sensitive or reproducible enough to rule out renal artery stenosis in a population of hypertensive patients with clinical clues suggestive for the presence of renal artery stenosis. Therefore, DSA remains the method of choice.
4. Selection of patients with a higher pre-test likelihood of having RAS resulted in a substantial increase in diagnostic performance.
5. Motion of the proximal renal arteries due to pulsations of the blood pressure and flow during the cardiac cycle is always present. The average full motion is comparable to or larger than currently used MRA voxel dimensions and effectively reduces spatial resolution.
6. Despite sustained breath-hold, significant near linear cranio-caudal motion of the distal renal artery is present. This motion adversely affects distal renal artery image quality on MRA and jeopardizes reliable clinical evaluation.
7. MRA image interpretation errors, MRA resolution limitations, and motion artifacts during MRA data acquistion, are the most frequent reasons for discrepancies between MRA and DSA with respect to the observed severity of atherosclerotic renal artery stenosis.

Samenvatting en conclusies

Hypertensie ('hoge bloeddruk') is een belangrijke risicofactor die kan leiden tot hart- en vaatziekten. Bij de meeste patiënten met hypertensie wordt geen duidelijke oorzaak voor de verhoogde bloeddruk gevonden, maar in een klein percentage (minder dan 5% van alle patiënten met hypertensie) wordt de oorzaak toegeschreven aan de gevolgen van een vernauwing in de slagader naar één of beide nieren ('nierarterie-stenose', ofwel 'renal artery stenosis'; afgekort RAS). In dit geval spreken we van renovasculaire hypertensie.

Behandeling door middel van percutane transluminale renale angioplastiek ('dotteren'), met of zonder het plaatsen van een stent, maakt het mogelijk om zo'n vernauwing op te heffen. Hierdoor kan de verhoogde bloeddruk verlagen of zelfs normaliseren. Een ander belangrijk voordeel van deze behandeling is dat de functie van de nier, die ook wordt aangedaan door RAS, kan worden verbeterd. Omdat behandeling mogelijk is, is het belangrijk dat patiënten met RAS tijdig worden geïdentificeerd. Al enkele decennia wordt intra-arteriële digitale subtractie angiografie (DSA) beschouwd als de beste test om RAS op te sporen. DSA is echter een invasieve procedure die patiënten blootstelt aan intra-arteriële catheters, contrastmiddelen die schadelijk voor de nieren kunnen zijn, en röntgenstraling. Daarom zijn er in de loop der tijd vele niet- of minimaal invasieve diagnostische alternatieven voor DSA ontwikkeld.

Diagnostische tests voor nierarterie-stenose

In hoofdstuk 2 hebben we een meta-analyse uitgevoerd die een samenvatting en vergelijking gaf van de betrouwbaarheid van computer tomografische angiografie (CTA), drie-dimensionale contrast-versterkte magneet resonantie angiografie (MRA), niet contrast-versterkte magneet resonantie angiografische technieken, echografie, captopril renografie en de captopril test, voor de diagnostiek van RAS bij patiënten bij wie op klinische gronden het vermoeden bestaat dat zij renovasculaire hypertensie hebben. DSA werd gebruikt als referentie test. Zogenaamde 'summary receiver-operating characteristic (ROC)' curves en de oppervlaktes onder deze ROC curves werden gebruikt voor analyse en onderlinge vergelijking.

Uit deze studie bleek dat zowel CTA en MRA significant beter presteerden dan de andere onderzochte niet- of minimaal invasieve tests. Gebaseerd op deze bevindingen, concludeerden we dat CTA en MRA de meest wenselijke tests lijken te zijn voor patiënten die worden verwezen voor de evaluatie van renovasculaire hypertensie. Echter, slechts een beperkt aantal gepubliceerde studies voldeden aan de inclusie criteria voor de meta-analyse. Daarom adviseerden we verder onderzoek.

CTA en MRA voor de diagnostiek van nierarterie-stenoses

In hoofdstuk 3, rapporteerden we de resultaten van de Renal Artery Diagnostic Imaging Study in Hypertension (RADISH). Deze grote prospektieve multicenter studie onderzocht de diagnostische betrouwbaarheid van CTA en MRA voor het opsporen van RAS in een groep van 356 patiënten die op klinische gronden verdacht werden van het hebben van een nierarterie-stenose. Al deze patiënten ondergingen zowel

CTA, MRA en de referentie test DSA. In tegenstelling tot hetgeen we verwachtten, bleken CTA en MRA een slechte sensitiviteit te hebben (varierend van 61% tot 69% (CTA) en van 57% tot 67% (MRA)) voor het opsporen van klinisch relevante RAS (atherosclerotische RAS met een afname van het lumen ≥50% en fibromusculaire dysplasie (FMD)). De specificiteit van CTA varieerde van 89% tot 97% en die van MRA van 77% tot 90%. Ook vonden we een matige interobserver overeenstemming, met kappa waarden varierend van 0.59 tot 0.64 voor CTA en van 0.40 tot 0.51 voor MRA. Aanvullende analyses wezen uit dat het missen van FMD aanzienlijk bijdroeg aan de slechte sensitiviteit. Door een subgroep van patiënten met een hoge prevalentie RAS te selecteren, kon de diagnostische betrouwbaarheid van CTA en MRA substantieel worden verbeterd, maar de sensitiviteit bleef onder de 90%.

We concludeerden dat CTA en MRA sensitief noch reproduceerbaar genoeg zijn om betrouwbaar klinisch relevante RAS op te sporen bij patiënten met klinische kenmerken die suggestief zijn voor de aanwezigheid van RAS. Voor dit doel blijft DSA daarom de aangewezen methode.

Limitaties van MRA voor het opsporen van nierarterie-stenoses

In hoofdstuk 4 hebben we de beweging van de proximale nierarteriën tijdens de hartcyclus gekwantificeerd. Dit onderzoek werd verricht bij 48 hypertensieve patiënten met mogelijk RAS. De beweging werd in kaart gebracht door middel van twee-dimensionale quantitative flow metingen en automatische contour-detectie. Het doel van deze studie was om objectieve gegevens te verkrijgen die gebruikt kunnen worden om renale MRA te verbeteren. We vonden een substantiële beweging van de proximale nierarteriën tijdens de hartcyclus, met een amplitude varierend van 1 tot 4 mm. De amplitude van deze beweging is vergelijkbaar met of groter dan de momenteel gangbare MRA voxel dimensies. Aangezien beweging resulteert in afname van de effectieve spatiële resolutie, concludeerden we dat er een vorm van correctie voor deze beweging nodig is om een meer accurate diagnostiek van RAS mogelijk te maken.

In hoofdstuk 5 zochten we naar een verklaring voor de zogenaamde 'blurring' en 'ringing' artefacten die, in wisselende mate, op het niveau van de distale nierarteriën en nieren bij MRA worden waargenomen. Deze artefacten belemmeren een betrouwbare klinische evaluatie van de verkregen beelden. In eerste instantie werden deze artefacten verklaard doordat de patiënten zouden hebben geademd tijdens de data acquisitie. Echter, het merendeel van de patiënten bleek tijdens de gehele MRA scanduur toch de adem te hebben ingehouden ('breath-hold'). Daarom werd een klinische studie verricht om de hypothese te testen of er beweging van de nieren is ondanks een goede breath-hold. Tevens werd gekeken of zo'n beweging correleert met MRA beeldkwaliteit. Computer simulaties werden uitgevoerd om een beter inzicht te verkrijgen in de effecten van beweging op MRA beeldkwaliteit. Vierentwintig patiënten ondergingen een breath-hold single slice twee-dimensionaal dynamisch turbo field-echo MRI onderzoek, gevolgd door MRA en de referentie test DSA. Tijdens breath-hold vonden we significante, vrijwel lineaire, craniale beweging van de nieren met een gemiddelde van 0.26 mm per seconde. De computer simulaties lieten zien dat lineaire beweging artefacten veroorzaakt. De verkregen MRA beelden ver-

toonden artefacten ter hoogte van de distale nierarteriën, die in ernst correleerden met de snelheid van beweging en die de bevindingen van de computer simulaties bevestigden. Deze artefacten verhinderen een betrouwbare klinische evaluatie. We concludeerden dat een vorm van bewegingscorrectie of technieken die de scanduur kunnen verkorten zullen moeten worden geimplementeerd om de nadelige effecten van de geobserveerde beweging op MRA beeldkwaliteit te verminderen.

In hoofdstuk 6 werd een retrospectieve analyse van de RADISH data verricht, om factoren te identificeren die de slechte sensitiviteit van MRA voor de detectie van atherosclerotische RAS kunnen verklaren. We vonden dat de meest frequente oorzaken van discrepantie tussen MRA en DSA incorrecte MRA beeld interpretatie, limitaties van de spatiële resolutie van MRA en bewegingsartefacten waren. Toekomstige ontwikkelingen die de huidige artefacten en limitaties van MRA data acquisitie kunnen oplossen en de MRA beeldkwaliteit kunnen verbeteren, zouden er uiteindelijk toe kunnen leiden dat MRA een meer accurate test wordt.

In hoofdstuk 7 werden de bevindingen van dit proefschrift in perspectief geplaatst en de huidige klinische bruikbaarheid van CTA en MRA als alternatieven voor DSA werden besproken. Ook werden de limitaties van MRA belicht. Ten slotte werden recente technische ontwikkelingen, die de betrouwbaarheid van CTA en MRA kunnen verbeteren, vermeld en werden er aanbevelingen voor toekomstige ontwikkelingen gedaan.

Conclusies

De conclusies van dit proefschrift zijn:

1. De meta-analyse geeft aan dat computer tomografische angiografie (CTA) en drie-dimensionale contrast-versterkte magneet resonantie angiografie (MRA) superieur zijn in vergelijking met andere niet- of minimaal invasieve tests voor de diagnostiek van nierarterie-stenoses bij patiënten verdacht voor het hebben van renovasculaire hypertensie. Hierbij werd intra-arteriële digitale subtractie angiografie als referentie test gebruikt. Aangezien er slechts een gering aantal CTA en MRA studies zijn gepubliceerd, werd verder onderzoek aanbevolen.
2. De meta-analyse vond een aanzienlijke variatie tussen de verschillende studies, in het bijzonder met betrekking tot prevalentie, dat mogelijk wijst op verschillen in patiënt selectie.
3. Vergeleken met de referentie test DSA, zijn CTA en MRA sensitief noch reproduceerbaar genoeg om nierartererie-stenosen uit te sluiten in een hypertensieve patiënten populatie met klinische kenmerken die suggestief zijn voor de aanwezigheid van nierarterie-stenoses. Derhalve blijft DSA voor dit doel de aangewezen test.
4. Het selecteren van patiënten met een hogere pre-test waarschijnlijkheid voor het hebben van een nierarterie-stenose resulteerde in een substantiële toename van de diagnostische betrouwbaarheid.
5. Beweging van de proximale nierarteriën als gevolg van pulsaties van de bloeddruk en het stromen van bloed tijdens de hartcyclus is altijd aanwezig. De gemiddelde beweging is vergelijkbaar met of groter dan huidige MRA voxel dimensies en redu-

ceert de effectieve spatiële resolutie.

6. Ondanks een goede breath-hold is significante, vrijwel lineaire, cranio-caudale beweging van de distale nierarteriën aanwezig. Deze beweging heeft een negatief effect op de MRA beeldkwaliteit van de distale nierarteriën en staat een betrouwbare klinische evaluatie in de weg.
7. Incorrecte MRA beeld interpretatie, MRA resolutie limitaties en bewegingsartefacten tijdens MRA data acquisitie, zijn de meest voorkomende oorzaken die leiden tot discrepanties tussen de bevindingen op MRA en DSA wat betreft de geobserveerde ernst van atherosclerotische nierarterie-stenoses.

Dankwoord

Allereerst wil ik alle patiënten bedanken, die deel hebben genomen aan de RADISH studie. Zonder hun bereidheid om de extra onderzoeken te ondergaan zou dit boekje er niet zijn geweest. Tevens gaat mijn dank uit naar alle artsen, laboranten, research nurses, doktersassistenten en anderen die betrokken zijn geweest bij de inclusie van patiënten, de beeldvorming en de logistiek van formulieren en beelden in Den Bosch, Maastricht, Nijmegen, Tilburg, Utrecht, en Veldhoven. Een aantal personen wil ik hieronder graag met name noemen.

Prof. Dr. J.M.A. van Engelshoven, geachte promotor en opleider, beste professor, ik ben u veel dank verschuldigd voor het in mij gestelde vertrouwen, uw wijze adviezen en beslissingen, uw enthousiasme en het prettige overleg. Ik hoop de komende jaren nog veel van u te mogen leren.

Prof. Dr. P.W. de Leeuw, geachte promotor, beste Peter, bedankt voor de prettige samenwerking en de waardevolle adviezen die je me in de loop der tijd hebt gegeven.

Dr. P.J. Nelemans, geachte co-promotor, beste Patty, om je te bedanken heb ik eigenlijk een apart hoofdstuk nodig. Je inzet, kennis en kunde hebben me enorm geholpen. Ook je geduld, humor en terechte kritiek op dwalingen in wetenschappelijk onderzoek (niet het onze!), waardeer ik ten zeerste.

Dr. A.A. Kroon, geachte co-promotor, beste Bram, ik wil je bedanken voor onze aangename samenwerking en je goede kritieken op de diverse manuscripten. Je inzet wat betreft inclusie van patiënten en het achterhalen van gegevens hebben in belangrijke mate bijgedragen aan het slagen van de RADISH studie.

De leden van de beoordelingscommissie Prof. Dr. K.M.L. Leunissen, Prof. Dr. P.J.E.H.M. Kitslaar, Dr. C.T. Postma, Prof. Dr. M.H. Prins en Priv.-Doz. Dr. med. S.O. Schönberg wil ik bedanken voor het kritisch beoordelen van het manuscript.

De leden van de RADISH studiegroep dank ik voor hun waardevolle commentaren tijdens ondermeer de plenaire sessies.

De volgende personen hadden de zware taak om zo'n 400 DSA, CTA, of MRA onderzoeken te beoordelen: Erik Beek, Professor van Engelshoven, Michiel de Haan, Professor B.K. Janevski, Mike Korst, Dick Koster, Tim Leiner, Jeff Maki, Kiam Oei en Wim van Zwam. Mijn dank hiervoor!

De radiologen en collega arts-assistenten van de afdeling Radiologie in Maastricht wil ik bedanken voor hun collegialiteit en belangstelling tijdens de periode van afronding van mijn proefschrift.

I wish to thank my international colleagues and friends in the field of MRA and renovascular hypertension for the useful discussions and enjoyable times we had. Although the results of RADISH were quite shocking to most of you (including myself), I would like to thank you for not shooting me for that (yet) and appreciate your comments and advices.

Karin Flobbe wil ik bedanken voor het creëren en beheren van de RADISH database en de Case Record Forms. Jouw creativiteit en gedrevenheid hebben ervoor gezord dat alle gegevens overzichtelijk en compleet beschikbaar waren. Dit is ook te danken aan Peggy Habets, die onvermoeibaar de data heeft ingevoerd en die ervoor zorgde dat elke 'missing' met een 'geeltje' retour kwam.

Fons Kessels; dankzij jou is alle statistiek kloppend en significant waar dat wenselijk was. Vele malen was je een prima adviseur en goede gesprekspartner. Ook kon je altijd de kritiek van reviewers prima pareren. Onze bijeenkomsten waren vaak kort maar krachtig, maar altijd stond de pot met drop klaar.

Etienne Lemaire wil ik bedanken voor zijn belangrijke hulp bij het scannen, het branden van CD-roms en zijn tips & trics om de uitvoering van MRA verder te verbeteren. Hij weet als geen ander patiënten te motiveren om de scanner in te gaan en een goede 'breath-hold' uit te voeren. Ik wens iedere onderzoeker zo'n goede hulp toe!

Marc Geerlings zorgde ervoor dat het inladen van digitale beelden op de werkstations zo efficiënt mogelijk verliep. De Fuzzy, Dali, Zonnebloem, GW2 en GW4 hebben heel wat data voor hun kiezen gehad. Ook mijn PC heb je diverse malen op miraculeuze wijze kunnen redden! De overige onderzoekers in de 'MRI kelder' wil ik ook bedanken voor de prettige tijd samen en ik wens hen veel succes met hun onderzoek en, voor sommigen, hun proefschrift.

Ook wil ik Dave Kaandorp, Robbert Nijenhuis en Kai Yiu Ho bedanken voor hun inspanningen en adviezen bij de 'motion' verhalen.

Geertjan van Zonneveld wil ik bedanken voor zijn inspanningen om het design en de lay-out van dit proefschrift te verzorgen. De overige medewerkers van de AV-dienst in het azM hebben me ook altijd prima geholpen.

Jeff Maki: one of the 'Godfathers' of MRA and good friend. Thanks for your excellent contributions to some of the articles in this thesis. I feel honoured to have you aboard and I hope we will be able to tackle the pitfalls and limitations of renal MRA soon!

Tim Leiner: mijn 'roomy', goede vriend, collega en paranimf. Samen hebben we heel wat mooie tijden meegemaakt in zowel 'The Home of MRA', als ook in binnen- en buitenland. Samen delen we veel passies, die niet altijd even goed voor de gezondheid zijn. Het voornemen om in 2004 samen een marathon te gaan lopen is daarop een uitzondering. Jouw gretigheid om onderzoek te doen werkt aanstekelijk en heeft mij keer op keer gemotiveerd in mijn eigen onderzoek.

Erik Smeets: beste vriend voor bijna 30 jaar. Wij hebben door de jaren heen, samen met Han Oei en andere vrienden, veel beleefd dat met wetenschappelijk onderzoek niets te maken had. Ik hoop dat we in de toekomst nog veel van dat soort momenten samen mogen beleven. Bedankt voor je bereidheid om de taak als paranimf op je te nemen.

Mijn ouders wil ik bedanken voor hun onvoorwaardelijke steun, liefde en alle kansen die ze me hebben gegeven. Ook mijn overige familie en schoonfamilie dank ik voor hun belangstelling en ondersteuning.

Lieve Suuske; zonder jouw geweldige steun, vertrouwen, inzet en geduld was en ben ik nergens! Tijdens mijn onderzoeksjaren hebben we samen drie fantastische kinderen gekregen, die je vaak alleen onder je hoede moest nemen als ik weer eens aan het werk was of naar een congres moest. Lieve Charlotte, Madeleine en Diederik; pappa's boekje is klaar!

About the Author

Godfried Boudewijn ('Bo') Christoffel Vasbinder was born on January 9, 1969 in Nijmegen, The Netherlands. From 1981 to 1988, he attended high school at Maasland College in Oss, The Netherlands (Atheneum β). This was interrupted by a one-year exchange studentship at Neosho High School, Neosho, Missouri, U.S.A (1985-86). In 1988, he started his medical training at Utrecht University Medical School, Utrecht, The Netherlands. In 1992, he received his MSc degree in Medicine and in January 1995, after two years of internship, he obtained his medical board certification. Also in 1995, he successfully completed the clinical part of the United States Medical Licensing Examination (USMLE).

In March of 1995, he was drafted to serve in the Dutch Armed Forces. During his tour of duty, he was a First Lieutenant general practitioner for the personnel of the Air Force Base at Soesterberg, The Netherlands, and also served as a flight surgeon for an F-16 squadron in Goose Bay, Newfoundland, Canada.

In September, he voluntarily chose to continue his military career as a resident (rank Captain) at the Department of Ear, Nose, and Throat Medicine of the Central Military Hospital in Utrecht.

In December 1998, he became a research fellow at the Department of Radiology of Maastricht University Hospital, The Netherlands. The results of the research he performed in Maastricht are presented in the current thesis. The author has presented his research and invited papers at many national and international medical conferences. For a portion of his work, he was nominated for the 2003 Ernst Schering Prize of the Dutch Radiological Society.

The author is currently a second-year Radiology resident in Maastricht.

He is married to Suuske Vasbinder-Verbeeten. Together, they have three children: Charlotte (1999), Madeleine (2000), and Diederik (2002).

List of Publications

Publications in Peer Reviewed Journals

1. Kaandorp DW, Vasbinder GBC, de Haan MW, Kemerink GJ, van Engelshoven JMA. Motion of the proximal renal artery during the cardiac cycle. J Magn Reson Imaging 2000;12(6):924-928.
2. Leiner T, de Weert TT, Nijenhuis RJ, Vasbinder GBC, Kessels AGH, Ho KY, van Engelshoven JMA. Need for background suppression in contrast-enhanced peripheral magnetic resonance angiography. J Magn Reson Imaging 2001;14(6): 724-733.
3. Stipkovits EM, Graamans K, Vasbinder GBC, van Dijk JE, Beek FJA. Assessment of vestibular schwannoma growth: application of a new measuring protocol to the results of a longitudinal study. Ann Otol Rhinol Laryngol 2001;110(4):326-330.
4. Vasbinder GBC, Nelemans PJ, Kessels AGP, Kroon AA, de Leeuw PW, van Engelshoven JMA. Diagnostic tests for renal artery stenosis in patients suspected of having renovascular hypertension: a meta-analysis. Annals of Internal Medicine 2001;135:401-411.
5. Vasbinder GBC. The use of CT angiography for the detection of renal artery stenosis. Imaging Decisions. 2002;6(2):11-14.
6. Vasbinder GBC, Maki JH, Nijenhuis RJ, Leiner T, Wilson GJ, Kessels AGH, Kaandorp DW, Ho KYJAM, van Engelshoven JMA. Motion of the distal renal artery during 3D contrast-enhanced breath-hold MRA. J Magn Reson Imaging. 2002 Dec;16(6):685-696.
7. Vasbinder GBC, Stolk MFJ, Ke MY, Jebbink HJA, van Berge Henegouwen GP, Akkermans LMA, Smout AJPM. Micturition is associated with phase III of the interdigestive migrating motor complex in man. Am J Gastroenterol. 2003 Jan;98(1):66-71.
8. Leiner T, de Vries M, Hoogeveen RM, Vasbinder GBC, Lemaire E, van Engelshoven JMA. Contrast-enhanced peripheral MR angiography at 3.0 Tesla: Initial experience with a whole-body scanner in healthy volunteers. J Magn Reson Imaging. 2003 May;17(5):609-14.
9. Yim PJ, Vasbinder GBC, Ho VB, Choyke PL. Isosurfaces as deformable models for magnetic resonance angiography. IEEE Trans Med Imaging. 2003 Jul;22(7): 875-81.
10. Kemerink GJ, de Haan MW, Vasbinder GBC, Frantzen MJ, Schultz FW, Zoetelief J, Jansen JT, van Engelshoven JMA. The effect of equipment set up on patient radiation dose in conventional and computed tomographic angiography of the renal arteries. BJR; in press.
11. Van Zwam WH, Vasbinder GBC, Kessels AGH, van Engelshoven JMA. Intra-observer variability in different 3D post-processing techniques. Submitted.

12. de Priester JA, Kroon AA, Giele EL, den Boer JA, Vasbinder GBC, Kessels AG et al. Automated post-processing and enhancement parameterization in magnetic resonance renography. Patterns in hypertensive patients with and without renal artery stenosis. Submitted.
13. Leiner T, Kessels AGH, Vasbinder GBC, de Haan MW, Kitslaar PJEHM, Ho KYJAM, Tordoir JHM, van Engelshoven JMA. The comparative accuracy of color duplex ultrasonography and contrast-enhanced magnetic resonance angiography for the diagnosis of peripheral arterial occlusive disease. Submitted.
14. Leiner T, Nijenhuis RJ, Vasbinder GBC, Kessels AGH, de Haan MW, van Engelshoven JMA. Detection of iliac artery stenosis with duplex ultrasonography, contrast-enhanced MRA and intra-arterial DSA. Submitted.
15. Vasbinder GBC, Nelemans PJ, Kessels AG, Kroon AA, Maki JH, Leiner T, Beek FJA, Korst MBJM, Flobbe K, de Haan MW, van Zwam WH, Postma CT, Hunink MGM, de Leeuw PW, van Engelshoven JMA. Computed tomographic angiography and magnetic resonance angiography for the diagnosis of renal artery stenosis: A comparative study with digital subtraction angiography. Results of the Renal Artery Diagnostic Imaging Study in Hypertension (RADISH). Submitted.
16. Vasbinder GBC, Nelemans PJ, Kessels AGH, Leiner T, Maki JH, de Haan MW, Korst MBJM, Koster D, Oei TK, Lohle PN, Teertstra JJ, Pasmans HM, Barentsz JO, van Engelshoven JMA. Pitfalls and limitations of contrast-enhanced renal magnetic resonance angiography for the detection of atherosclerotic renal artery stenosis. Submitted.
17. van Assen HC, Vasbinder GBC, Stoel BC, Putter H, van Engelshoven JMA, Reiber JHC. Quantitative assessment of the morphology of renal arteries from X-ray images; Quantitative Vascular Analysis (QVA). Submitted.
18. de Haan MW, Kessels AGH, Vasbinder GBC, Beek FJA, Korst MBJM, Leiner T, Maki JH, van Zwam WH, de Leeuw PW, van Engelshoven JMA. Fibromuscular dysplasia of the renal arteries: comparison of spiral CT angiography, MR angiography and conventional angiography. Submitted.
19. Wilson GJ, Maki JH, Eubank WB, Vasbinder GBC, Kessels AGH, Hoogeveen RM. A Direct Comparison Study to Determine the Utility of Sensitivity Encoding (SENSE) for Renal MRA. Submitted.